Stony Brook University

Applications of Physics and Geometry to Finance

A Dissertation Presented

by

Jaehyung Choi

to

The Graduate School

in Partial Fulfillment of the Requirements

for the Degree of

Doctor of Philosophy

in

Physics

Stony Brook University

May 2014

Stony Brook University

The Graduate School

Jaehyung Choi

We, the dissertation committee for the above candidate for the

Doctor of Philosophy degree, hereby recommend

acceptance of this dissertation.

Robert J. Frey - Dissertation Advisor
Research Professor, Department of Applied Mathematics and Statistics

Jacobus Verbaarschot - Co-Advisor
Professor, Department of Physics and Astronomy

Alfred S. Goldhaber - Chairperson of Defense
Professor, Department of Physics and Astronomy

Dominik Schneble - Committee Member
Associate Professor, Department of Physics and Astronomy

Noah Smith - External Committee Member
Assistant Professor, College of Business

This dissertation is accepted by the Graduate School.

Charles Taber
Dean of the Graduate School.

Abstract of the Dissertation

Applications of Physics and Geometry to Finance

by

Jaehyung Choi

Doctor of Philosophy

in

Physics

Stony Brook University

2014

Market anomalies in finance are the most interesting topics to academics and practitioners. The chances of the systematic arbitrage are not only the counter-examples to the efficient market hypothesis but also the sources of profitable trading strategies to the practitioners. Approaches to finding, predicting, and explaining the anomalies by using ideas from physics and geometry had not been permeated.

In the first part, I develop monthly momentum and weekly contrarian strategies with stock selection rules based on various measures from risk management and analogy of momentum in physics. The

better performance and risk profile are achieved by the alternative strategies implemented in diverse asset classes and markets.

The concept of spontaneous symmetry breaking is suggested for modeling the arbitrage dynamics. In the model, the arbitrage strategy is considered as being in the symmetry breaking phase and the phase transition between arbitrage mode and no-arbitrage mode is triggered by a control parameter. It is also tested with contrarian strategies in various markets.

In the last part, I prove the correspondence between Kähler manifold and information geometry of signal processing models under conditions on transfer function. The various advantages of introducing the Kähler manifold are visited. Several implications to time series models are also given in the Kählerian information geometry.

Contents

List of Figures

List of Tables

Acknowledgements

Every particle in nature interacts with other particles. It is well-known in theoretical physics that the elementary particles exchange 4-momentum and quantum numbers under given gauge coupling constants. This law of nature is not limited to the strings or elementary particles but also applied to the social behavior of human-being. We interact with other people and exchange ideas and experience under given relationships. This is one of the most important and advanced human activities. Although we don't know what the exact model of the interaction is, I believe that we know the effective model at least. In that sense, it is my honor to make the relationship with the great people I've met and learned their precious experience and knowledge while working together.

First of all, I want to express the greatest gratitude to my academic advisor Dr. Robert J. Frey who consistently supported my research and guided me to quantitative finance. I had learned not only knowledge on quantitative finance but also his endeavor and passion toward real world problems. I also would like to thank Dr. Jacobus Verbaarschot, the co-advisor in Physics, who helped me with administrative processes which made this interdisciplinary study possible. I thank Dr. Alfred S. Goldhaber for being the chairperson of the defense committee and providing valuable advice on the dissertation

and presentation. I also thank Dr. Dominik Schneble for serving a committee member. I am also grateful to Dr. Young Shin Aaron Kim, Dr. Andrew P. Mullhaupt, and Dr. Svetlozar T. Rachev for collaboration and valuable advice in research. I am also grateful to Dr. Sangmin Lee at Department of Physics in Seoul National University for his advice and guidance to string theory.

Additionally, I also want to thank Kendal Beer, Joe Haggenmiller, and Greg Frank from Presagium, Pacome Breton, Lucilia Ferraz, Dr. Giri Pemmasani, and Pauline H. Weatherby from FQS Capital and Harbor Financial Management.

I also want to thank my old and new friends and colleagues from Stony Brook Physics, Stony Brook Quantitative Finance Program, and Seoul National University. They are not limited to followings: Yikang Chai, Jay Hyun Cho, Sungwan Cho, Sungtae Cho, Heeje Cho, Gongjun Choi, Sungsoo Choi, Youme Choi, Fangfei Dong, Xu Dong, Jonghyoun Eun, Saebyeok Jeong, Tengjie Jia, Wonseok Kang, Dongkyu Kim, Keunyoung Kim, Mihwa Kim, Kyunghee Koh, Changhyun Koo, Daesu Lee, Siyeon Lee, Sojeong Lee, Un Jung Lee, Yeunhwan Lim, Rong Lin, Soohyung Min, Eungook Moon, Yu Mu, Yookyung Noh, Hyeyun Park, Yein Park, Hyejin Ryu, Taeho Ryu, Barret Shao, Hyunoo Shim, Jaewon Song, Michael Tiano, Angela Tsao, Naoshi Tsuchida, Xiang Xi, Wenjie Xu, Riyu Yu, Xiao Yu, Ke Zhang, Yuzhong Zhang, and Xiaoping Zhou. I also want to inform that my friend, the late E.J. Eun Jung Rhee is always remembered.

Finally, I would like to deeply thank my family. I could not have completed the Ph.D. degree in U.S. and this dissertation without their love, warmth, and support.

Vita and Publication

In the first two years of research in Physics, I wrote two published papers on AdS/CFT correspondence in string theory. During the turmoils of financial crisis in 2008, I was motivated by the complexity of the financial markets and begun to have an interest in finance again since I had invested in stocks while I had worked as a software developer for mandatory military service. After switching to finance, I published one paper and finished several preprints. The list of the papers is following:

1. Jaehyung Choi, Spontaneous symmetry breaking of arbitrage, Physica A 391 (2012) 3206-3218

2. Jaehyung Choi, Physical approach to price momentum and its application to momentum strategy, arXiv:1208.2775 and SSRN 2128946

3. Jaehyung Choi, Sungsoo Choi, Wonseok Kang, Momentum universe shrinkage effect in price momentum, arXiv:1211.6517 and SSRN 2180556

4. Jaehyung Choi, Young Shin Kim, Ivan Mitov, Reward-risk momentum strategies using classical tempered stable distribution, arXiv:1403.6093 and SSRN 2141105

5. Jaehyung Choi, Maximum drawdown, recovery, and momentum, arXiv:1403.8125 and SSRN 2418515

6. Jaehyung Choi, Andrew P. Mullhaupt, Kählerian information geometry for signal processing, arXiv:1404.2006

There exists the overlap between the papers listed above and this dissertation.

Chapter 1

Introduction

After Bachelier's seminal paper [14] and its re-discovery [30], random walk theory has been the most crucial cornerstone in economics and finance. An assumption that price dynamics is governed by stochastic process has become popular and useful in asset valuation theories such as option pricing theory [18, 74] or interest rate models [31, 103, 104]. However, the assumption also claims that prices of financial instruments cannot be predicted exactly because of the nature of Brownian motion. This unpredictable nature of financial markets helps economists to establish a belief that there are no tools to find arbitrage opportunities and to make money systematically in the financial markets. It is also imposed that successful investors are considered nothing but luckier than others. The idea is crystallized in the form of the efficient market hypothesis by Eugene Fama [38] and Paul Samuelson [89]. According to the efficient market hypothesis, financial markets are informationally efficient and this efficiency cannot make participants systematically achieve excessive returns over the market portfolio in the long run. Although there are three slightly different versions of the hypothesis to cover more general cases, what the hypothesis generally emphasizes has not been changed.

However, many market practitioners intrinsically believe an idea that the market could be predictable regardless of their methods used for forecast and investment because it is partially or totally inefficient. The idea is opposite to the belief of proponents for the efficient market hypothesis and it is empirically supported by the fact that there are actual market anomalies which are used as the sources of systematic arbitrage trading. These anomalies and trading strategies include fundamental analysis, technical analysis, pair trading, price momentum, sector momentum, mutual fund arbitrage, volatility arbitrage, merger arbitrage, January effect, and weekend effect etc. The anomalies let market participants create profits by utilizing the trading strategies based on the market inefficiencies. Even if the market is efficient in the long run, practitioners assure that they are able to find opportunities and timings that the market stays in the inefficient phase within very short time intervals. The existence of a shortly inefficient market state is guaranteed by the success of high frequency trading based on quantitative analysis and algorithmic execution in a short time scale automated by computers. In these cases, the arbitrage does not have the traditional definition that non-negative profit is gained almost surely. It can create positive expected return with high probability but there are also downside risks which make the portfolio underperform. This kind of arbitrage is called statistical arbitrage and the arbitrage in this paper means mostly statistical arbitrage.

Not only the practitioners but some academic researchers also have different opinions to the efficient market hypothesis. They have taken two approaches to check the validity of the efficient market hypothesis. On the one hand, the market anomalies of which the practitioners believe the existence

are empirically scrutinized. Some results on the famous market anomalies are reported in academic literatures and seem to be statistically significant while their origins are not clearly revealed yet. For more detailed discussions on the market anomalies, see Singal [93] or Lo and MacKinlay [67]. On the other hand, psychological and behavioral aspects of investors begin to be paid attention in order to find the explanatory theories on the market anomalies [54, 55, 91]. The behavioral economists focus on cognitive biases such as over- and under-reaction to news/events and bounded rationality of investors [29]. They claim that those biases can create the inefficiencies in the market. The cognitive biases lead the investors to group thinking and herding behavior that most of investors think and behave in the similar ways. The good examples of herding are speculative bubbles, their collapses, market crashes, and panics during financial crises.

Among these market anomalies, price momentum has been the most well-known example to both groups. Since Jegadeesh and Titman's seminal paper [53], it has been reported that the prices of financial instruments exhibit the momentum effect that the future price movement tends to keep the same direction along which it has moved during a given past period. It is also realized that the momentum strategy, a long-short portfolio based on the momentum effect, has been a profitable trading strategy in the stock markets of numerous developed and emerging countries during a few decades even after its discovery [87, 88]. In addition to the existence in equity markets, the momentum effect large enough to implement as the trading strategy is also found in other asset classes such as foreign currency exchange [78], bond [11], futures [11, 76], and commodities markets [37].

In spite of its success in profitability over diverse asset classes and markets, its origin has not been fully understood in the frame of traditional mainstream finance. This is why the momentum effect is one of the most famous market anomalies. Attempts to explain the momentum effect with factor analysis have failed [40] and the reason why the momentum effect has persisted over decades still remains mysterious. The Fama-French three factor model is able to explain only parts of the momentum return [40]. The lead-lag effect or auto-/cross-sectional correlation between equities are one of the possible answers to the momentum effect [62, 66]. The sector momentum is another partial interpretation on the anomaly [75]. Additionally, the behavioral aspects of investors such as collective response to financial news and events have broadened the landscape of understanding on the momentum effect [16, 33, 48, 101]. Transaction cost is also considered a factor caused the momentum effect [61]. Unfortunately, none of these explanations are capable of providing the entire framework for explaining why the momentum of price dynamics exists in many financial markets.

Not only demystification on the origins of the price momentum, pursuit on the profitability and implementability of the momentum effect in financial markets also has been interesting to academics and practitioners. For example, although several studies [1, 10, 23, 58, 63] found that the momentum strategies in some Asian markets such as Japanese stock market are not profitable, Asness et al. [11] discovered that the momentum strategy in Japan becomes lucrative, when it is combined with other negatively correlated strategies such as value investment. Not only in several stock markets, the hybrid portfolio of value and momentum also outperforms each of the value and momentum

portfolios across the assets. Their study paid attention to the implementation of the momentum strategy combining with fundamental value investment factors such as book-market (BM) ratio[1] which also has been used to unveil the origins of the momentum effect in Fama-French three factor analysis. In other words, their work can be understood as the construction of the hybrid portfolio to increase the profitability and stability of the portfolios based on the momentum strategy. Moreover, the selection criteria for the hybrid portfolio are considered as the multiple factors related to the momentum returns whether they are positively correlated or negatively correlated. Academically, this observation has the important meaning in the sense that these multiple filters can explain their contributions to the momentum returns. In practical viewpoint, it is definitely the procedure for generating trading profits in the markets.

Another method for improving the profitability of the momentum strategy is introducing various selection rules to the construction of the momentum portfolio. First of all, simple variation on the original momentum selection rule can be made. Moskowitz et al. [76] suggested new trading strategies based on time series momentum which constructs the momentum portfolios by time series regression theory. It is not simply from cumulative return during a lookback period as a sorting variable but from an autoregressive model of order one which can forecast the future returns under given conditions such as the past returns and volatilities. The forecasted return is used as the selection criterion for the time series momentum strategy. The time series momentum

[1]It is also related to price-book (PB) ratio inversely. Many literatures on momentum mostly use BM ratio as a momentum-driven factor and PB ratio also known as PBR is frequently mentioned in fundamental analysis of stocks.

strategy performs very well even during market crisis. It also shares the common component which drives the momentum return with the cross-sectional momentum strategy across many asset classes. This fact imposes that the momentum strategy is improved by the modified cumulative return criterion and there is a possibility to find the better momentum strategies in performance and risk.

Besides only considering the cumulative return, the introduction of alternative proxies for the portfolio selection rules has been also worth getting attention. George and Hwang [43] used 52-week high price[2] as a selection criterion and the momentum portfolio based on the 52-week high price generated stronger returns. Additionally, the tests with the momentum portfolios, which are doubly-sorted by the cumulative return or sector momentum and the 52-week high price, exhibit the superiority of the 52-week high price criterion. The factor analysis also shows that the return from the 52-week high price factor is not only stronger than the traditional or sector momentum factors but also statistically more significant and important in the momentum return modeling. The dominance of the 52-week high momentum criterion is also observed in the various international stock markets [63].

Reward-risk measures are also able to serve as the ranking criteria. Rachev et al. [79] used the reward-risk measures as the sorting criteria for their momentum portfolios instead of the cumulative return over the estimation period. In their work, Value-at-Risk, Sharpe ratio, R-ratio, and STARR ratio were used as alternative ranking rules. In the S&P 500 universe from 1996 to 2003, their momentum portfolios constructed by the reward-risk measures provided

[2]The 52-week high price is the highest price during last 52 weeks, i.e. 1 year.

the better risk-adjusted returns than the traditional momentum strategy. In addition to that, the new momentum portfolios had lower tail indexes for winner and loser baskets. In other words, these momentum strategies based on the reward-risk measures obtained the better risk-adjusted returns with acceptance of the lower tail risk.

Back to physics, the momentum in price dynamics of a financial instrument is also an intriguing phenomenon because the persistent price dynamics and its reversion can be understood in terms of inertia and force. The selection rules of the momentum strategy is directly related to the ways of how to define and measure "physical" momentum in price dynamics of the instrument. When the instrument is considered as a particle in an one-dimensional space, the price momentum is also calculated if mass and velocity are defined. Since the momentum effect exists, it can be concluded that price of an equity has an inertia that makes the price keep their direction of movements until external forces are exerted. In this analogy, the external force corresponds to any exogenous market events and information such as good/bad news, changes in psychology and macroeconomic situation, and imbalance in supply and demand. This idea is also able to explain why the cumulative return based momentum strategy generates the positive expected returns. However, it has been not much attractive to physicists yet. Most of the econophysics community doesn't have been interested in trading strategy and portfolio management so far.

Physicists also have become interested in the characteristics of financial markets as complex systems. Mainly, econophysics and statistical mechanics communities have used their methodologies to analyze the financial markets and several research fields have attracted their interests. In the sense of cor-

relation, the financial markets are interesting objects. Since there are many types of interactions between market building blocks such as markets-markets, instruments-instruments, and investors-investors, correlations and correlation lengths are important. In other directions, speculation and its collapse are always hot topics because they are explained as collective behavior in physics. The analysis on speculation gives some partial answers that speculations have patterns including the resilience effect. Additionally, market crash or collapse of a bubble can be understood by the log-periodic pattern. For more details, see [68, 69, 85, 95, 96] and references therein.

In particular, Sornette introduced the concept of spontaneous symmetry breaking (SSB) of stock price to explain speculation and to resolve the growth stock paradox [94]. He pointed out that economic speculation is understood as price dynamics caused by desirable/undesirable price symmetry. If stocks of a certain company are desirable to hold, investors try to buy the equities at extremely high prices which are the spontaneous symmetry breaking mode. However, when the equities are not desirable any more, the investors do not want to hold it and try to sell them as soon as possible to avoid damages from the downslide of price caused by the situation that nobody in the market prefers the equities. In his paper, the phase transition is induced by riskless interest rate above risk-adjusted dividend growth rate which also expresses herding in the sense that large growth rate gets more attention from investors and it leads to herding. Positive dividend payment breaking the symmetry makes the price positive and this is why the positive price is observed. These are the origins of speculation in economic valuation. The result is also related to the well-known financial valuation theory called the Gordon-Shaprio

formula. His work is important in speculation modeling not only because symmetry breaking concept is applied to finance but also because speculation, its collapse, and market crash are indispensable parts of the market dynamics.

From the mathematical viewpoint, the financial markets are interesting research topics. The stochastic calculus is one of the most popular topics and is heavily used in real world problem solving. However, the application of differential geometry to finance is relatively rare except for information geometry. Since the concept of Riemannian differential geometry was introduced to statistics [52, 80], information geometry has been developed in various directions. The statistical curvature as the differential geometric analogue of information loss and sufficiency was proposed by Efron [36]. The α-dual description of information geometry was found by Amari [2]. Not limited to statistical inference, the information geometry has become popular in many different fields such as information theoretic generalization of Expectation-Maximization algorithm [72] and hidden Markov model [73], interest rate modeling [21], phase transition [51, 106], and string theory [47]. More applications can be found in the literature [9] and references therein.

In particular, the well-known applications of information geometry are time series analysis and signal processing. Ravishanker et al. [81] found the information geometry of autoregressive moving average (ARMA) model in the coordinate system of poles and zeros. It was also extended to fractional integrated ARMA model [82]. Barbaresco [15] also found the information geometry of autoregressive (AR) model in the reflection coefficient coordinates. The Bayesian predictive priors outperforming Jeffreys' prior were information theoretically derived for the AR models by Komaki [59].

The Kähler manifold is one of the most popular research topics in differential geometry. Since the manifold is equipped with good properties such that metric tensors and Levi-Civita connection are derived from Kähler potential and that Ricci tensor is obtained from the determinant of the metric tensor, many implications of the Kähler manifold are found in mathematics and theoretical physics. In that sense, Barbaresco's paper [15] deserves to get attention because it is the paper introducing the Kähler manifold to the information geometry of time series models. Unfortunately, the reason why the Kähler manifold for time series analysis is introduced was not clear in the paper. Moreover, any specific conditions for the Kähler manifold were not given.

Based on these backgrounds, this dissertation concentrates on the applications of physical and geometrical concepts to finance. Several momentum and contrarian portfolios based on reward-risk measure and analogy of physical momentum are constructed. The geometric method is also developed for signal processing and time series model. The structure of the dissertation is as follows. In next chapter, the brief introduction and the portfolio construction based on the momentum strategy are given. The implementation of the momentum/contrarian strategies using maximum drawdown and consecutive recovery is tested in Chapter 3. Reward-risk momentum strategies using classical tempered stable distribution are implemented in Chapter 4. The analogy of physical momentum is applied to the construction of contrarian strategy in Chapter 5. The arbitrage is understood with spontaneous symmetry breaking concept and application to momentum strategy is given in Chapter 6. The correspondence between Kähler manifold and information geometry of signal

processing filter is proven in Chapter 7. In Chapter 8, we make the conclusion of the dissertation.

Chapter 2

Fundamentals of momentum and contrarian strategies

The momentum strategy is one of the famous trading strategies which use market anomalies. It is well-known that the strategy that buys past winners, short-sells past losers in returns, and then holds the portfolio for some periods in the U.S. market enables to provide positive expected returns in intermediate time frames such as 1–12 months [53]. The basic assumption of the strategy is that since price has momentum in its dynamics, it tends to move along the direction it has moved. Based on the assumption, the financial instruments which have shown good performance in the past are highly probable to gain profits in the future. Opposite to winners, it is likely that losers in the past would underperform the benchmark in the monthly time frame.

Over other trading strategies such as pair trading or merger arbitrage strategies, it is advantageous that the momentum strategy is able to be exploited at any time and in any markets. Pair trading is utilized only when the correlation of two instruments weakens and when investors can find it. Merger arbitrage is able to make benefits if M&A rumors or news begin to be spread

in the market and if there is a price gap between actual and buy prices. When using these strategies, the investors become relatively passive to market conditions and events. However, in the case of the momentum strategy, if they look back at the price history, market participants make use of momentum strategy and the trading frequency is up to their time frames from high frequency trading to long-term investment. In addition to that, unlike merger arbitrage which is possible only in equity markets, momentum strategy can be applied to various asset markets including local equity, global index/equity [87, 88], currency [78], commodity [37], future [11, 76], and bond markets [11].

The most important variables of the momentum strategy are the length of the lookback (or estimation) period J, length of the holding period K, and sorting criterion ψ. The traditional momentum strategy uses the cumulative return during the lookback period as a ranking criterion, i.e. a triplet of the traditional momentum strategy is $(J, K, \psi = p^{(0)})$ [53]. On the reference day ($t = 0$), the cumulative returns of all instruments in the market universe during the periods from $t = -J$ to $t = -1$ are calculated. After sorting the instruments in the order of the ascending criterion, numbers of ranking groups are constructed and each of the ranking groups has the same number of the instruments. As an instance, if there are 200 equities and we consider 10 groups, each of sorted ranking groups has 20 equities as group constituents. Following the convention of Jegadeesh and Titman [53], the loser group who has the worst performers in the market is named as R1 and the winner group with the best performers is the last one, R10. And then the momentum portfolio is constructed by buying the winners and short-selling the losers with the same size of positions in cash in order to make the composite portfolio

dollar-neutral. For the winner and loser portfolios, each group member is equally weighted in the group in which it is. The constructed momentum portfolio is held until the end of the holding period ($t = K$). On the last day of the holding period ($t = K$), the momentum portfolio is liquidated by selling the winner group off and buying the loser group back.

On the first day of each unit period, the momentum portfolio is constructed as explained in the previous paragraph. For examples, a weekly momentum portfolio is selected in every Monday unless it is not a holiday. Monthly portfolios are formulated on the first business day in every month. For multiple-period holding strategies, there exists overlapping period between two different strategies. The reasons of this construction are followings. First of all, the momentum return from this construction is not dependent with the starting point of the strategy formation. For example, when we implement the 12-month lookback and 12-month holding momentum strategy, construction of the portfolio occurs at the beginning of each year. Since the return results are always interfered by the seasonal effects such as January effect or others related to business cycle and taxation, it is difficult to discern the momentum effect from the seasonal effects. Second, the portfolios from overlapped periods can generate the larger numbers of return samples to fortify the statistical significance. Since the dataset here only has twelve years of historical data comparing with other studies which uses much longer time periods as datasets, its statistical significance could be lowered by the smaller size of our samples if we use the non-overlapped portfolios. Third, Jegadeesh and Titman [53] reported that there were not big differences between the returns by the overlapped and non-overlapped portfolios. Finally, the portfolio construction

here can be considered as diversification which helps to mitigate large return fluctuation of the momentum portfolio. For example, in the case of 12-month holding strategies, we have twelve different portfolios at a given moment and it is definitely diversification of the portfolio. Based on these reasons, it is more sensible that the overlapping portfolios are used in our case.

When we buy the winner and loser portfolios which provide expected returns for those groups of r_W and r_L respectively, the return by the momentum portfolio r_Π is simply $r_\Pi = r_W - r_L$ because we short-sell the losers in the portfolio. When we implement the trading strategy in the real financial markets, a transaction cost including brokerage commission and tax is always important because they actually erode the trading profits. The implemented momentum return or transaction-cost-adjusted return r_I is

$$\begin{aligned} r_I &= r_\Pi - c \\ &= (r_W - r_L) - (c_W + c_L) \end{aligned}$$

where c_W and c_L are the transaction costs for winner and loser group, respectively. In general, c_L is greater than c_W because the short-selling is usually much more difficult than buying. Since the transaction cost is an one-time charge, its effect on the implemented return per unit period becomes smaller as the holding period is lengthened.

When the expected return of the momentum portfolio for a given (J, K, ψ) strategy is negative, the strategy can become profitable by simply switching to the contrarian strategy $(J, K, \psi^\dagger)$ that buys the past loser group and short-sells the past winner group, exactly the opposite position to the momentum

portfolio. Contrasting to the momentum strategy following the price trend, the contrarian strategy is based on the belief that there is the reversion of price dynamics. If equities have performed well during the past few periods, investors try to sell those stocks to put the profits into their pockets. The investors who bought those equities long time ago are able to make large enough profits even when the price recently has gone slightly downward. However, buyers who recently purchased the equities might not have enough margins yet from their inventories and want not to lose money from the current downward movement because of risk aversion. The only option those investors can take is just selling their holdings off. This herding behavior makes the reversion of price and it is probable to make profits from short-selling if a smarter investor knows when it would be. For the opposite case, it is also possible to buy the past losers to get advantages of using the herding because the losers are temporarily undershot by investors' massive selling force and the equities tend to recover their intrinsic values. On the way of price recovery, the short-sellers need to buy back what they sold in the past in order to protect their accounts and the serial buy-back can boost the price dynamics to the upward direction which also causes feedback that causes consequential massive buy-backs by other short-sellers. How the initial anomaly can be amplified and be grown is modeled in Shleifer and Vishny [92].

The momentum and contrarian strategies look contradictory to each other but they have only the different time horizons in which each of strategies works well. Usually, in three to twelve months scale, the equity follows the trends [53] but the reversal effect is dominant at the longer and shorter scales than the monthly scale [35, 66]. For the contrarian strategy, the portfolio return

$r_{\Pi^\dagger}$ is given by

$$r_{\Pi^\dagger} = r_L - r_W = -r_\Pi.$$

The transaction cost adjusted return r_I for the contrarian strategy is

$$\begin{aligned} r_I &= r_{\Pi^\dagger} - c \\ &= (r_L - r_W) - (c_W + c_L). \end{aligned}$$

When implementability of a given strategy in the real markets is the main concern, we need to focus on whether or not it is possible to take actual profits from the strategy among the momentum and contrarian strategies. In this sense, the profitability of the strategy with absolute (implemented) return $\tilde{r}_I$ can be measured by

$$\tilde{r}_I = |r_W - r_L| - (c_W + c_L)$$

and tells whether the potential trading profit can exceed the barrier of the transaction cost. The actual positive return from the momentum/contrarian trading strategies can be taken into the pocket when $\tilde{r}_I$ is positive. However, the transaction cost is not considered because the out/under-perfomance is our main concern.

As mentioned above, the method for measuring the price momentum is the momentum strategy with the physical momentum as a ranking criterion. There are total eleven types of candidates for physical momentum including the original cumulative return momentum. On the reference day ($t = 0$), each

physical momentum for equities over the estimation periods is calculated and is used for sorting the equities. The ranking for each criterion constructs the momentum portfolios. After holding the portfolio during the given period, it is liquidated to get the momentum profit. The positive implemented returns and Sharpe ratios from implemented return exhibit the robustness of the physical momentum strategies. If their returns beat that of the traditional momentum strategy, it is obvious that the physical momentum definition really has a merit to introduce and there is a practical reason to use the momentum strategies based on the physical momentum as an arbitrage strategy.

For the lookback period, some stocks which don't have enough trading dates are ignored from the analysis. In general, this case happens to companies which are enlisted to the market universe amid of the lookback period. If an equity is traded on only one day during the estimation period, it is neglected from our consideration for the momentum strategy universes because it is impossible to calculate alternative ranking criteria for these stocks. Since all possible candidates for the alternative momentum need to be compared with other criteria over the same sample, it is obvious not to consider these equities with only one trading day in the estimation period. The companies delisted amid of the holding periods don't cause the same problem because only the lookback return is important in sorting the equities and constructing the momentum portfolios. In this case, the returns for the delisted companies are calculated from the prices on the first and last trading days in the holding periods.

As mentioned before, the reason why the momentum strategy generates positive expected return has attracted the interest of researchers but it is

not clearly revealed yet. The sector momentum is considered one of possible explanations [75]. A behavioral approach to momentum also can give more explanations such as under-reaction [48, 101] or over-reaction [33] of market participants to news or psychology [16]. It is ambiguous whether the momentum effect comes from either which of them or from a combination of these possible explanations. However, this dissertation focuses on how to use the strategy based on symmetry breaking rather than what makes markets inefficient.

Chapter 3

Maximum drawdown, recovery, and momentum

One of the most popular risk measures is maximum drawdown. It is defined as the worst cumulative decline from a peak in a given period. The maximum drawdown is also used in the definitions of the Calmar ratio and Sterling ratio in order to assess the performance and risk of mutual funds and hedge funds. Several advantages of the maximum drawdown over VaR and CVaR are followings. First of all, it is more insightful than other risk measures. When two historical price charts are given, it is more straightforward to find which asset has the smaller maximum drawdown. Additionally, it is easier to calculate the drawdown directly from time series. Moreover, there is no model dependency.

In this chapter, we introduce multiple composite ranking criteria stemmed from the maximum drawdown and successive recovery in order to construct alternative momentum/contrarian-style portfolios. The monthly momentum and weekly contrarian strategies based on the alternative stock selection rules are implemented in U.S. and South Korea stock markets. The alternative

strategies outperform the traditional cumulative return based strategies in performance and risk. In particular, the drawdown measures provide the better trend-following strategies in monthly scale and the recovery criteria work well with the weekly strategies. The outperformance is also found in the Fama-French three-factor model. The structure of the paper is following. In the next section, the new ranking rules based on the maximum drawdown and sequential recovery are defined. In section 3.2, datasets and methodology are introduced. The performance and risk profile of the alternative portfolios are found in section 3.3. The factor analysis is given in section 3.4. We close the chapter with conclusion in section 3.5.

3.1 Construction of stock selection rules

As mentioned before, the maximum drawdown is the worst successive loss among declines from peaks to troughs during a given period. It is defined by

$$\text{MDD} = \max_{\tau \in (0,T)} \left(\max_{t \in (0,\tau)} \big(P(t) - P(\tau) \big) \right)$$

where $P(t)$ is the log-price at time t. The expression can be represented in terms of return

$$\text{MDD} = - \min_{\tau \in (0,T)} \left(\min_{t \in (0,\tau)} R(t,\tau) \right)$$

where $R(t,\tau)$ is the log-return between t and τ. The maximum drawdown is regarded as the worst-case scenario to an investor who starts his/her invest-

ment at any moment in that period. It is obvious for the investor to prefer the lower maximum drawdown to the higher one.

The maximum drawdown is closely related to the price momentum. In particular, the maximum drawdown is associated with the direction of the price momentum. In the case of positive momentum, it is a part of mean-reversion process if the size of the maximum drawdown is small. Additionally, if it is large enough, the maximum drawdown is more likely to break the upward trend and generate new downward trend-following stage. Meanwhile, it is one of the largest components for the downside momentum. The larger maximum drawdown would be much preferred for short position.

The successive recovery to the maximum drawdown is defined by

$$\mathrm{R} = R(t^*, T)$$

where t^* is the moment for the end of the maximum drawdown formation. It encodes how much loss from the worst decline is recovered by the short-term reversal. Similar to the maximum drawdown, it is also helpful to understanding the price momentum. When an asset price is on the upward trend, it is regarded as the support to the original trend. Meanwhile, in downside momentum, the recovery is a reversal to the overall trend. It is obvious that an asset with stronger recovery is favored than an asset with weaker recovery.

In these spirits, the maximum drawdown and consecutive recovery are indispensable in the processes of analyzing and detecting signals for price trend. It is obvious that these measures should be incorporated into the momentum analysis and momentum ranking criteria considered these measures need to

be considered in portfolio construction. It is possible to construct new composite selection rules stemming from the maximum drawdown and recovery. For example, even when two assets have the same cumulative return, one with the larger maximum drawdown can be penalized in the ranking measure. In other case, assets with stronger short-term mean-reversion to the maximum drawdowns can be preferred in the alternative ranking system.

Before developing alternative selection rules, we need to take a closer look on the cumulative return. A given estimation period is chronologically decomposed into three periods. The first period is the peak formulation phase from the beginning of the estimation period to the peak before the downfall. The next stage is the period for the creation of the maximum drawdown. The last stage is the recovery period from the trough associated with the maximum drawdown to the end of the estimation period. The above decomposition on the cumulative return C is represented with the returns in the three different phases:

$$\begin{aligned} \mathrm{C} &= R_I + R_{II} + R_{III} \\ &= \mathrm{PP} - \mathrm{MDD} + \mathrm{R} \end{aligned}$$

where PP is the log-return during the pre-peak period.

With the decomposition, it is possible to construct hybrid indicators using the maximum drawdown and recovery. Taking weighted average with more weights on certain specific period is one way of the construction. Many possible combinations with the maximum drawdown and consecutive recovery are given in Table 3.1.

Table 3.1: Description on alternative selection rules using maximum drawdown and recovery

Portfolio name	Criterion	Weights on R_t
C	Cumulative return	(1,1,1)
M	MDD	(0,1,0)
R	Recovery	(0,0,1)
RM	Recovery–MDD	(0,1,1)
CM	Cumulative return-MDD	(1,2,1)
CR	Cumulative return+Recovery	(1,1,2)
CMR	Cumulative return–MDD+Recovery	(1,2,2)

The C strategy is the benchmark strategy. It is the traditional momentum/contrarian strategy that employs the cumulative return as the ranking criterion. The M and R portfolios are constructed by using the maximum drawdown and recovery as the ranking rule, respectively. More complicated selection rules are stemmed from weighted averages on certain periods. The RM strategy utilizes the difference between the recovery and maximum drawdown. It encodes how much losses are recovered by the short-term reversion. The CM strategy not only considers the cumulative return and but also pays attention to the period of the maximum drawdown. It is a penalty to the assets with the large drawdowns. In the similar way, it is possible to assign the weights on only the recovery period or both of the maximum drawdown and recovery for the CR and CMR strategies, respectively.

3.2 Dataset and methodology

3.2.1 Dataset

The datasets for this study consist of the KOSPI 200 universe, SPDR U.S. sector ETFs, and S&P 500 universe.

South Korea equity market: KOSPI 200

The KOSPI 200 is a stock benchmark index that is the value-weighted and sector-diversified index with 200 stocks in South Korea stock markets. Historical price information and component-roster are downloaded from Korea Exchange. The period from January 2003 to December 2012 is considered.

U. S. equity market: SPDR sector ETFs

Sector ETFs are selected for simulating sector momentum with the alternative stock selection rules. In particular, the SPDR U.S. sector ETFs are chosen because it is the collection of ETF products for which the equal length of price history is available. The time span covers from January 1999 to December 2012. The SPDR U.S. sector ETFs consist of XLB (Materials), XLE (Energy), XLF (Financial), XLI (Industrial), XLK (Technology), XLP (Consumer Staples), XLU (Utilities), XLV (Health Care), and XLY (Consumer Discretionary).

U. S. equity market: S&P 500

The price information and roster of the S&P 500 historical components are collected from the Bloomberg. The covered time horizon is from January 1999

to December 2012.

3.2.2 Methodology

The basic methodology for portfolios construction is the momentum-style (or contrarian) portfolios given in Jegadeesh and Titman [53]. Based on given selection rules during 6 months (weeks) of estimation period, assets in market universes are sorted in ascending order. In this study, most criteria will be used in increasing order except for the maximum drawdown. Then several ranking baskets are fomulated. In the cases of the S&P 500 and KOSPI 200 universes, numbers of groups are 10 and three baskets are formed for U.S. sector ETFs. The group 1 is for losers that exhibit the worst ranking scores and the last group is for the best performers in the selection rules. Each group is constructed as an equal-weighted portfolio. The winner group is at long (short) position and the loser group is at short (long) position. After 6 months (weeks) of the holding period, each basket is liquidated. The portfolio is constructed at the beginning of every month, i.e. it is the overlapping portfolio.

The risk measures for the portfolio performance are calculated from the daily time series of the overlapping portfolio. The risk model for VaR, CVaR, and Sharpe ratio is the ARMA(1,1)-GARCH(1,1) model with classical tempered stable (CTS) innovation. This model is suggested by Kim et al. [57] and the same model is also used for momentum portfolio construction [26]. For more information, consult with Kim et al. [57] and references therein.

3.3 Results

3.3.1 South Korea equity market: KOSPI 200

Weekly results

In Table 3.2, the recovery related strategies outperform the traditional mean-reversion strategy obtaining weekly 0.073% under the volatility of 2.841%. In particular, the best performer is the recovery portfolio with the weekly returns of 0.146%, two-times larger than the original contrarian strategy, and the excellent performance is achieved under much smaller standard deviation of 1.757%, almost 1.1% lower than the C strategy. The CR and CMR strategies also obtain the better performance under smaller fluctuation. The portfolio returns are weekly 0.086% and 0.078% under the standard deviations of 2.665% and 2.865%. Meanwhile, the maximum drawdown strategies such as the M, CM, and RM strategies underperform the benchmark strategy in the weekly scale.

The outperformance of the R, CR, and CMR strategies are based on the strong reversal of each ranking basket. First of all, the loser groups of every alternative contrarian strategies perform as well as the loser in the mean-reversion portfolio. The performance of the long positions is in the range from 0.241%–0.314% and the return fluctuations are smaller or comparable with the loser basket in the benchmark strategy. In particular, the loser group in the recovery measure exhibits not only the best performance but also the lowest deviation measure among all the loser baskets. Additionally, the winner basket of the R, CR, and CMR portfolios perform poorer than other portfolios

Table 3.2: Summary statistics and risk measures of weekly 6/6 contrarian portfolios in South Korea KOSPI 200

Criterion	Portfolio	Summary statistics				Risk measures				
		Mean	Std. Dev.	Skewness	Kurtosis	Fin. Wealth	Sharpe	$VaR_{95\%}$	$CVaR_{95\%}$	MDD
C	Winner (W)	0.1961	3.8032	-1.2946	6.7809	1.0119	0.0685	1.7519	2.5310	67.27
	Loser (L)	0.2692	4.3576	-1.1792	7.6903	1.3889	0.0813	1.6808	2.5153	63.00
	L – W	0.0731	2.8417	0.1864	1.8644	0.3770	0.0148	1.6864	2.4245	33.66
M	Winner (W)	0.2583	2.5125	-1.4858	7.4210	1.3330	0.0842	1.1302	1.6413	50.11
	Loser (L)	0.2574	4.7328	-1.1544	7.0878	1.3281	0.0681	1.9362	2.7975	67.43
	L – W	-0.0010	3.1694	-0.2546	2.7173	-0.0049	0.0140	1.7974	2.5476	60.08
R	Winner (W)	0.1688	4.0728	-1.5786	9.1786	0.8712	0.0603	1.6462	2.2375	72.17
	Loser (L)	0.3143	3.3376	-1.4649	9.7503	1.6220	0.1003	1.2523	1.8700	51.78
	L – W	0.1455	1.7567	0.0996	1.8461	0.7508	0.0465	1.1494	1.3907	30.09
RM	Winner (W)	0.2279	3.4532	-1.5951	8.4947	1.1762	0.0753	1.5765	2.1820	65.22
	Loser (L)	0.2575	4.5200	-1.0493	6.8847	1.3286	0.0730	1.7822	2.6200	63.92
	L – W	0.0295	2.7489	0.3269	2.2130	0.1524	0.0131	1.6210	2.3542	36.66
CM	Winner (W)	0.2258	3.4946	-1.2486	5.8310	1.1654	0.0737	1.6513	2.4019	61.34
	Loser (L)	0.2594	4.5592	-1.1455	7.4612	1.3384	0.0780	1.8532	2.7334	64.35
	L – W	0.0335	3.0442	0.1036	2.4027	0.1730	0.0165	1.8081	2.6182	41.05
CR	Winner (W)	0.1551	3.9277	-1.4040	7.7612	0.8003	0.0611	1.7428	2.4508	70.98
	Loser (L)	0.2408	4.2109	-1.1877	8.4200	1.2424	0.0808	1.6678	2.4696	63.16
	L – W	0.0857	2.6649	0.3887	1.4694	0.4421	0.0163	1.6105	2.2866	33.30
CMR	Winner (W)	0.1829	3.6266	-1.3528	6.8595	0.9439	0.0662	1.6819	2.3703	66.13
	Loser (L)	0.2609	4.4422	-1.1052	7.4757	1.3461	0.0778	1.7475	2.5888	63.42
	L – W	0.0779	2.8645	0.2827	2.0772	0.4022	0.0165	1.7426	2.5012	33.34

including the cumulative return contrarian portfolio.

According to Table 3.2, the outperformance of the recovery portfolios such as the R and CR portfolios is achieved by taking less risks. The portfolios are less riskier in every risk measures than the other portfolios by the alternative ranking rules including the cumulative return. The R portfolio provides the largest Sharpe ratio and the CR strategy is one of the top 4 in Sharpe ratio. The lowest 95% VaRs and CVaRs are featured by the R and CR portfolios. In particular, the R strategy exhibits 1.149% daily VaR and 1.391% daily CVaR, the smallest risk measures. An interesting caveat is that the CVaR is much decreased than the VaR. This indicates the existence of the much thinner downside tail in the R portfolio performance. The maximum drawdowns of these two portfolios are also lower than all other strategies.

The each ranking basket in the R and CR portfolios is also less riskier than other competitive ranking groups. The winner and loser groups of these two portfolios exhibit lower VaRs and CVaRs. The loser in the recovery criterion achieves the lowest VaR and CVaR with 1.252% and 1.870%, respectively. The Sharpe ratios of the loser groups are the top 2 largest ones among the other alternative and benchmark strategies. The maximum drawdown of the recovery loser is also smaller than the long position in the traditional contrarian portfolio. For winner groups, the tendency is slightly weaker. Although the short baskets are less riskier in 95% VaR and CVaR, the Sharpe ratios and maximum drawdowns are worse than those of the winner and loser in the C criterion. However, the riskier short position is more attractive for the profitability of the entire portfolio.

Monthly results

In Table 3.3, it is found that the maximum drawdown criterion and related stock selection rules provide the alternative momentum strategies outperforming the traditional momentum strategy. The best strategy is the momentum portfolio by the composite rule of cumulative return and maximum drawdown. The monthly average return of 1.433% with the volatility of 7.036% is obtained by the CM portfolio while the cumulative return criterion provides the trend-following strategy with the monthly return of 1.331% and the standard deviation of 6.826%. The CMR and RM strategies are the next best performers with the monthly returns of 1.311% and 1.280% and the standard deviations of 6.729% and 6.241%, respectively. The performance of these portfolios are slightly worse but the volatility levels are also lower than that of the momentum strategy. The CR and M strategies also perform well although the strategies underperform the benchmark strategy. Meanwhile, the recovery strategy obtains the worst performance in monthly scale.

The momentum strategies associated with the maximum drawdown exhibit strong momentum in each ranking group basket. The winner basket of the CM strategy achieves monthly 1.701%, the strongest upside momentum among all long positions including the cumulative return winner. Additionally, the return volatility of the position is only 8.062%, almost 10% smaller than that of the momentum winner. The performance of the CMR winner is as good as the benchmark winner and the fluctuation is relatively lower. In addition to that, the loser groups of the M, RM, CM, and CMR strategies underperform the traditional momentum loser. The short basket of the CM strategy, one of the

Table 3.3: Summary statistics and risk measures of monthly 6/6 momentum portfolios in South Korea KOSPI 200

Criterion	Portfolio	Summary statistics					Risk measures			
		Mean	Std. Dev.	Skewness	Kurtosis	Fin. Wealth	Sharpe	$VaR_{95\%}$	$CVaR_{95\%}$	MDD
C	Winner (W)	1.6292	8.7334	-0.4543	2.2045	1.8573	0.0775	1.7825	2.6373	64.48
	Loser (L)	0.2987	8.9425	-0.8357	5.5529	0.3405	0.0641	1.9006	2.6312	65.46
	W – L	1.3305	6.8258	0.0217	0.6760	1.5167	0.0545	2.5163	3.2597	59.87
M	Winner (W)	1.3075	5.5705	-0.5793	3.5011	1.4905	0.0885	1.1644	1.6563	46.13
	Loser (L)	0.2841	9.5852	-0.8019	4.3932	0.3239	0.0591	2.0981	2.8616	67.36
	W – L	1.0234	6.5769	-0.3515	1.0627	1.1667	0.0322	2.2287	2.7281	54.58
R	Winner (W)	1.3299	8.7707	-0.7226	3.1472	1.5161	0.0818	1.8927	2.8033	69.11
	Loser (L)	0.9559	6.7652	-1.3312	6.0955	1.0898	0.0936	1.2107	1.7995	55.58
	W – L	0.3740	4.0823	0.9101	2.2150	0.4264	0.0127	1.6553	2.3164	37.97
RM	Winner (W)	1.5416	7.5704	-0.2469	1.5551	1.7574	0.0828	1.7765	2.6339	58.39
	Loser (L)	0.2613	9.3531	-0.7718	5.4615	0.2978	0.0613	2.0245	2.8005	67.25
	W – L	1.2803	6.2406	-0.3327	1.5967	1.4596	0.0569	2.5490	3.2939	52.06
CM	Winner (W)	1.7005	8.0623	-0.3032	1.7154	1.9386	0.0785	1.6763	2.4660	59.37
	Loser (L)	0.2676	9.1117	-0.8241	5.4601	0.3051	0.0635	1.9590	2.6871	66.38
	W – L	1.4330	7.0357	-0.1969	0.5758	1.6336	0.0611	2.4930	3.1834	59.16
CR	Winner (W)	1.5449	8.8493	-0.5423	2.4918	1.7611	0.0778	1.8826	2.7816	67.88
	Loser (L)	0.4421	8.6716	-0.8298	6.2348	0.5040	0.0643	1.7340	2.4558	63.74
	W – L	1.1028	6.5956	0.2097	0.9879	1.2571	0.0404	2.3883	3.1240	62.37
CMR	Winner (W)	1.5557	8.2241	-0.3319	1.7862	1.7735	0.0754	1.8104	2.6763	62.70
	Loser (L)	0.2451	9.1274	-0.8155	5.5803	0.2794	0.0625	1.9074	2.6450	66.39
	W – L	1.3106	6.7290	-0.2114	0.7663	1.4941	0.0575	2.5282	3.2651	58.32

3 worst performers in the loser groups, underperforms the loser group in the cumulative return. The short baskets in the RM and CMR strategies also show the stronger downside momentum than the loser group of the traditional momentum strategy.

The risk profiles for the momentum portfolios in Table 3.3 indicate that the portfolios ranked by the maximum drawdown related selection rules are less riskier in many reward-risk measures than the benchmark. For example, most of the alternative momentum strategies exhibit lower 95% VaR and CVaR levels. Even for RM and CMR portfolios, the difference in risk measure is just a few basis points. Additionally, lower maximum drawdown is featured by the alternative portfolios except for the CR portfolio. Moreover, higher Sharpe ratios than the C-strategy are achieved by the CM, CMR, and RM strategies. In overall, choosing these composite ranking criteria related to the maximum drawdown is better at risk management.

Each ranking group in the drawdown strategies exhibits better risk characteristics. Lower 95% VaR, CVaR, and maximum drawdown levels are achieved by the winner groups comparing with the long basket of the momentum portfolios. Additionally, the Sharpe ratios of the long baskets are larger than that of the momentum winner group. The better reward-risk and smaller risk measures are favorable for the long position. Meanwhile, the loser groups are under greater exposure to the risk with higher 95% VaR, 95% CVaR, and maximum drawdown. The Sharpe ratios for the short baskets are weaker than the momentum loser. For short position, the larger risk of losing money is more desirable.

3.3.2 U.S. equity market: SPDR sector ETFs

Weekly results

As shown in Table 3.4, the strong performance of the RM, CR, and CMR contrarian portfolios is obtained in the ETF universe. In particular, the CR strategy is the best performer among all the other contrarian strategies and is the only alternative strategy that outperforms the benchmark portfolio. The portfolio with the weekly performance of 0.094% and the volatility of 1.648% is not only greater but also less volatile than the cumulative return portfolio. The other recovery portfolios such as the CMR and RM strategies show good performance but the fluctuations of the weekly returns are larger than the traditional contrarian portfolio. Although the performance of the R strategy is not the best result, its standard deviation is at the lowest level, 1.217%.

The outperformance of the CR portfolio is based on the strong reversal in its ranking groups. The similar size of the reversion is achieved by every loser group in the alternative measures. In particular, the loser basket in the CR portfolio exhibits the strongest turn-around of 0.127%. Additionally, the volatility is the second lowest one among all the alternative ranking rules. Its strong mean-reversion is not limited to the loser group. The average weekly return of the CR winner is 0.034%, the poorest performance among all the short baskets including the benchmark. Moreover, the standard deviation of the performance is at one of the highest levels. The combination of the poorer performance and larger volatility in the CR short position makes the entire portfolio more likely to get profits.

According to Table 3.4, taking less risk leads to the outperformance of the

Table 3.4: Summary statistics and risk measures of weekly 6/6 contrarian portfolios in U.S. sector ETF

Criterion	Portfolio	Summary statistics					Risk measures			
		Mean	Std. Dev.	Skewness	Kurtosis	Fin. Wealth	Sharpe	$VaR_{95\%}$	$CVaR_{95\%}$	MDD
C	Winner (W)	0.0397	2.5424	-1.0070	5.6347	0.2876	0.0477	1.1783	1.4955	53.08
	Loser (L)	0.1274	2.9360	-0.4862	7.3610	0.9226	0.0408	1.2427	1.5333	60.12
	L – W	0.0877	1.7279	0.6594	7.4927	0.6350	0.0001	0.4469	0.6055	29.74
M	Winner (W)	0.0615	2.1450	-1.2742	7.7993	0.4454	0.0529	1.0917	1.4038	44.84
	Loser (L)	0.1116	3.3237	-0.3631	5.7091	0.8083	0.0441	1.3652	1.7236	63.96
	L – W	0.0501	2.1195	0.3290	5.5900	0.3629	0.0210	0.5570	0.7526	49.03
R	Winner (W)	0.0654	2.8563	-0.8552	6.0406	0.4735	0.0460	1.1853	1.5648	61.57
	Loser (L)	0.1133	2.5224	-0.6937	6.5736	0.8206	0.0537	1.2192	1.4816	46.81
	L – W	0.0479	1.2174	0.5730	3.7388	0.3470	0.0000	0.3403	0.4426	17.91
RM	Winner (W)	0.0467	2.3858	-1.0909	6.1818	0.3384	0.0511	1.1193	1.4491	52.07
	Loser (L)	0.1158	3.1071	-0.3805	6.5959	0.8382	0.0408	1.2903	1.5781	60.78
	L – W	0.0690	1.7563	0.7227	9.7128	0.4998	0.0000	0.4724	0.6073	33.84
CM	Winner (W)	0.0537	2.3661	-1.0646	5.4095	0.3891	0.0506	1.1356	1.4503	48.73
	Loser (L)	0.1197	3.1199	-0.4035	6.9313	0.8663	0.0399	1.2742	1.5995	63.77
	L – W	0.0659	1.8692	0.6222	8.1724	0.4772	0.0068	0.4846	0.6459	42.43
CR	Winner (W)	0.0335	2.6260	-1.0225	5.6197	0.2428	0.0458	1.1733	1.5236	57.61
	Loser (L)	0.1270	2.8685	-0.4025	7.3544	0.9198	0.0408	1.3345	1.6153	56.89
	L – W	0.0935	1.6477	0.7112	6.8603	0.6770	0.0000	0.4504	0.5750	20.46
CMR	Winner (W)	0.0463	2.4735	-0.9579	5.0344	0.3353	0.0496	1.1432	1.4590	53.24
	Loser (L)	0.1208	3.0348	-0.3624	6.7464	0.8744	0.0398	1.3061	1.5975	61.50
	L – W	0.0745	1.7891	0.7205	8.0367	0.5392	0.0000	0.5092	0.6519	32.00

CR strategy. The 95% VaR, CVaR, maximum drawdown of the strategy are 0.450%, 0.575%, and 20.46%, the second lowest VaR, CVaR, and maximum drawdown levels among the alternative portfolios. The CR portfolio also exhibit lower CVaR and maximum drawdown levels and the comparable size of VaR with the traditional contrarian portfolio. An interesting caveat is that the recovery portfolio exhibits the best risk profiles in every risk measures. Its 95% VaR, CVaR, and maximum drawdown are 0.340%, 0.443%, and 17.91% that are much lower than the risk measures of the traditional mean-reversion strategy. Meanwhile, the poorer risk measures are obtained by the other portfolios of which the construction rules are associated with the maximum drawdown.

Similar to the entire portfolio level, the better risk management in each ranking basket is provided by considering the recovery measure in the stock selection rules. In particular, the recovery criterion has the best loser group both in performance and risk. All the risk measures of the recovery loser are lower than any other loser groups of the alternative strategies including the benchmark strategy. Moreover, the largest Shape ratio among the loser baskets is achieved by the loser in the recovery criterion. Opposite to the loser basket, the winner group in the recovery portfolio exhibits the worst risk measures and Sharpe ratio. Since the winner basket in the contrarian strategy is actually going short, the risky assets are helpful to gain the profit for the overall portfolio.

Monthly results

The alternative momentum portfolios constructed by the maximum drawdown related criteria outperform the cumulative momentum strategy in the SPDR

U.S. sector ETFs universe. According to the summary statistics given in Table 3.5, the monthly performance of 0.172% under the standard deviation of 3.565% is achieved by the CMR strategy, the best performer among all criteria while the traditional momentum strategy generates monthly 0.117% under the volatility of 3.552%. The portfolio return is increased by almost 50% and the standard deviation is changed less than 1%. The RM and CM strategies with monthly returns of 0.138% and 0.121% are also followed by the C strategy. The both strategies are also less volatile than the cumulative return momentum strategy. The performance by the R and CR strategies are not only as good as the C strategy but also less volatile.

Regardless of criterion, the outperformance of the alternative portfolios is based on the strong momentum in each ranking basket. The winner and loser groups in the alternative portfolios consistently perform as well as the ranking groups of the traditional momentum strategy. In particular, the strongest momentum in the baskets is achieved by the CMR strategy: the long basket outperforms and the short basket underperforms that of the benchmark strategy. The winner and loser groups in the CM and RM portfolios are also under the strong trend-following phenomena. Other recovery related ranking rules also exhibit the same pattern. For example, the R and CR criteria also provide the strong momentum at the ranking group level.

In Table 3.5, the alternative portfolios are less riskier than the traditional momentum portfolio. First of all, the maximum drawdown of every strategy is lower or comparable with the benchmark case. Additionally, the 95% VaR and CVaR levels indicate that the recovery related selection rules are good at handling the severe losses. In particular, the RM portfolio takes low risk

Table 3.5: Summary statistics and risk measures of monthly 6/6 momentum portfolios in U.S. sector ETF

Criterion	Portfolio	Summary statistics				Risk measures				
		Mean	Std. Dev.	Skewness	Kurtosis	Fin. Wealth	Sharpe	$VaR_{95\%}$	$CVaR_{95\%}$	MDD
C	Winner (W)	0.3742	4.5444	-0.7738	1.3970	0.6062	0.0518	1.3639	1.7161	48.23
	Loser (L)	0.2568	5.3434	-0.6718	1.6714	0.4160	0.0373	1.4811	1.7675	65.48
	W – L	0.1174	3.5522	-0.1950	1.6853	0.1903	0.0001	0.5529	0.7246	39.55
M	Winner (W)	0.2820	3.6813	-0.8993	2.3732	0.4569	0.0540	1.2180	1.5566	44.57
	Loser (L)	0.1869	5.7772	-0.4749	0.9533	0.3027	0.0361	1.6286	1.9842	64.60
	W – L	0.0951	3.5423	-0.1730	1.7801	0.1541	-0.0025	0.7813	1.0325	38.14
R	Winner (W)	0.3616	5.0347	-0.7006	1.7317	0.5859	0.0491	1.5282	1.9039	59.12
	Loser (L)	0.2463	4.3456	-0.6546	1.3965	0.3990	0.0452	1.3462	1.6252	49.28
	W – L	0.1154	2.7612	-0.2002	0.9125	0.1869	0.0001	0.3750	0.5204	29.21
RM	Winner (W)	0.3568	4.0697	-0.9282	1.9866	0.5780	0.0488	1.2738	1.6263	46.52
	Loser (L)	0.2191	5.4810	-0.5295	1.1879	0.3549	0.0371	1.4805	1.8016	63.39
	W – L	0.1377	3.2694	-0.4041	3.0940	0.2231	-0.0000	0.5050	0.6658	35.87
CM	Winner (W)	0.3810	4.2173	-0.8257	1.6097	0.6172	0.0458	1.2515	1.6113	44.80
	Loser (L)	0.2599	5.4694	-0.5744	1.2093	0.4210	0.0322	1.5393	1.8406	63.52
	W – L	0.1211	3.4904	-0.3021	2.1704	0.1962	0.0000	0.6991	0.8904	37.85
CR	Winner (W)	0.4015	4.6474	-0.7771	1.4298	0.6504	0.0541	1.4251	1.8317	50.05
	Loser (L)	0.2911	5.0446	-0.5675	1.6271	0.4716	0.0420	1.3626	1.6324	61.33
	W – L	0.1104	3.2966	-0.3510	1.2258	0.1788	0.0001	0.3790	0.4868	36.23
CMR	Winner (W)	0.4009	4.3287	-0.8553	1.5424	0.6495	0.0469	1.2709	1.6388	46.38
	Loser (L)	0.2286	5.4417	-0.5751	1.2593	0.3703	0.0331	1.5221	1.8123	64.15
	W – L	0.1724	3.5652	-0.3392	1.9933	0.2792	0.0000	0.6383	0.7834	40.65

with achieving the better performance. The substantially less-riskier portfolios constructed by the R and CR criterion are also as good in performance as the trend-following strategy by cumulative return. Considering almost 50%-increased monthly return, the reward-risk ratio of the CMR portfolio is also improved because the risk measure of the portfolio is only slightly increased.

The alternative momentum strategies constructed by the maximum drawdown related measures are less riskier at the levels of the ranking baskets. The lower VaR and CVaR levels for the winner and the higher levels for the losers are found in the cases of the maximum drawdown strategies such as the M, MR, CM, and CMR strategies. These strategies also exhibit the smaller (larger) maximum drawdown for the winner (loser) group. Meanwhile, the opposite situation is observed in the ranking groups of the R and CR strategies. The strategies show the larger (smaller) VaR and CVaR levels for the winner (loser) groups than that of the cumulative return strategy.

3.3.3 U. S. equity market: S&P 500

Weekly results

In Table 3.6, the alternative weekly contrarian portfolios constructed by the M, R, and CR criteria outperform the traditional contrarian portfolio. In particular, the recovery measure provides the best portfolio both in performance and volatility. The weekly return of 0.045% under the weekly standard deviation of 1.894% is achieved and both numbers are significantly improved with respect to the benchmark case. The CR strategy is also followed by the cumulative return mean-reversion strategy and its volatility level is one of the

smallest ones. Although the maximum drawdown portfolio exhibits the second best average return, its performance is based on the largest volatility.

The alternative contrarian portfolios exhibit strong reversal at the level of each ranking basket. The loser groups in the R and CR portfolios achieve the largest weekly returns of 0.202% and 0.185%, respectively. In particular, the smallest standard deviation of 2.944% among the losers is achieved by the recovery loser although its weekly return is larger than the losers in any other portfolios including the benchmark loser group. While the winners in the alternative criteria show as consistent performance as the traditional contrarian winner basket, the winner group in maximum drawdown features the weakest weekly performance of 0.094% which is desirable to the short position. Moreover, the return fluctuation is also the smallest volatility among the winner baskets.

The recovery associated portfolios are less riskier than the traditional reversal portfolio according to the risk measures in Table 3.6. With the Shape ratio, every alternative strategies exhibit larger Sharpe ratios than the benchmark contrarian strategy. Additionally, the R, RM, CMR, and CR portfolios are less riskier in the 95% VaR and CVaR. Moreover, only the R and CR portfolios feature lower maximum drawdowns than the cumulative return strategy and the maximum drawdown of the R portfolios is at the lowest level and 50% decreased. More interesting finding is that the lowest level of the risk is achieved by the risk measures of the recovery portfolio. Meanwhile, the portfolios related to the maximum drawdown are exposed to the more risks. In particular, the risk measures of the M portfolio are at the worst level.

In each ranking basket, the recovery based portfolio is also more compat-

Table 3.6: Summary statistics and risk measures of weekly 6/6 contrarian portfolios in U.S. S&P 500

Criterion	Portfolio	Summary statistics				Risk measures				
		Mean	Std. Dev.	Skewness	Kurtosis	Fin. Wealth	Sharpe	$VaR_{95\%}$	$CVaR_{95\%}$	MDD
C	Winner (W)	0.1545	3.4269	-0.8186	6.8648	0.7970	0.0560	1.3386	1.7016	63.77
	Loser (L)	0.1685	4.6130	-0.1908	11.7318	0.8693	0.0494	1.3727	1.7022	81.06
	L – W	0.0140	2.7235	0.5559	18.0504	0.0722	-0.0018	0.5749	0.7774	68.14
M	Winner (W)	0.0941	1.8080	-1.7153	14.3482	0.4858	0.0665	0.9660	1.2390	42.75
	Loser (L)	0.1330	5.4226	-0.0581	8.7693	0.6862	0.0367	1.5473	1.9427	84.81
	L – W	0.0388	4.2834	0.5514	11.5404	0.2004	0.0108	0.8726	1.1586	85.89
R	Winner (W)	0.1571	4.2265	-0.5915	8.0259	0.8106	0.0485	1.4418	1.8567	72.18
	Loser (L)	0.2024	2.9440	-0.5202	9.3128	1.0442	0.0770	1.1436	1.4756	59.09
	L – W	0.0453	1.8942	-0.3874	14.1420	0.2336	0.0029	0.4783	0.6290	34.65
RM	Winner (W)	0.1418	2.8429	-1.1089	7.5609	0.7319	0.0609	1.2627	1.6121	57.66
	Loser (L)	0.1205	4.9787	-0.2042	10.1750	0.6216	0.0429	1.4418	1.8103	84.29
	L – W	-0.0214	3.1059	0.3535	21.3982	-0.1103	0.0074	0.5464	0.7585	77.06
CM	Winner (W)	0.1329	2.8026	-0.9900	5.7244	0.6860	0.0617	1.2509	1.5900	57.59
	Loser (L)	0.1385	4.9616	-0.2106	10.4703	0.7146	0.0433	1.4433	1.8060	84.00
	L – W	0.0055	3.2731	0.5005	19.5205	0.0286	0.0044	0.6020	0.8273	78.42
CR	Winner (W)	0.1602	3.6578	-0.7068	7.0300	0.8264	0.0536	1.3591	1.7390	65.75
	Loser (L)	0.1848	4.3762	-0.0598	12.1970	0.9536	0.0517	1.3629	1.6812	78.68
	L – W	0.0247	2.5212	0.4148	15.3566	0.1272	-0.0009	0.5745	0.7780	60.46
CMR	Winner (W)	0.1379	3.1150	-1.0011	6.9205	0.7116	0.0562	1.3127	1.6669	60.12
	Loser (L)	0.1432	4.7905	-0.1819	11.2766	0.7388	0.0463	1.4082	1.7604	82.92
	L – W	0.0053	2.9710	0.4719	21.3172	0.0272	0.0056	0.5547	0.7546	74.13

ible with the risk profile of the contrarian strategy. Its loser basket exhibits the lowest risk measures such as 95% VaR, CVaR, and maximum drawdown. For example, the R and CR portfolios achieve the lowest 95% VaRs, CVaRs, maximum drawdowns in the loser groups, i.e. long postions. Additionally, the Sharpe ratio of the long position in the recovery portfolio is significantly larger than other portfolios including the benchmark portfolio and the CR criterion provides the second largest Sharpe ratio for the loser group. Meanwhile, the risk exposure of the winner in the recovery and CR measures is at the most dangerous degree and worse than those of the benchmark winner. The VaR, CVaR, and maximum drawdown of the recovery portfolio hit the worst levels.

Monthly results

The maximum drawdown related momentum portfolios exhibit the better performance in the S&P 500 universe. The summary statistics in Table 3.7 show that the monthly return of 0.185% and the standard deviation of 6.240% are achieved by the CM strategy, the best performer among all the alternative strategies while the monthly return of 0.135% and the standard deviation of 5.869% are obtained by the traditional momentum strategy. The portfolios by other maximum drawdown based rules such as the CMR, M, and RM strategies are followed by the benchmark strategy in performance measure. These three portfolios generate monthly 0.179%, 0.160%, and 0.152%, respectively. Meanwhile, the recovery portfolios such as the R and CR criteria show poorer performance with smaller standard deviations. For example, the CR strategy slightly underperforms the original strategy by 10% and its volatility is also decreased by 10%.

Table 3.7: Summary statistics and risk measures of monthly 6/6 momentum portfolios in U.S. S&P 500

Criterion	Portfolio	Summary statistics				Risk measures				
		Mean	Std. Dev.	Skewness	Kurtosis	Fin. Wealth	Sharpe	$VaR_{95\%}$	$CVaR_{95\%}$	MDD
C	Winner (W)	0.5207	5.4226	-0.8283	1.0570	0.5936	0.0548	1.6548	1.9514	56.70
	Loser (L)	0.3862	8.1115	0.0315	3.7771	0.4402	0.0369	1.8685	2.0034	80.28
	W – L	0.1345	5.8692	-1.5902	9.5354	0.1533	0.0060	1.1323	1.4689	65.05
M	Winner (W)	0.3996	2.9461	-1.6477	5.3286	0.4555	0.0659	1.1147	1.4830	42.61
	Loser (L)	0.2398	8.8190	0.0228	1.9067	0.2734	0.0315	2.0026	2.1785	81.31
	W – L	0.1597	7.1307	-0.8664	3.9332	0.1821	0.0008	1.5681	1.7568	69.40
R	Winner (W)	0.5030	6.6957	-0.5231	1.4928	0.5735	0.0517	1.7725	2.0429	72.42
	Loser (L)	0.5907	4.9978	-1.1764	4.6055	0.6734	0.0679	1.3524	1.6042	58.84
	W – L	-0.0876	3.1151	-0.7435	2.6854	-0.0999	0.0167	0.5746	0.7087	41.29
RM	Winner (W)	0.4912	4.4369	-0.9406	1.4538	0.5600	0.0542	1.5068	1.8224	52.14
	Loser (L)	0.3391	8.5186	0.0410	2.7849	0.3865	0.0341	1.8999	2.0506	81.15
	W – L	0.1522	5.9310	-1.8047	10.2498	0.1735	0.0075	1.1213	1.3830	66.01
CM	Winner (W)	0.4824	4.6982	-0.9008	1.3118	0.5499	0.0589	1.5884	1.8747	53.69
	Loser (L)	0.2976	8.5087	0.0268	2.7663	0.3393	0.0343	1.9262	2.0662	81.41
	W – L	0.1848	6.2404	-1.5782	8.4758	0.2106	0.0059	1.2391	1.5414	67.73
CR	Winner (W)	0.4980	5.6849	-0.7882	0.7682	0.5678	0.0573	1.7250	1.9887	60.49
	Loser (L)	0.3777	7.7708	-0.0968	4.5905	0.4306	0.0407	1.8039	1.9443	78.66
	W – L	0.1203	5.2923	-1.4184	8.9592	0.1372	0.0002	0.9499	1.2799	60.28
CMR	Winner (W)	0.5196	4.9916	-0.8961	1.2364	0.5923	0.0539	1.6096	1.9175	55.17
	Loser (L)	0.3408	8.3077	0.0104	3.3067	0.3886	0.0363	1.8954	2.0390	81.05
	W – L	0.1787	5.9297	-1.7243	10.3269	0.2037	0.0078	1.1499	1.4681	65.58

The outperformance of the maximum drawdown momentum strategies is achieved by the poorer performance in the loser groups. Most loser groups of the alternative strategies underperform that of the momentum strategy. Except for the R-strategy, the short baskets of the composite ranking criteria provide 0.240%–0.378% while the cumulative return loser group obtains monthly 0.386%. When the baskets are in short-selling, the underperformance generates the profit for the long/short portfolios. The returns of the alternative long baskets are more consistent regardless of criterion. The performance of the winners is slightly worse than 0.521% by the momentum winner group but in the narrow range of 0.482%–0.520% except for the M-strategy which earns monthly 0.400%. Additionally, the winners in maximum drawdown related measures are less volatile than the recovery or cumulative return winners.

The outperformance of the maximum drawdown momentum strategies is achieved by taking low downside risk. According to the risk measures given in Table 3.7, the alternative strategies except for the M and CM portfolios tend to exhibit lower 95% VaR and CVaR measures. Even with the CM criterion, the performance of the portfolio is almost 50% improved and the risk measures are only 10% increased. In addition to that, the Sharpe ratios of the maximum drawdown strategies are greater than those of the recovery strategies and cumulative return based strategy. Additionally, the lower maximum drawdown is another characteristic of the maximum drawdown portfolios.

The risk measures of each ranking group support the outperformance of the maximum drawdown momentum strategies. The lower (higher) 95% VaR, CVaR, and maximum drawdown levels for winner (loser) groups are achieved by the maximum drawdown related stock selection rules. Its long position is

less riskier than that of the momentum strategy while the opposite position is under the greater risk of losing money. This opposite behavior enables the portfolios profitable. Additionally, the higher Sharpe ratios are obtained by these strategies. Meanwhile, the recovery related strategies such as the R and CR strategies exhibit the higher (lower) 95% VaR, CVaR, and maximum drawdown for the winner (loser) groups.

3.3.4 Overall results

Regardless of asset class and market, the alternative portfolios constructed by the maximum drawdown and consecutive recovery achieve the better performance than the original momentum and contrarian strategies. In particular, employing the composite ranking rules are superior to using the only cumulative return, maximum drawdown, and recovery measures.

In weekly scale, the contrarian portfolios constructed by the recovery measures exhibit the outperformance over the traditional contrarian strategy. The R, CR, and CMR criteria are the best stock selection rules for the weekly contrarian strategy in any markets. The high performance and low volatility are featured by the portfolios. The historical cumulative returns of these portfolios are found in Figure 3.1.

For momentum portfolio construction, the maximum drawdown related measures are the best stock selection rules. The CM criterion provides the portfolios performing well in three different markets. The CMR and RM selection rules also predict future winners and losers well. Additionally, the volatility levels of the portfolio returns are relatively lower when the overall

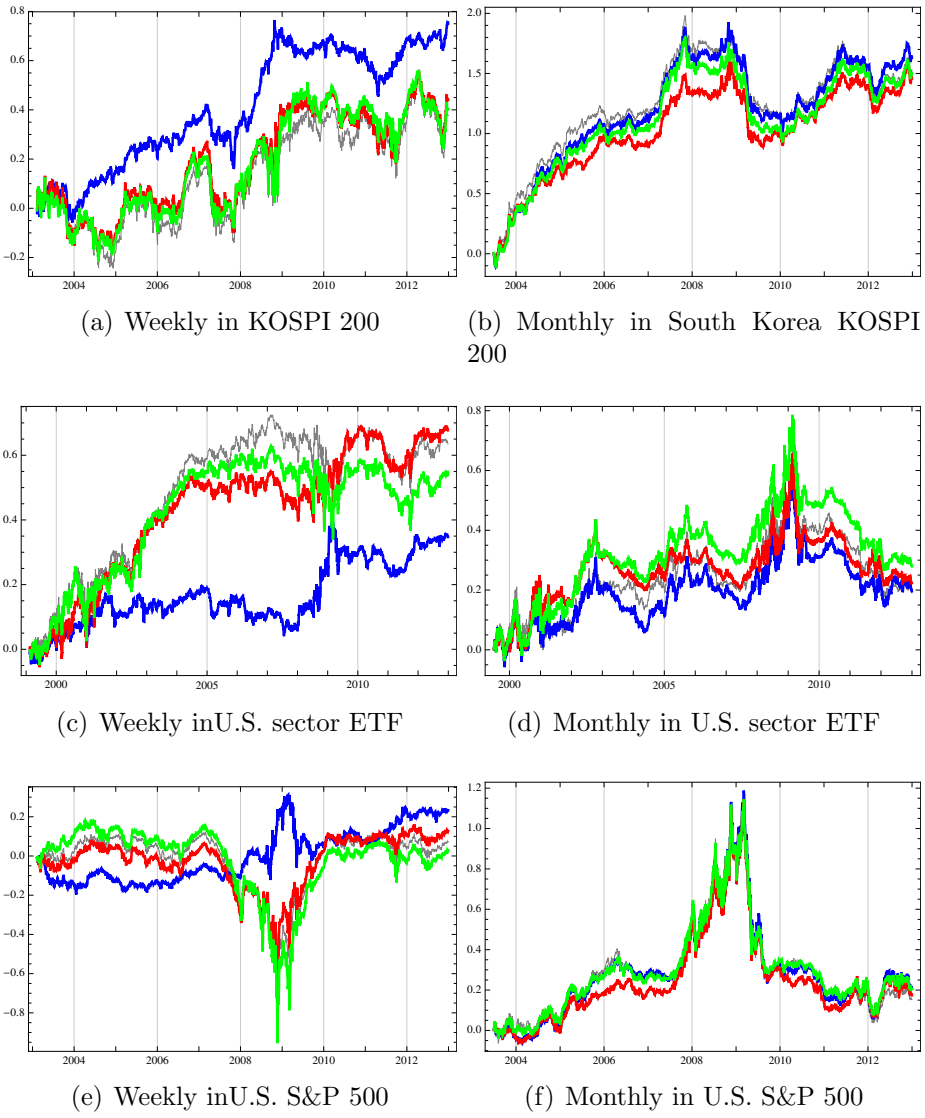

(a) Weekly in KOSPI 200

(b) Monthly in South Korea KOSPI 200

(c) Weekly inU.S. sector ETF

(d) Monthly in U.S. sector ETF

(e) Weekly inU.S. S&P 500

(f) Monthly in U.S. S&P 500

Figure 3.1: For weekly contrarian, cumulative returns for the traditional contrarian (gray), R (blue), CR (red), and CMR (green). For monthly momentum, cumulative returns for the traditional momentum (gray), CM (blue), RM (red), and CMR (green).

performance is considered. The cumulative returns of these portfolios are also given in Figure 3.1.

It is noteworthy that the price components related to the past and future

directions expected by the momentum and reversal are important factors for portfolio construction in any time scale. For momentum, the maximal drawdown should be minimized for the winner but maximized for the loser because the winner is expected to outperform the loser. Meanwhile, the recovery for short-term contrarian should be smaller for losers. If the recovery is too large for the losers, it is considered that the asset already spent the fuel for the reversion and it is hard to exhibit the reversal.

The performance of the alternative portfolios is not the price of taking more risk. The alternative portfolios are less riskier in the better risk profiles such as VaR, CVaR, and maximum drawdown. It is also interesting that the risk measures of each ranking group are also well-matched to the purpose of portfolios construction: The winners (losers) groups are less (more) riskier in monthly scale. The ranking groups of the weekly contrarian strategy exhibit the opposite characteristics.

3.4 Factor analysis

As shown in the previous section, the maximum drawdown and consecutive recovery provide the useful stock selection rules for more profitable portfolios with low risk. The factor analysis with the Fama-French three-factors [40] also tests the outperformance of the alternative strategies. We focus on the S&P 500 universe.

3.4.1 Weekly

In Table 3.8, the intercepts and factor exposures of alternative contrarian strategies are given. All Fama-French three-factor alphas are negative except for the recovery portfolio. The positive and statistically significant alpha is achieved only by the recovery strategy. The R and CR portfolios exhibit greater alpha than the three-factor alpha of the traditional contrarian strategy. The intercepts for all other contrarian strategies are negative and smaller than the benchmark alpha.

Table 3.8: Fama-French regression of weekly 6/6 contrarian portfolios in U.S. S&P 500

Criterion	Portfolio	Factor loadings				
		$\alpha(\%)$	β_{MKT}	β_{SMB}	β_{HML}	R^2
C	Winner (W)	-0.0494	1.1237**	0.2532**	0.2906**	0.8744
	Loser (L)	-0.0965	1.4406**	0.1721*	0.6591**	0.8445
	L – W	-0.0471	0.3169**	-0.0810	0.3685**	0.1602
M	Winner (W)	0.0047	0.6754**	-0.1448**	-0.1222**	0.8471
	Loser (L)	-0.1897*	1.5955**	0.3761**	1.0971**	0.8638
	L – W	-0.1945	0.9201**	0.5209**	1.2193**	0.6798
R	Winner (W)	-0.0994	1.3435**	0.2755**	0.6570**	0.9080
	Loser (L)	0.0309	1.0689**	0.0088	0.1174**	0.9458
	L – W	0.1303*	-0.2746**	-0.2667**	-0.5396**	0.4502
RM	Winner (W)	-0.0222	0.9763**	0.1229**	0.1081**	0.8745
	Loser (L)	-0.1723*	1.5370**	0.2604**	0.8106**	0.8645
	L – W	-0.1500	0.5606**	0.1374	0.7025**	0.4339
CM	Winner (W)	-0.0271	0.9579**	0.1506**	0.0442	0.8520
	Loser (L)	-0.1517	1.5166**	0.2565**	0.8286**	0.8554
	L – W	-0.1246	0.5586**	0.1059	0.7844**	0.4150
CR	Winner (W)	-0.0587	1.1904**	0.2685**	0.3697**	0.8814
	Loser (L)	-0.0650	1.3810**	0.1372	0.5804**	0.8428
	L – W	-0.0063	0.1906**	-0.1313	0.2108*	0.0643
CMR	Winner (W)	-0.0445	1.0426**	0.2018**	0.1728**	0.8671
	Loser (L)	-0.1345	1.4811**	0.2159**	0.7355**	0.8492
	L – W	-0.0900	0.4386**	0.0141	0.5628**	0.2847

** 1% significance * 5% significance

The factor exposure of the recovery portfolio is unique. The R portfolio exhibits negative exposures to all the Fama-French three factors. Additionally, the negative exposures are all statistically significant. The CR and C portfolios show weak dependence on the market and value factors and negative exposure on the size factor. The R^2 values of the C, CR, and CMR portfolios are relatively smaller.

The performance of the winner and loser baskets is explicable by the Fama-French three-factor model with high R^2 values. Most of the factor exposures are positive and statistically significant. Meanwhile, the intercepts for the ranking baskets are negative and not statistically significant in most cases. The loser groups of the M and RM portfolios exhibit statistically significant alphas.

3.4.2 Monthly

The intercepts and factor loadings of the alternative momentum strategies are given in Table 3.9. All the intercepts of the regression model are positive except for the recovery strategy. Additionally, most of the portfolios outperform the cumulative return strategy if no factor exposure is given.

Different factor structures by the types of the stock selection rules are found. The first type of the ranking rules are the selection rules associated with the maximum drawdown. The alphas of the maximum drawdown related portfolios are greater than other strategies including the traditional momentum. In particular, the positive and statistically significant intercept is achieved only by the M strategy. Additionally, the larger portions of the returns by the

Table 3.9: Fama-French regression of monthly 6/6 momentum portfolios in U.S. S&P 500

Criterion	Portfolio	Factor loadings				
		$\alpha(\%)$	β_{MKT}	β_{SMB}	β_{HML}	R^2
C	Winner (W)	-0.0855	1.0061**	0.3656**	-0.0642	0.7869
	Loser (L)	-0.5270	1.5391**	0.1749	0.3457*	0.8026
	W – L	0.4415	-0.5330**	0.1906	-0.4099	0.2057
M	Winner (W)	0.1109	0.6204**	-0.1077	-0.0089	0.7824
	Loser (L)	-0.8071*	1.6119**	0.4258*	0.4787**	0.8300
	W – L	0.9180*	-0.9916**	-0.5334*	-0.4876**	0.6036
R	Winner (W)	-0.3169	1.2997**	0.2715**	0.3641**	0.9033
	Loser (L)	0.0056	1.0678**	0.0955	0.0389	0.9299
	W – L	-0.3225	0.2319**	0.1760	0.3252**	0.2925
RM	Winner (W)	-0.0081	0.8703**	0.2145*	-0.0413	0.8274
	Loser (L)	-0.6613	1.5904**	0.3701*	0.3803**	0.8307
	W – L	0.6532	-0.7202**	-0.1556	-0.4217*	0.4112
CM	Winner (W)	-0.0367	0.8847**	0.2958**	-0.0899	0.7880
	Loser (L)	-0.6901*	1.5843**	0.3056	0.4203**	0.8189
	W – L	0.6533	-0.6996**	-0.0098	-0.5102*	0.3475
CR	Winner (W)	-0.1586	1.0704**	0.3174**	0.0841	0.8193
	Loser (L)	-0.4931	1.4920**	0.1695	0.2650	0.8050
	W – L	0.3345	-0.4216**	0.1479	-0.1810	0.1296
CMR	Winner (W)	-0.0355	0.9483**	0.2934**	-0.0714	0.7970
	Loser (L)	-0.6101	1.5711**	0.2503	0.3486*	0.8148
	W – L	0.5747	-0.6229**	0.0431	-0.4200*	0.2863

** 1% significance * 5% significance

maximum drawdown strategies are explained by the Fama-French three-factor model with higher R^2. The strategies are much exposed to the market factor and the value factor. The portfolio returns are negatively correlated with the size factor.

Contrary to the maximum drawdown based portfolios, the recovery portfolios such as the R and CR portfolios have the smaller intercepts than other strategies. In particular, the negative intercept is obtained by the R portfolio. The returns of these strategies are weakly dependent with the market and value factors but exhibit the positive exposures on the size factor than the

drawdown portfolios. The R^2 values are relatively lower.

The winner and loser baskets in each portfolio are well-explained by the Fama-French three-factor model with high R^2 values. The differences in intercept and factor exposure with respect to the ranking criterion are originated from the characteristics in factor structure of each basket. The winner basket of the recovery momentum strategy not only has the a smaller intercept but also exhibits more exposures on all the three factors than the loser basket. Meanwhile, the maximum drawdown portfolios are opposite: the higher alpha, less exposures to the Fama-French factors.

3.5 Concluding remarks

In this chapter, we test the monthly momentum and weekly contrarian strategies with the alternative stock selection rules originating from maximum drawdown and consecutive recovery. The selection rules include not only the maximum drawdown and successive recovery but also the composite indices of them. The alternative portfolios are implemented in U.S. and South Korea equity markets.

In every markets, the performance of the alternative strategies is superior to the benchmark strategies. Additionally, the best portfolios are related to the construction rules that are related to the past and future directions expected by momentum and reversal. In weekly scale, the recovery related measures provide the better contrarian portfolios in the markets, i.e. smaller recovery expects more reversal. The R, CR, and CMR portfolios show the

outperformance.

In monthly scale, the maximum drawdown associated strategies outperform the traditional momentum strategy, i.e. smaller maximum drawdown gives stronger momentum. The CM strategy is the overall best performer in every market. The CMR and CM portfolios are as good as the CM strategy.

The risk measures for the portfolios indicate that the portfolios are less riskier than the benchmark strategy. The portfolios tend to exhibit the lower VaR, CVaR, and maximum drawdown in the markets. The similar pattern is also observed at the levels of each long/short basket.

The factor analysis also shows that the unique pattern by the stock selection rules exists. In weekly, the intercept of the recovery portfolio is the largest one. The maximum drawdown portfolios have the higher intercept and larger exposures to the market and value factors than the traditional momentum strategy.

In future, the stock selection criteria based on the maximum drawdown and recovery will be tested in shorter time scales such daily and intraday frequencies. It will be useful to test the performance and risk of the alternative portfolios in various equity markets.

Chapter 4

Reward-risk momentum strategies using classical tempered stable distribution

In this chapter, we extend the approach based on the reward-risk measures suggested by Rachev et al. [79] to many different directions. First of all, the reward-risk measure based momentum portfolios are constructed in diverse asset classes including currency markets, commodity markets, global stock benchmark indices, South Korea KOSPI 200 universe, SPDR U.S. sector ETFs, and S&P 500 universe. Secondly, more robust tests by using a different time horizon and removing survivor bias with the component-change log are performed in the S&P 500 universe. Finally, the Fama-French factor analysis on the reward-risk portfolios is conducted. The structure of this paper is followings: In next section, we briefly cover a risk model and reward-risk measures used as stock selection rules for momentum-style portfolio construction. In section 4.2, datasets and methodology are introduced. The performance and risk measures of the strategies are given in section 4.3. The Fama-French factor analysis is conducted in section 4.4. We close the chapter in section 4.5.

4.1 Risk model and reward-risk measures

4.1.1 Risk model

It is important to decide a risk model for the calculation of reward-risk measures. Considering the distributional properties of a financial asset price such as autocorrelation and volatility clustering, the ARMA(1,1)-GARCH(1,1) model is chosen. Additionally, we assume that the innovation of the model is generated from classical tempered stable (CTS) distribution [86] in order to model skewness and kurtosis. The ARMA-GARCH-CTS model is proposed by Kim et al. [57] and this paper follows it.

An infinitely divisible random variable X is said to follow the CTS distribution, $X \sim \text{CTS}(\alpha, C_+, C_-, \lambda_+, \lambda_-, m)$ if its Levy triplet (σ^2, ν, γ) satisfies following conditions:

$$\begin{aligned} \sigma &= 0 \\ \nu(dx) &= (C_+ e^{-\lambda_+ x}\mathbb{I}_{x>0} + C_- e^{-\lambda_- |x|}\mathbb{I}_{x<0})\frac{dx}{|x|^{\alpha+1}} \\ \gamma &= m - \int_{|x|>1} x\nu(dx) \end{aligned}$$

where $C_+, C_-, \lambda_+, \lambda_-$ are all positive, $\alpha \in (0, 2)$, and $m \in \mathbb{R}$. From the viewpoint of risk management, important CTS parameters are α and λ_-. The tail index α tells how fat both tails are and the lager tail index is achieved by the thinner tail. The downside tail is controlled by λ_-. Similar to the tail index α, the thinner downside tail is described by the larger λ_- parameter.

4.1.2 Reward-risk measures

Sharpe ratio

The Sharpe ratio is the ratio of expected excessive return to standard deviation for excessive return [90], i.e. it is a reward per deviation. It is defined with

$$\mathrm{SR}(r) = \frac{E(r - r_f)}{\sigma(r - r_f)}$$

where r_f is a risk-free rate. A portfolio with higher Sharpe ratio is considered the better portfolio than a portfolio with lower Sharpe ratio. Additionally, the portfolio with the highest Sharpe ratio in Markowitz framework is the tangency portfolio [70].

Conditional Value-at-Risk

In order to define conditional Value-at-Risk (CVaR), Vale-at-Risk (VaR) needs to be defined. The VaR is represented with

$$\mathrm{VaR}_{(1-\alpha)100\%} = -\inf\{l | P(r > l) \leq 1 - \alpha\}$$

where $0 < \alpha < 1$.

The CVaR, also known as average Value-at-Risk (AVaR), is the expected loss worse than the VaR [83, 84]. The CVaR is defined by

$$\mathrm{CVaR}_{(1-\alpha)100\%}(r) = \mathrm{ETL}_{\alpha 100\%}(r) = \frac{1}{\alpha}\int_0^{\alpha} \mathrm{VaR}_{(1-\beta)100\%} d\beta$$

where $0 < \alpha < 1$. When severe losses hit a given VaR level, the CVaR tells

how seriously bad in average those losses are, i.e. it is the average loss of the extreme losses. For continuous distributions, it is identical to the extreme tail loss (ETL).

An advantage of CVaR over VaR is the coherency of the risk measure [8, 20, 84]. The definition of the coherent risk measure is given in the original literatures on the coherent risk measures [8, 20, 84]. Another advantage is that the CVaR encodes more information on the downside tail. For example, even if the VaR levels of two different portfolios are same, one with the fatter tail exhibits the larger CVaR.

Stable tail adjusted return ratio

The Sharpe ratio considers deviations along downside and upside directions. Since the deviation in the upward direction is not an actual risk, much attention on the downslide risk should be paid. The stable tail adjusted return ratio (STARR) is introduced by Martin et al. [71] in order to distinguish the risk from the deviation. The standard deviation in the denominator of the Sharpe ratio definition is replaced with the CVaR. The STARR is defined by

$$\mathrm{STARR}_{(1-\alpha)100\%} = \frac{E(r - r_f)}{\mathrm{CVaR}_{(1-\alpha)100\%}(r - r_f)}$$

where $0 < \alpha < 1$. In this paper, the linearized version of STARR is used in the paper and the linearized STARR is defined by

$$\mathrm{STARR}_{(1-\alpha)100\%} = E(r - r_f) - \mathrm{CVaR}_{(1-\alpha)100\%}(r - r_f).$$

Since larger CVaR is achieved by riskier assets, the STARR for riskier assets becomes smaller. Meanwhile, less riskier, larger STARR.

Rachev ratio

The return distribution of financial assets has two tails, i.e. downside and upside tails. The upper tails are favorable but the lower tails are undesirable. The Rachev ratio (R-ratio) is the ratio of the expected upward tail gain to the expected downside tail loss. It is defined by

$$\mathrm{RR}(\alpha,\beta) = \frac{\mathrm{CVaR}_{(1-\alpha)100\%}(r_f - r)}{\mathrm{CVaR}_{(1-\beta)100\%}(r - r_f)}$$

where $0 \leq \alpha, \beta \leq 1$. The higher R-ratio is more preferred.

Classification of the reward-risk measures

These reward-risk measures can be categorized into two classes. The first class includes ratio-based measures such as R-ratio and Sharpe ratio. With the ratio measures, the reward is scaled by the risk. The second class is risk-based measures. The CVaR is one of the measures in this category and the linearized STARR is also a member in the second group.

4.2 Dataset and methodology

4.2.1 Dataset

Various asset classes and markets are employed in order to conduct robust tests on the profitability of the reward-risk momentum strategies. The datasets consist of currency markets, commodity markets, global stock benchmark indices, South Korea KOSPI 200 universe, SPDR U.S. sector ETFs, and U.S. S&P 500 universe.

Currency markets

The historical currency prices are downloaded from Bloomberg and the length of the covered period is 20 years from January 1993 to December 2012. The currency rates are spot prices in U.S. dollar and obtained with respect to Eastern Standard Timezone. The instruments are followings: ARSUSD (Argentina), AUDUSD (Australia), BRLUSD (Brazil), CADUSD (Canada), CHFUSD (Swiss), CLPUSD (Chile), CNYUSD (China), COPUSD (Columbia), CZKUSD (Czech), DEMUSD (German), DKKUSD (Denmark), EGPUSD (Egypt), EURUSD (Euro), GBPUSD (U.K.), GHSUSD (Ghana), HKDUSD (Hong Kong), HUFUSD (Hungary), IDRUSD (Indonesia), ILSUSD (Israel), INRUSD (India), ISKUSD (Iceland), JPYUSD (Japan), KESUSD (Kenya), KRWUSD (South Korea), MXNUSD (Mexico), MYRUSD (Malaysia), NGNUSD (Nigeria), NOKUSD (Norway), NZDUSD (New Zealand), PENUSD(Peru), PHPUSD (Philippines), PLNUSD (Poland), RUBUSD (Russia), SARUSD (Saudi), SEKUSD (Sweden), SGDUSD (Singapore), THBUSD (Thai), TRYUSD (Turkey), TWDUSD (Taiwan), VEFUSD (Venezuela), XAFUSD (Central Africa), and

ZARUSD (South Africa).

Commodity markets

The commodity price information between January 1993 and December 2012 is collected from Bloomberg. The historical price of a generic future contract is obtained. The whole momentum universe includes following tickers: BO (Soybean Oil: CBT), C (Corn: CBT), CC (Cocoa: NYB), CL (WTI: NYM), CO (Brent:N YM), COA (Coal: NYM), CT (Cotton: NYB), DA (Milk: CME), DL (Ethanol: CBT), FC (Feeder Cattle: CME), GC (Gold: CMX), HG (Copper: CMX), HO (Heating Oil: NYM), HU(Gasoline: NYM) JO (Orange Juice: NYB), KC (Coffee: NYB), LA (Aluminium Primary: LME), LC (Live Cattle: CME), LCO (Cobalt: LME), LH (Lean Hogs: CME), LL (Lead: LME), LN (Nickel: LME), LT (Tin: LME), LX (Zinc: LME), LY (Aluminium Alloy: LME), MOL (Molybden: LME), NG (Natural Gas: NYM), O (Oat: CBT), OR (Rubber: SGX), PA (Palladium: NYM), PB (Pork Belly: CME), PGP (Polypropylen: NYM), PL (Platinum: NYM), PN (Propane: NYM), QS (Gas Oil: ICE), RR (Rice: CBT), S (Soybean: CBT), SB (Sugar: NYB), SI (Silver: CMX), SM (Soybean Meal: CBT), TO (Dubai: NYM), W (Wheat: CBT), and XB (RBOB Gasoline: NYM).

Global stock benchmark indices

The daily data of global stock benchmark indices are downloaded from Bloomberg. The time horizon covers the period from January 1993 to December 2012. The indices are converted to dollar values and the considered index tickers are AEX (Netherland), AS51 (Australia), BEL20 (Belgium), CAC 40 (France), CCMP

(U.S. NASDAQ), DAX (German), FBMKLCI (Malaysia), FSSTI (Singapore), FTSEMIB-MIB30 (Italy), HSI (Hong Kong), IBEX (Spain), IBOV (Brazil), IGBC (Columbia), IGBVL (Peru), INDU (U.S. Dow Jones), IPSA (Chile), JCI (Indonesia), KOSPI (South Korea), MERVAL (Argentina), MEXBOL (Mexico), NKY (Japan), NZSE50FG (New Zealand), OMX (Sweden), PCOMP (Philiphine), PSI20 (Portuguese), RTSI$ (Russia), SENSEX (India), SET (Thailand), SHCOMP (China), SMI (Swiss), SPTSX (Canada), SPX (U.S. S&P 500), SX5E (Euro), TWSE (Taiwan), UKX (U.K.), and VNINDEX(Vietnam).

South Korea equity market: KOSPI 200

The price history and component-change log are obtained from Korea Exchange. The market universe for the momentum strategy consists of the recent 10-year (2003–2012) components of the KOSPI 200 which is one of main benchmark indices in Korean stock markets.

U.S. equity market: SPDR sector ETFs

The data for SPDR U.S. sector ETFs are collected from Bloomberg. Among various sector ETFs, SPDR sector ETFs are chosen because the same length of historical price is available for all industry sectors. The time horizon is the period between January 1999 and December 2012. The ETF universe includes XLB (Materials), XLE (Energy), XLF (Financial), XLI (Industrial), XLK (Technology), XLP (Consumer Staples), XLU (Utilities), XLV (Health Care), and XLY (Consumer Discretionary).

U.S. equity market: S&P 500

The price data and component-change log for S&P 500 components are downloaded from Bloomberg. The time span covers from January 2003 to December 2012.

4.2.2 Methodology

The portfolio construction for this study is identical to the traditional momentum portfolio construction in Jegadeesh and Titman [53]. The only difference is the usage of alternative ranking criteria for the formation of momentum ranking groups. For comparison, the first criterion is cumulative return over a ranking period. Other stock selection rules used for portfolio construction are the reward-risk measures introduced in the previous section: Sharpe ratio, CVaR, STARR, and R-ratio. Among these reward-risk measures, Sharpe ratio, STARR, and R-ratio are already used in Rachev et al. [79] and CVaR is newly adopted in this paper.

Given a ranking rule calculated from the past six months of estimation period, assets are sorted from the highest risk to the lowest risk and grouped into several baskets. In this paper, the size of the groups is 3 except for the KOSPI 200 and S&P 500 universes which use 10 different ranking groups. Assets with the highest risk form a loser basket and the safest assets are assigned to a winner basket. Momentum return is the return difference between the winner and loser quantiles after a holding period. The six months of holding period are used in this study. In every six months, the new portfolio is constructed and maintained until the end of the holding period, i.e. it is a

non-overlapping portfolio.

The price data are converted into summary data which contain the reward-risk measures and cumulative returns over the periods. Some summary results for several instruments in certain periods are ignored if enough numbers of data points in the period are not given. The minimum number of the data in the period is 21 days corresponding to the trading dates in one month. This ignorance is reasonable for the case that some instruments could have few data points during the period. In this case, it is impossible to estimate the parameters of the CTS distribution by using maximum likelihood estimation with very small numbers of data points. The Sharpe ratio, VaR, CVaR, STARR, and R-ratio are calculated in daily scale. The maximum drawdown is obtained from the entire history of the portfolio performance.

4.3 Results

4.3.1 Currency markets

According to the summary statistics of the strategies found in Table 4.1, the R-ratio based strategies in the currency universe outperform the traditional momentum strategy which obtains the monthly return of 0.33% and the standard deviation of 2.33%. In particular, the R-ratio(50%, 9X%)-based portfolios achieve monthly 0.44%–0.52%. The standard deviations of these portfolios are about 20% smaller than that of the original momentum strategy. In addition to that, the average monthly returns of the R-ratio(9X%,9X%) portfolios are in the range between 0.31% and 0.36%. The volatility levels of these strate-

gies are also 40% lower than that of the cumulative return portfolio. Other reward-risk measures such as Sharpe ratio, CVaRs, and STARR ratios provide the portfolios underperforming the traditional trend-following strategy and these portfolios except for the Sharpe ratio based strategy are not less volatile.

With the R-ratio(50%,9X%) criteria, the momentum of each ranking basket becomes stronger. The winner groups of the R-ratio(50%,9X%) portfolios outperform that of the benchmark strategy. Additionally, they are the best winner groups among all the reward-risk momentum portfolios. Opposite to the winner baskets, the loser baskets of the R-ratio(50%,9X%) strategies are the worst performers among all the selection rules including the cumulative return. The lagging in the short basket enables the strategies beat the traditional momentum strategy. The short baskets of the R-ratio(9X%,9X%) portfolios show substantial downside momentum but the opposite baskets are not as strong as the winner portfolio of the cumulative return based strategy. The pattern of skewness also explains why the momentum by the alternative ranking rules tends to be stronger. For all the reward-risk momentum portfolios, the long (short) baskets exhibit larger (smaller) skewness than the cumulative return strategy does.

The dominant performance of the reward-risk strategies is achieved by taking less risk. In Table 4.2, it is obvious that every R-ratio strategies exhibit lower 95% VaR and CVaR levels. Another remarkable characteristic of the reward-risk portfolios is that the maximum drawdowns of 10.96%–14.83% are significantly smaller than 26.90% by the cumulative return portfolio. Moreover, the top 3 largest Sharpe ratios are achieved by the R-ratio(50%,X%)

Table 4.1: Summary statistics of monthly 6/6 momentum portfolios in currency markets

Criterion	Portfolio	Summary statistics				
		Mean	Std. Dev.	Skewness	Kurtosis	Final Wealth
Cumulative return	Winner (W)	0.0321	2.0745	-0.7740	5.4388	0.0751
	Loser (L)	-0.3050	2.3322	-0.1929	2.5957	-0.7138
	W – L	0.3371	2.3313	-0.1021	1.0460	0.7889
Sharpe ratio	Winner (W)	-0.1120	2.0836	-0.6513	2.7086	-0.2620
	Loser (L)	-0.1464	1.8203	-0.2558	3.1569	-0.3426
	W – L	0.0344	1.8672	-0.1799	1.4097	0.0806
CVaR(99%)	Winner (W)	-0.1505	1.1370	-0.0961	11.2495	-0.3522
	Loser (L)	-0.2853	2.5900	-0.4855	2.1489	-0.6677
	W – L	0.1348	2.1998	0.4062	2.5712	0.3155
CVaR(95%)	Winner (W)	-0.1715	1.1056	0.0751	13.8207	-0.4012
	Loser (L)	-0.2184	2.6403	-0.3228	1.6908	-0.5110
	W – L	0.0469	2.3552	0.1908	2.6448	0.1098
CVaR(90%)	Winner (W)	-0.1743	1.1531	0.1157	11.8002	-0.4078
	Loser (L)	-0.1944	2.6707	-0.3040	1.6134	-0.4549
	W – L	0.0201	2.4136	0.1001	2.4119	0.0471
STARR(99%)	Winner (W)	-0.1533	1.1495	-0.1178	10.8946	-0.3586
	Loser (L)	-0.2692	2.5865	-0.4183	1.8526	-0.6299
	W – L	0.1159	2.2168	0.3393	2.3994	0.2713
STARR(95%)	Winner (W)	-0.1761	1.1052	0.0937	13.8560	-0.4120
	Loser (L)	-0.2534	2.6841	-0.4140	2.1140	-0.5929
	W – L	0.0773	2.3860	0.2367	2.7273	0.1809
STARR(90%)	Winner (W)	-0.1573	1.1573	0.1509	11.7092	-0.3680
	Loser (L)	-0.2025	2.6763	-0.2977	1.6779	-0.4739
	W – L	0.0452	2.4405	0.0818	2.3401	0.1059
R-ratio(99%,99%)	Winner (W)	-0.0133	1.7425	-0.0727	1.5723	-0.0310
	Loser (L)	-0.3182	1.8715	-0.5392	3.1297	-0.7447
	W – L	0.3050	1.5420	0.2915	2.8258	0.7137
R-ratio(95%,95%)	Winner (W)	0.0058	1.7369	-0.4895	0.9809	0.0135
	Loser (L)	-0.3549	1.7668	-0.3822	3.3337	-0.8305
	W – L	0.3607	1.4942	-0.0412	1.5296	0.8441
R-ratio(90%,90%)	Winner (W)	-0.0144	1.8151	-0.7065	2.0349	-0.0337
	Loser (L)	-0.3773	1.6853	-0.3615	3.9879	-0.8830
	W – L	0.3629	1.4896	-0.2404	2.2522	0.8492
R-ratio(50%,99%)	Winner (W)	0.0737	2.1660	-0.7656	3.0856	0.1725
	Loser (L)	-0.4499	1.4829	-0.6964	4.8830	-1.0529
	W – L	0.5237	1.8569	-0.2688	3.1975	1.2254
R-ratio(50%,95%)	Winner (W)	0.0722	2.0517	-0.7429	3.2594	0.1690
	Loser (L)	-0.4370	1.5174	-0.5894	4.5845	-1.0225
	W – L	0.5092	1.7138	-0.1580	3.8655	1.1916
R-ratio(50%,90%)	Winner (W)	0.0402	2.0641	-0.6512	2.3895	0.0940
	Loser (L)	-0.3994	1.5007	-0.5285	4.7091	-0.9346
	W – L	0.4395	1.7131	-0.0681	4.2952	1.0285

strategies. Besides the R-ratio strategies, the highest Sharpe ratio and lowest maximum drawdown are obtained by the Sharpe ratio momentum strategy. The reward-risk measures of any other ranking criteria are worse than those

of the traditional momentum. The R-ratio(50%,95%) and R-ratio(50%,90%) strategies are characterized by larger CTS tail index α values which control the both tails simultaneously. Most of the other reward-risk strategies generally have larger λ_- parameters than the benchmark strategy.

With the VaR and CVaR levels of each ranking basket, the selection rules are categorized into two groups. The first class of the reward-risk measures are characterized by higher (lower) VaR and CVaR levels for the winner (loser) group. The R-ratios and Sharpe ratio are included in this class. The second class is opposite to the first class, i.e. the winner (loser) group is less (much) riskier than that of the cumulative return strategy. The second class consists of the CVaR and the STARR criteria. The same classification is also applied to the CTS parameters. For the criteria in the first class, the λ_- values of the winners are greater than the loser groups. In particular, for the R-ratio(50%,9X%) strategies, the λ_- parameters of the long (short) position are larger (smaller) than that of the traditional momentum winner. This explain why the winner (loser) groups of the R-ratio(50%,9X%) portfolios outperform (underperform) the momentum winner (loser). For the second class, the situation is opposite to the first class. The downside tail indices of the winner portfolios are below the levels of the downside tail indices for the loser. Additionally, the smaller λ_- for the winners and larger λ_- for the losers are found. It is the reason why these strategies are not as good as the strategies by the selection rules in the first class strategies or the cumulative return portfolio.

Table 4.2: Summary risk statistics of monthly 6/6 momentum portfolios in currency markets

Criterion	Portfolio	CTS parameters			Risk measures			
		α	λ_+	λ_-	Sharpe	$\text{VaR}_{95\%}$	$\text{CVaR}_{95\%}$	MDD
Cumulative return	Winner (W)	0.3265	1.2321	1.2063	0.0000	0.3200	0.4291	29.98
	Loser (L)	1.0536	0.5899	0.5726	-0.0001	0.2962	0.4555	64.37
	W – L	0.1465	1.3847	1.4100	0.0002	0.3261	0.4293	26.90
Sharpe ratio	Winner (W)	0.0584	1.4679	1.4174	-0.0000	0.3445	0.4729	47.73
	Loser (L)	0.3092	1.0731	1.0843	-0.0001	0.2958	0.3679	46.76
	W – L	0.1027	1.4560	1.4315	0.0113	0.3963	0.4520	24.25
CVaR(99%)	Winner (W)	1.2291	0.2897	0.2671	0.0000	0.1712	0.2174	42.02
	Loser (L)	0.0500	1.6772	1.5845	-0.0125	0.4893	0.6918	62.23
	W – L	0.0501	1.5106	1.5468	0.0031	0.4540	0.6377	27.70
CVaR(95%)	Winner (W)	1.2847	0.2185	0.2040	0.0000	0.1810	0.2169	43.36
	Loser (L)	0.0500	1.7227	1.6260	-0.0064	0.5036	0.7111	59.02
	W – L	0.0500	1.5408	1.5664	-0.0021	0.4585	0.6398	32.19
CVaR(90%)	Winner (W)	1.3343	0.1935	0.1847	-0.0000	0.1811	0.2105	44.36
	Loser (L)	0.0500	1.7320	1.6572	-0.0022	0.4989	0.7077	56.78
	W – L	0.0500	1.5443	1.5765	-0.0034	0.4734	0.6584	33.55
STARR(99%)	Winner (W)	1.2225	0.2841	0.2664	0.0000	0.1706	0.2201	42.07
	Loser (L)	0.0500	1.6806	1.5912	-0.0116	0.4772	0.6733	61.92
	W – L	0.0501	1.5352	1.5734	0.0039	0.4420	0.6174	27.76
STARR(95%)	Winner (W)	1.2881	0.2160	0.2041	0.0000	0.1633	0.2162	43.43
	Loser (L)	0.0500	1.7078	1.6164	-0.0093	0.5025	0.7101	61.57
	W – L	0.0502	1.5230	1.5469	-0.0001	0.4690	0.6604	32.61
STARR(90%)	Winner (W)	1.2620	0.2207	0.2205	0.0000	0.1637	0.2127	43.90
	Loser (L)	0.0500	1.6719	1.6098	-0.0036	0.5105	0.7212	58.21
	W – L	0.0500	1.5199	1.5387	-0.0020	0.4835	0.6797	33.22
R-ratio(99%,99%)	Winner (W)	0.0500	1.6266	1.6361	0.0054	0.3023	0.4289	35.24
	Loser (L)	0.3003	1.0894	1.0830	0.0022	0.2316	0.3535	63.39
	W – L	0.5974	1.1324	1.2882	0.0127	0.2212	0.3161	14.44
R-ratio(95%,95%)	Winner (W)	0.0500	1.6630	1.6881	0.0094	0.3294	0.4600	35.65
	Loser (L)	0.4629	0.9745	0.9448	-0.0002	0.2304	0.3563	64.74
	W – L	0.1903	1.5207	1.6450	0.0264	0.2452	0.3418	12.25
R-ratio(90%,90%)	Winner (W)	0.0501	1.6728	1.6901	0.0125	0.3336	0.4658	34.57
	Loser (L)	0.9131	0.6500	0.5814	0.0014	0.2211	0.3371	65.09
	W – L	0.2621	1.2970	1.3826	0.0250	0.2816	0.3495	10.96
R-ratio(50%,99%)	Winner (W)	0.0500	1.6440	1.6473	0.0116	0.3919	0.5533	27.00
	Loser (L)	1.3377	0.3170	0.2621	-0.0001	0.1780	0.2770	67.89
	W – L	0.0624	1.5050	1.5960	0.0363	0.3310	0.4512	14.83
R-ratio(50%,95%)	Winner (W)	0.0500	1.5884	1.5990	0.0243	0.3717	0.5262	28.34
	Loser (L)	1.1848	0.3975	0.3456	-0.0001	0.2248	0.3424	68.16
	W – L	1.2444	0.5611	0.5777	0.0326	0.3044	0.3960	13.30
R-ratio(50%,90%)	Winner (W)	0.0505	1.6138	1.6224	0.0147	0.3646	0.5146	33.36
	Loser (L)	1.2180	0.3736	0.3352	-0.0001	0.2299	0.3613	65.65
	W – L	1.2080	0.5865	0.5558	0.0264	0.2920	0.3800	12.46

4.3.2 Commodity markets

Similar to the currency market, it is found that the reward-risk portfolios in commodity markets also beat the cumulative return based strategy. According to Table 4.3, the alternative momentum strategies in the commodity markets exhibit negative average returns regardless of ranking criterion and outperform the traditional trend-following strategy with the monthly return of -0.79%. Those strategies are also less volatile with smaller standard deviation than the benchmark strategy with the volatility of 5.59%. The R-ratio strategies generate the larger average returns of -0.33%– -0.06% and the smaller standard deviations in the range of 3.99%–4.31%. In particular, the R-ratio(50%,9X%) strategies achieve the best performance among the R-ratio criteria. The next best portfolios are the Sharpe ratio and CVaR(90%) strategies with monthly -0.22% and -0.26%, respectively.

In the commodity markets, the reward-risk measures are good at filtering the momentum signal. The behaviors of the winner and loser groups are similar to the case in the currency universe. All winner groups in the alternative ranking rules are followed by the winner basket of the traditional momentum portfolio in performance. The best winner performer is the R-ratio(50%,90%) portfolio with monthly 0.72%. The CVaR(99%) and Sharpe ratio criteria provide the next best winner baskets with monthly 0.66% and 0.61%. These long positions of the alternative strategies are at the lower volatility levels than that of the cumulative return strategy. Additionally, all the loser groups underperform the loser group of the cumulative return criterion. The poor performance in short position is desirable for increasing the profitability of the

Table 4.3: Summary statistics of monthly 6/6 momentum portfolios in commodity markets

Criterion	Portfolio	Summary statistics				
		Mean	Std. Dev.	Skewness	Kurtosis	Final Wealth
Cumulative return	Winner (W)	0.4143	5.1784	-1.0806	5.2535	0.9694
	Loser (L)	1.2053	4.8953	-0.2249	1.3746	2.8204
	W – L	-0.7910	5.5935	-0.2445	0.2579	-1.8510
Sharpe ratio	Winner (W)	0.6064	5.1466	-0.8979	3.6700	1.4190
	Loser (L)	0.8273	4.3070	-0.6332	2.5603	1.9360
	W – L	-0.2209	4.5718	-0.0674	-0.3583	-0.5170
CVaR(99%)	Winner (W)	0.6631	3.6342	-0.8517	3.5270	1.5517
	Loser (L)	0.9276	5.2643	-0.2828	1.2405	2.1706
	W – L	-0.2645	4.3264	-0.2562	0.9318	-0.6189
CVaR(95%)	Winner (W)	0.5997	3.4050	-0.7986	3.9883	1.4033
	Loser (L)	0.9575	5.3540	-0.3387	1.2568	2.2406
	W – L	-0.3578	4.4633	-0.2766	0.6479	-0.8373
CVaR(90%)	Winner (W)	0.5338	3.3410	-0.9823	4.0281	1.2491
	Loser (L)	0.9718	5.4232	-0.3288	1.1617	2.2741
	W – L	-0.4380	4.5934	-0.1550	0.4317	-1.0250
STARR(99%)	Winner (W)	0.5907	3.7046	-1.0038	4.3935	1.3823
	Loser (L)	0.9294	5.2586	-0.2552	1.4219	2.1747
	W – L	-0.3387	4.3930	-0.2675	0.9513	-0.7925
STARR(95%)	Winner (W)	0.5376	3.5036	-0.9090	3.6746	1.2580
	Loser (L)	0.9299	5.3508	-0.2844	1.3115	2.1759
	W – L	-0.3923	4.4493	-0.3029	0.5762	-0.9179
STARR(90%)	Winner (W)	0.4963	3.5004	-1.0908	4.9997	1.1613
	Loser (L)	0.9559	5.4563	-0.2540	1.2031	2.2367
	W – L	-0.4596	4.7060	-0.1914	0.5041	-1.0754
R-ratio(99%,99%)	Winner (W)	0.5915	4.4427	-0.8225	3.0958	1.3840
	Loser (L)	0.8540	4.3695	-0.4970	1.3058	1.9984
	W – L	-0.2626	4.0172	0.0491	0.2316	-0.6144
R-ratio(95%,95%)	Winner (W)	0.5374	4.2729	-1.0231	4.3569	1.2576
	Loser (L)	0.8656	4.1993	-0.2917	1.5985	2.0255
	W – L	-0.3282	3.9956	-0.1576	0.1118	-0.7679
R-ratio(90%,90%)	Winner (W)	0.5887	4.4228	-1.0648	4.6065	1.3775
	Loser (L)	0.8720	4.1982	-0.3809	1.7478	2.0406
	W – L	-0.2834	4.0549	-0.2807	0.2554	-0.6631
R-ratio(50%,99%)	Winner (W)	0.5581	4.8855	-1.1222	4.5402	1.3059
	Loser (L)	0.7970	4.1559	-0.6035	2.6882	1.8650
	W – L	-0.2390	4.1749	-0.1373	0.8693	-0.5592
R-ratio(50%,95%)	Winner (W)	0.5819	4.6565	-0.9870	4.0067	1.3616
	Loser (L)	0.8092	4.2402	-0.5323	2.5387	1.8936
	W – L	-0.2274	4.2693	-0.3293	0.5660	-0.5320
R-ratio(50%,90%)	Winner (W)	0.7209	4.7138	-0.8867	3.0352	1.6868
	Loser (L)	0.7806	4.3313	-0.4248	2.3588	1.8266
	W – L	-0.0597	4.3054	-0.4928	0.9752	-0.1397

momentum portfolio.

The risk profiles of these reward-risk strategies are more impressive. As seen in Table 4.4, the maximum drawdowns of the strategies are in the range

of 52.20–71.68%, substantially smaller than that of the traditional trend-following strategy, 85.75%. The 95% VaRs and CVaRs by the reward-risk strategies are also below the 95% VaR and CVaR levels of the original momentum portfolio. Moreover, the Sharpe ratios of the alternative strategies, except for the STARR(90%) strategy, are larger than that of cumulative return strategy. The different patterns in the risk characteristics are also observed as it is found in the currency markets. The CVaR and STARR strategies exhibit larger λ_- values than the momentum strategy. Meanwhile, with the R-ratio and Sharpe ratio, the λ_- values of the portfolios are smaller than that of the benchmark strategy except for some R-ratio portfolios.

The risk patterns of the long/short positions also show the superiority of the alternative reward-risk strategies. The smaller VaR and CVaR levels are achieved by the winner groups of these strategies. Since the long baskets of the reward-risk strategies outperform that of the traditional momentum, the lower VaR and CVaR levels of the winner groups impose that these groups generate the more profits by accepting the lower risks. The Sharpe ratios and maximum drawdowns of the long baskets are superior to the reward-risk measures of the winner basket by the cumulative return selection rule. Other ranking portfolios feature lower VaR and CVaR levels for the winner groups but larger risk measures for the loser groups. The lower risk acceptance of the long positions is also cross-checked by the higher λ_- values than that of the long position for the momentum portfolio. In the case of short position, the CTS downside tail indices of R-ratio and Sharpe ratio strategies are smaller than the short position of the cumulative return. Meanwhile, the CVaR and STARR strategies have larger λ_- values.

Table 4.4: Summary risk statistics of monthly 6/6 momentum portfolios in commodity markets

Criterion	Portfolio	CTS parameters			Risk measures			
		α	λ_+	λ_-	Sharpe	$\text{VaR}_{95\%}$	$\text{CVaR}_{95\%}$	MDD
Cumulative return	Winner (W)	1.3720	0.9916	0.6312	0.0350	1.0760	1.5650	61.66
	Loser (L)	0.1958	2.0049	1.9494	0.0604	1.1308	1.5448	35.93
	W – L	0.9216	1.4964	1.3690	-0.0176	1.3787	1.8632	85.75
Sharpe ratio	Winner (W)	0.4635	2.0927	1.6750	0.0430	1.1685	1.6479	59.19
	Loser (L)	0.8170	1.2921	1.2816	0.0414	1.1398	1.5368	43.66
	W – L	0.9183	1.3461	1.1814	0.0005	1.4338	1.9571	58.31
CVaR(99%)	Winner (W)	0.9785	1.2509	1.1633	0.0445	0.7570	1.0685	42.33
	Loser (L)	0.2422	2.2452	1.9497	0.0489	1.2025	1.6235	44.40
	W – L	1.0338	1.1273	1.5324	-0.0160	0.9733	1.2693	59.71
CVaR(95%)	Winner (W)	0.9448	1.3126	1.1662	0.0492	0.7446	1.0528	43.76
	Loser (L)	0.0500	2.4102	2.1969	0.0437	1.2350	1.6702	44.85
	W – L	0.9278	1.3522	1.5423	-0.0146	1.0126	1.3319	64.68
CVaR(90%)	Winner (W)	0.9245	1.3392	1.1408	0.0463	0.7632	1.0823	43.76
	Loser (L)	0.0501	2.3793	2.1784	0.0439	1.2369	1.6871	44.56
	W – L	0.3408	1.9163	2.0487	-0.0179	1.0914	1.4583	71.68
STARR(99%)	Winner (W)	0.9331	1.3316	1.1827	0.0388	0.7990	1.1277	49.08
	Loser (L)	0.0500	2.4853	2.2204	0.0436	1.2130	1.6169	44.50
	W – L	1.1206	1.0505	1.3073	-0.0130	1.0099	1.3323	62.34
STARR(95%)	Winner (W)	0.9266	1.3549	1.1489	0.0440	0.7475	1.0581	46.89
	Loser (L)	0.2859	2.1234	1.9041	0.0441	1.2462	1.6939	44.85
	W – L	0.9204	1.3606	1.6227	-0.0160	0.9901	1.3005	66.57
STARR(90%)	Winner (W)	0.9181	1.3089	1.0937	0.0453	0.7500	1.0689	46.40
	Loser (L)	0.0501	2.3661	2.1507	0.0437	1.2607	1.7114	38.78
	W – L	0.9370	1.2727	1.4695	-0.0187	1.0747	1.4262	71.56
R-ratio(99%,99%)	Winner (W)	0.4814	1.7380	1.6970	0.0329	1.0402	1.3394	52.62
	Loser (L)	0.9261	1.5171	1.1059	0.0544	1.1560	1.6415	39.32
	W – L	0.9285	1.3067	1.5299	-0.0129	1.2503	1.6093	65.03
R-ratio(95%,95%)	Winner (W)	0.5422	1.7836	1.6769	0.0377	1.0174	1.3677	53.89
	Loser (L)	0.9138	1.4485	1.1528	0.0517	1.1874	1.6781	39.76
	W – L	0.9954	1.2907	1.3079	-0.0129	1.1978	1.5729	70.98
R-ratio(90%,90%)	Winner (W)	0.0500	2.4029	2.2400	0.0438	1.0362	1.3952	53.33
	Loser (L)	0.8122	1.5034	1.2426	0.0487	1.2531	1.7657	37.30
	W – L	1.2229	0.9370	0.9757	-0.0060	1.1654	1.5548	70.40
R-ratio(50%,99%)	Winner (W)	0.1966	2.2214	2.0415	0.0399	1.0994	1.4746	56.55
	Loser (L)	1.0158	1.0838	0.9312	0.0433	0.9920	1.4269	38.76
	W – L	1.2547	0.9740	0.9249	-0.0021	1.0660	1.4203	60.97
R-ratio(50%,95%)	Winner (W)	0.9164	1.4355	1.2057	0.0409	1.0998	1.4837	53.13
	Loser (L)	0.9421	1.2119	1.0704	0.0432	0.9968	1.4152	43.02
	W – L	1.4945	0.6476	0.5690	0.0017	1.0466	1.4391	58.70
R-ratio(50%,90%)	Winner (W)	0.9074	1.6374	1.3227	0.0483	1.0802	1.4626	51.92
	Loser (L)	0.9641	1.2459	1.0570	0.0433	1.0282	1.4610	42.76
	W – L	0.9620	1.3896	1.3335	0.0055	1.0946	1.4697	52.20

4.3.3 Global stock benchmark indices

As seen in Table 4.5, the outperformance of the alternative portfolios is also attained in the global stock benchmark index universe. While the cumulative return criterion obtains monthly 0.51% with standard deviation of 4.23%, the best performers are the R-ratio(90%,90%) and R-ratio(95%,95%) portfolios with 0.63% and 0.58%, respectively. The standard deviations of these strategies are 3.47% and 3.16%, much less volatile than the traditional momentum strategy. Accepting smaller return fluctuations, the STARR(90%), Sharpe ratio, and R-ratio(50%,90%) also provide higher average returns than the benchmark strategy. The performance of the R-ratio(50%,90%) and R-ratio(99%,99%) strategies are comparable with the cumulative return portfolio and the volatility level of those portfolios are significantly lower. Smaller standard deviations are also obtained by the other selection rules.

The strong performance of the winner baskets in the reward-risk strategies is found in the global benchmark index universe regardless of criterion. The winner groups obtain 0.86%–1.18% and the top 4 best long positions are from the R-ratio criteria. The long basket in the Sharpe ratio portfolio is also followed by the cumulative return winner group. Additionally, the volatility levels of these winner baskets are lower than the the benchmark case. The skewness of every R-ratio long position is greater than the traditional momentum case, i.e. the downside tails of the R-ratio strategies are thinner. For loser groups, the average returns are in the range of 0.46–0.60% while the cumulative return loser group achieves 0.49%. Although the loser groups of the reward-risk momentum strategies tend to perform slightly better than the

Table 4.5: Summary statistics of monthly 6/6 momentum portfolios in global stock benchmark indices

Criterion	Portfolio	Summary statistics				
		Mean	Std. Dev.	Skewness	Kurtosis	Final Wealth
Cumulative return	Winner (W)	0.9905	5.9325	-1.1304	3.7568	2.3178
	Loser (L)	0.4851	6.6008	-0.7938	3.0113	1.1350
	W – L	0.5054	4.2311	0.1320	0.8529	1.1827
Sharpe ratio	Winner (W)	1.0586	5.8729	-1.2502	4.7906	2.4772
	Loser (L)	0.5297	5.8772	-0.8649	3.6942	1.2396
	W – L	0.5289	3.3999	-0.1069	0.5636	1.2377
CVaR(99%)	Winner (W)	0.8723	4.9680	-1.1605	3.9285	2.0412
	Loser (L)	0.5861	7.3019	-0.7672	1.9657	1.3715
	W – L	0.2862	3.9970	0.4240	2.8749	0.6697
CVaR(95%)	Winner (W)	0.8593	4.9428	-1.3736	5.1772	2.0107
	Loser (L)	0.5398	7.3079	-0.7509	1.7926	1.2632
	W – L	0.3194	4.0510	0.3798	2.4666	0.7475
CVaR(90%)	Winner (W)	0.9216	5.0045	-1.2665	4.8889	2.1566
	Loser (L)	0.4636	7.2697	-0.7344	1.6345	1.0848
	W – L	0.4580	4.0226	0.3939	2.3733	1.0718
STARR(99%)	Winner (W)	0.9361	4.9617	-1.3080	4.4615	2.1905
	Loser (L)	0.5785	7.2497	-0.7217	1.7708	1.3537
	W – L	0.3576	4.0123	0.3719	3.0792	0.8368
STARR(95%)	Winner (W)	0.9017	5.0220	-1.3293	4.9186	2.1100
	Loser (L)	0.5332	7.1981	-0.7311	1.8412	1.2477
	W – L	0.3685	3.9964	0.2788	2.7878	0.8623
STARR(90%)	Winner (W)	1.0039	5.0770	-1.3917	5.4502	2.3490
	Loser (L)	0.4689	7.1887	-0.7465	1.7680	1.0972
	W – L	0.5350	3.9795	0.4948	2.9160	1.2518
R-ratio(99%,99%)	Winner (W)	1.0947	5.7644	-0.7168	2.2020	2.5617
	Loser (L)	0.6166	5.8873	-1.0293	2.9335	1.4429
	W – L	0.4781	2.8936	0.5906	3.8428	1.1188
R-ratio(95%,95%)	Winner (W)	1.1799	5.9191	-0.6809	2.5225	2.7610
	Loser (L)	0.5993	5.9333	-0.9607	3.0226	1.4025
	W – L	0.5806	3.1583	0.1902	3.4522	1.3585
R-ratio(90%,90%)	Winner (W)	1.1711	5.9908	-0.8077	3.3492	2.7405
	Loser (L)	0.5449	6.0320	-1.0438	3.5434	1.2751
	W – L	0.6262	3.4709	0.1290	2.5468	1.4653
R-ratio(50%,99%)	Winner (W)	0.9422	5.9046	-1.0095	4.1233	2.2049
	Loser (L)	0.5731	5.8747	-0.9605	4.1299	1.3410
	W – L	0.3692	3.0054	-0.0994	2.6143	0.8639
R-ratio(50%,95%)	Winner (W)	0.9426	5.8568	-0.9330	4.1479	2.2058
	Loser (L)	0.5306	5.9947	-1.0009	3.6159	1.2415
	W – L	0.4121	3.3019	-0.1268	2.0959	0.9643
R-ratio(50%,90%)	Winner (W)	1.0995	6.0004	-0.9742	4.4194	2.5729
	Loser (L)	0.5948	6.0052	-0.9199	3.6425	1.3919
	W – L	0.5047	3.3742	-0.2066	2.0993	1.1810

original momentum strategy, smaller skewness is obtained by the short positions of the R-ratio and Sharpe-ratio portfolios. The smaller skewness imposes that the loser baskets are exposed to the more downside tail risk which are

likely to generate the profits from the short positions.

In Table 4.6, it is found that the reward-risk strategies, in particular, the R-ratio strategies are less riskier than the traditional trend-following strategy. With 95% VaR and CVaR, all the reward-risk strategies, except for the STARR(99%) strategy, are less riskier than the benchmark strategy. Additionally, the maximum drawdowns of the R-ratio strategies are substantially lower than that of the cumulative return strategy. The Sharpe ratio, CVaR, and STARR momentum portfolios exhibit the comparable sizes of maximum drawdowns. Larger Sharpe ratios are obtained by the Sharpe ratio, R-ratio(90%,90%), R-ratio(50%,90%), and R-ratio(95%,95%) strategies. In this sense, the reward-risk portfolios generate more profits under less exposure to the risk. In particular, the R-ratio and Sharpe ratio criteria are better both in performance and risk.

The maximum drawdown of each ranking group is also well-matched to the purpose of the group. The winner baskets of the reward-risk strategies exhibit smaller maximum drawdowns and the maximum drawdowns of the losers are higher. The 95% VaR and CVaR levels of these portfolios are slightly different with the maximum drawdown. The CVaR and STARR criteria feature lower VaRs and CVaRs than the long basket of the R-ratio and Sharpe ratio portfolio. The short baskets of the alternative portfolios obtain lower VaR and CVaR values than the momentum strategy.

Table 4.6: Summary risk statistics of monthly 6/6 momentum portfolios in global stock benchmark indices

Criterion	Portfolio	CTS parameters			Risk measures			
		α	λ_+	λ_-	Sharpe	$\text{VaR}_{95\%}$	$\text{CVaR}_{95\%}$	MDD
Cumulative return	Winner (W)	0.0500	2.0979	1.9009	0.0968	0.6016	0.8975	66.04
	Loser (L)	0.0503	1.8561	1.7458	0.0150	1.1133	1.6152	59.87
	W – L	0.0500	1.9911	1.9836	0.0397	0.8778	1.2456	39.25
Sharpe ratio	Winner (W)	0.1611	1.9514	1.7597	0.0890	0.6364	0.9404	61.60
	Loser (L)	0.8824	1.2630	1.1015	0.0478	0.9627	1.4030	56.83
	W – L	0.0500	1.8594	1.8528	0.0450	0.7009	0.9868	36.68
CVaR(99%)	Winner (W)	0.7714	1.5418	1.2731	0.0811	0.6222	0.9331	57.18
	Loser (L)	0.0501	1.9593	1.8333	0.0588	0.9804	1.4291	64.82
	W – L	0.0505	1.8343	1.9519	-0.0156	0.8550	1.1789	38.42
CVaR(95%)	Winner (W)	0.0500	2.0608	1.9121	0.0784	0.6208	0.9172	58.40
	Loser (L)	0.0500	1.8935	1.7896	0.0563	0.9796	1.4324	64.76
	W – L	0.0501	1.7456	1.8405	-0.0131	0.8602	1.1868	39.25
CVaR(90%)	Winner (W)	0.0500	2.1249	1.9480	0.0842	0.6146	0.8973	57.76
	Loser (L)	0.0500	1.9191	1.8091	0.0532	0.9805	1.4302	64.79
	W – L	0.0500	1.7962	1.8969	-0.0041	0.8606	1.1760	40.41
STARR(99%)	Winner (W)	0.1835	2.0098	1.8181	0.0850	0.6149	0.9185	59.81
	Loser (L)	0.0502	1.9893	1.8419	0.0580	0.9843	1.4329	62.56
	W – L	1.3829	0.3941	0.4447	-0.0000	0.8781	1.3049	38.01
STARR(95%)	Winner (W)	0.0500	2.1778	1.9757	0.0887	0.5990	0.8842	60.07
	Loser (L)	0.0501	1.9396	1.8233	0.0555	0.9902	1.4404	63.10
	W – L	0.0500	1.7790	1.8637	0.0005	0.8368	1.1590	40.45
STARR(90%)	Winner (W)	0.0500	2.2164	2.0290	0.0899	0.5915	0.8724	61.03
	Loser (L)	0.0501	1.9499	1.8431	0.0522	1.0621	1.5389	62.43
	W – L	0.0500	1.7647	1.8517	0.0077	0.8716	1.2138	39.07
R-ratio(99%,99%)	Winner (W)	0.0500	1.9375	1.8094	0.0682	0.7317	1.0762	61.95
	Loser (L)	0.0530	2.0874	1.9035	0.0667	0.6960	1.0160	59.22
	W – L	0.0500	1.8410	1.8344	0.0285	0.5720	0.7874	26.74
R-ratio(95%,95%)	Winner (W)	0.0500	1.8674	1.7495	0.0814	0.7375	1.0939	61.81
	Loser (L)	0.0500	1.9943	1.8418	0.0563	0.7425	1.0792	60.21
	W – L	0.0500	1.9181	1.8727	0.0386	0.5661	0.7748	28.23
R-ratio(90%,90%)	Winner (W)	0.0500	1.9043	1.7863	0.0815	0.7076	1.0518	63.97
	Loser (L)	0.0501	1.8711	1.7454	0.0482	0.7780	1.1356	60.17
	W – L	0.0500	1.8931	1.8639	0.0442	0.5518	0.7645	30.55
R-ratio(50%,99%)	Winner (W)	0.0500	2.0586	1.8799	0.0616	0.6885	1.0175	61.59
	Loser (L)	0.0500	1.8478	1.7322	0.0530	0.8224	1.2045	63.54
	W – L	0.0500	1.6900	1.7341	0.0318	0.5997	0.8451	26.25
R-ratio(50%,95%)	Winner (W)	0.0500	2.1160	1.9211	0.0741	0.6881	1.0143	60.93
	Loser (L)	0.0500	1.8117	1.7401	0.0474	0.8394	1.2234	61.02
	W – L	0.0500	1.8467	1.8361	0.0328	0.5631	0.7899	27.79
R-ratio(50%,90%)	Winner (W)	0.0500	2.0039	1.8754	0.0878	0.6834	1.0134	62.75
	Loser (L)	0.0501	1.8849	1.7849	0.0537	0.8326	1.2112	59.56
	W – L	0.0500	2.0022	1.9599	0.0422	0.5403	0.7582	23.14

4.3.4 South Korea equity market: KOSPI 200

In the KOSPI 200 universe, the reward-risk momentum strategies not only outperform the cumulative return strategy but also feature lower volatility. According to the summary statistics of the reward-risk strategies in Table 4.7, the best strategies are given by the STARR criteria. The STARR(90%) achieves monthly 1.62% with the volatility of 6.73% while the cumulative return provides monthly 0.97% with the standard deviation of 7.56%. The STARR(95%) and STARR(99%) portfolios are the next top performer obtaining the average returns of 1.53% and 1.50% and the monthly return fluctuation levels of the portfolios are 6.68% and 5.98%, respectively. The CVaR portfolios also obtain better performance and are less volatile than the cumulative return. The CVaR(99%), CVaR(95%) and CVaR(90%) based strategies generate 1.48%, 1.35%, and 1.24%, respectively. These CVaR criteria also have smaller standard deviations, 6.27%–6.94%.

Similar to other asset classes, the R-ratio(50%,9X%) strategies also feature better performance than the traditional momentum strategy. The R-ratio(50%,99%) and R-ratio(50%,95%) strategies generate the monthly profits of 1.15%. The two alternative portfolios with the monthly volatility levels of 4.45%–4.67% are much less volatile not only than the original trend-following strategy but also than the CVaR and STARR portfolios. The R-ratio(50%,90%) portfolio with the average return of 1.00% and the volatility of 4.46% is still better in performance and risk. Although the Sharpe ratio strategy is slightly poorer in performance than the benchmark strategy, the standard deviation of the performance is much reduced. Meanwhile, the R-

Table 4.7: Summary statistics of monthly 6/6 momentum portfolios in South Korea KOSPI 200

Criterion	Portfolio	Summary statistics				
		Mean	Std. Dev.	Skewness	Kurtosis	Final Wealth
Cumulative return	Winner (W)	1.4398	9.0217	-0.3171	2.2066	1.6414
	Loser (L)	0.4684	9.1068	-0.4597	4.1819	0.5339
	W – L	0.9714	7.5597	0.0182	0.7296	1.1074
Sharpe ratio	Winner (W)	1.8949	8.1841	-0.4886	2.1096	2.1602
	Loser (L)	0.9584	8.0359	-0.8615	5.0522	1.0925
	W – L	0.9365	5.6301	0.3053	0.5808	1.0677
CVaR(99%)	Winner (W)	1.3118	5.7065	-0.6048	2.8393	1.4955
	Loser (L)	-0.1689	9.9050	-1.5460	10.0696	-0.1925
	W – L	1.4807	6.2786	1.0819	5.9193	1.6880
CVaR(95%)	Winner (W)	1.2905	5.5849	-0.4143	2.5666	1.4712
	Loser (L)	-0.0613	10.2952	-1.1747	7.5463	-0.0699
	W – L	1.3519	6.9397	0.5886	3.6766	1.5411
CVaR(90%)	Winner (W)	1.2074	5.5331	-0.6038	3.1926	1.3765
	Loser (L)	-0.0341	10.2453	-1.0795	6.6876	-0.0388
	W – L	1.2415	6.7954	0.3954	2.8837	1.4153
STARR(99%)	Winner (W)	1.3306	5.8878	-0.7975	4.3349	1.5169
	Loser (L)	-0.1647	9.8757	-1.5148	10.2862	-0.1878
	W – L	1.4953	5.9833	0.7815	4.3467	1.7046
STARR(95%)	Winner (W)	1.3460	5.7153	-0.5123	3.2865	1.5344
	Loser (L)	-0.1814	10.1670	-0.9790	6.8045	-0.2068
	W – L	1.5274	6.6811	0.3329	2.4814	1.7412
STARR(90%)	Winner (W)	1.3591	5.5502	-0.6069	3.7614	1.5494
	Loser (L)	-0.2631	10.2472	-0.9260	6.0243	-0.2999
	W – L	1.6222	6.7347	0.1402	1.9444	1.8493
R-ratio(99%,99%)	Winner (W)	1.4438	7.8759	-0.7614	2.3934	1.6459
	Loser (L)	0.9616	7.6100	-1.3860	5.6460	1.0963
	W – L	0.4821	4.3156	-0.2820	-0.0043	0.5496
R-ratio(95%,95%)	Winner (W)	1.3230	7.7621	-0.6399	3.4614	1.5082
	Loser (L)	0.8531	7.7857	-1.2492	5.0462	0.9725
	W – L	0.4699	4.6851	0.2020	0.2420	0.5357
R-ratio(90%,90%)	Winner (W)	1.5087	7.4916	-0.3809	2.7238	1.7199
	Loser (L)	0.8257	7.5730	-1.3530	5.6923	0.9413
	W – L	0.6829	4.5874	0.3489	0.5876	0.7785
R-ratio(50%,99%)	Winner (W)	1.7095	7.6654	-0.7838	3.7805	1.9488
	Loser (L)	0.5574	7.9100	-1.3168	6.6333	0.6355
	W – L	1.1521	4.4496	0.2340	0.3793	1.3134
R-ratio(50%,95%)	Winner (W)	1.7754	7.8268	-0.7106	3.8838	2.0239
	Loser (L)	0.6279	7.7797	-1.1171	5.5356	0.7158
	W – L	1.1474	4.6714	0.3849	1.4663	1.3081
R-ratio(50%,90%)	Winner (W)	1.7137	7.5797	-0.6446	3.6913	1.9537
	Loser (L)	0.7159	7.9767	-0.9611	5.0985	0.8161
	W – L	0.9978	4.4564	0.3819	1.8013	1.1375

ratio(9X%,9X%) strategies underperform the momentum strategy although the strategies are less volatile in the deviation measure. Every reward-risk strategy is under larger skewness than the cumulative return strategy.

The behaviors of winner and loser deciles are followings. With the STARR and CVaR selection rules, the winner groups underperform that of the traditional momentum strategy by 0.10%. However, the loser groups perform much poorly than the loser group of the cumulative return strategy by 0.60%–0.70%. The different amounts of the shifts make the reward-risk strategies more profitable. Meanwhile, the winner and loser groups of the Sharpe ratio and R-ratio strategies tend to outperform the original trend-following strategy. The long/short positions of all the reward-risk portfolios exhibit the smaller skewness than the benchmark strategy.

The less riskier performance of the reward-risk strategies are also cross-checked with the risk characteristics given in Table 4.8. The maximum drawdowns of all the reward-risk strategies are substantially decreased. In particular, the maximum drawdowns of the R-ratio(50%,9X%) strategies are 17.31%–24.63%, significantly smaller than 63.97% of the traditional momentum strategy. The STARR portfolios also achieve 27.97%–33.46% and the CVaR criteria obtain 32.74%–35.92% of maximum drawdowns. The maximum drawdown of the Sharpe ratio portfolio is 49.57% which is higher than other criteria but still smaller than the benchmark case. More interesting caveat is that all the R-ratio momentum portfolios are remarkably less riskier because their VaRs and CVaRs are decreased by 30%–40%. The 95% VaR and CVaR levels of the STARR(99%), STARR(90%), Sharpe ratio, and CVaR(99%) strategies are also lower than those of the trend-following strategy. In addition to that, the λ_{-} values of all the R-ratio portfolios are larger than that of the momentum strategy. This fact indicates that those portfolios are under the lower tail risk. The Sharpe ratios of the Sharpe ratio, CVaR(99%) and R-ratio(50%,9X%)

Table 4.8: Summary risk statistics of monthly 6/6 momentum portfolios in South Korea KOSPI 200

Criterion	Portfolio	CTS parameters			Risk measures			
		α	λ_+	λ_-	Sharpe	$\text{VaR}_{95\%}$	$\text{CVaR}_{95\%}$	MDD
Cumulative return	Winner (W)	0.8478	2.1575	1.2321	0.0574	1.3611	1.9685	63.36
	Loser (L)	0.7857	2.6316	1.3006	0.0597	1.7720	2.5289	61.04
	W – L	0.7958	1.8394	1.8233	0.0301	1.8387	2.4195	63.97
Sharpe ratio	Winner (W)	0.7768	2.3318	1.2925	0.0857	1.3897	2.0182	63.52
	Loser (L)	0.6705	2.8222	1.3440	0.0793	1.4732	2.0966	57.35
	W – L	0.0500	3.2275	3.0301	0.0386	1.4387	1.9039	49.57
CVaR(99%)	Winner (W)	0.7763	2.1096	1.3939	0.0856	1.2377	1.7574	43.27
	Loser (L)	0.8115	2.1446	1.0821	0.0435	1.8999	2.7423	76.76
	W – L	1.4470	0.5609	1.1020	0.0404	1.7143	2.1861	32.74
CVaR(95%)	Winner (W)	0.7997	1.9605	1.3082	0.0845	1.1781	1.7147	42.86
	Loser (L)	0.8220	2.5174	1.1561	0.0444	2.0738	2.8467	74.27
	W – L	0.8787	1.1987	1.8770	0.0270	1.9567	2.4884	35.70
CVaR(90%)	Winner (W)	0.4379	2.3799	1.7123	0.0852	1.2029	1.7302	43.77
	Loser (L)	0.8320	2.5104	1.1420	0.0461	2.0740	2.9225	72.88
	W – L	1.1769	0.8078	1.5383	0.0172	1.9343	2.5135	35.92
STARR(99%)	Winner (W)	0.7518	2.0932	1.4361	0.0826	1.2487	1.7661	48.34
	Loser (L)	0.8042	2.0746	1.0620	0.0446	1.8875	2.7616	76.01
	W – L	1.4385	0.5687	1.0741	0.0399	1.6948	2.1915	27.97
STARR(95%)	Winner (W)	0.6662	2.2644	1.5439	0.0869	1.2036	1.7098	45.15
	Loser (L)	0.7992	2.1960	1.1022	0.0423	2.0961	2.9631	73.99
	W – L	1.2638	0.7440	1.3256	0.0333	2.0472	2.5786	30.97
STARR(90%)	Winner (W)	0.6063	2.3069	1.6306	0.0868	1.1812	1.6821	44.97
	Loser (L)	0.8128	2.1695	1.0729	0.0415	2.0908	2.9479	73.93
	W – L	1.3431	0.6194	1.3335	0.0301	1.9072	2.3904	33.46
R-ratio(99%,99%)	Winner (W)	0.8585	2.7585	1.2858	0.0800	1.3245	1.9144	59.63
	Loser (L)	0.8275	2.1835	1.1921	0.0732	1.3315	1.9277	62.41
	W – L	0.7841	1.9352	1.9353	0.0219	1.2057	1.6272	36.54
R-ratio(95%,95%)	Winner (W)	0.8744	2.8021	1.3169	0.0708	1.2916	1.8392	62.61
	Loser (L)	0.8931	2.0968	1.1701	0.0704	1.4142	2.0419	64.15
	W – L	0.3083	3.4434	3.5048	0.0159	1.2456	1.6523	37.59
R-ratio(90%,90%)	Winner (W)	0.7927	3.0129	1.5758	0.0744	1.3054	1.8505	57.92
	Loser (L)	0.8319	2.2215	1.1868	0.0717	1.4654	2.1195	62.89
	W – L	0.7879	1.8989	2.1168	0.0192	1.2328	1.6690	25.50
R-ratio(50%,99%)	Winner (W)	0.7840	3.3015	1.6325	0.0763	1.3522	1.9132	58.96
	Loser (L)	0.8136	2.3232	1.1549	0.0642	1.4451	2.0702	62.14
	W – L	0.8466	1.6880	1.8100	0.0495	1.2995	1.7366	17.31
R-ratio(50%,95%)	Winner (W)	0.8499	4.6116	1.8431	0.0761	1.3130	1.8300	58.86
	Loser (L)	0.8250	2.3388	1.1320	0.0629	1.3904	2.0094	61.30
	W – L	0.7449	2.1419	2.2175	0.0480	1.2479	1.6763	22.01
R-ratio(50%,90%)	Winner (W)	0.8037	3.9623	1.7733	0.0779	1.3327	1.8677	58.31
	Loser (L)	0.8393	2.0942	1.0814	0.0629	1.4042	2.0388	61.13
	W – L	0.7499	2.0112	2.2066	0.0398	1.2411	1.6618	24.63

criteria are higher than that of the cumulative return portfolio.

The risk profile of each ranking basket is also consistent with the purpose

of the ranking group. The winner (loser) groups of the reward-risk portfolios feature smaller (larger) risk measures such as VaR, CVaR, and maximum drawdowns. Larger (smaller) Sharpe ratios are available for the winner (loser) groups. It is also supported by the CTS parameter λ_- of each basket. The λ_- values for the winner (loser) deciles are greater (smaller) than that of the long (short) basket in the momentum portfolio. The risk characteristics of the ranking deciles in the R-ratio strategies are slightly different with other portfolios. The R-ratio strategies are also less riskier in the level of both ranking baskets. The winner and loser groups of the R-ratio portfolios are less riskier in 95% VaR and CVaR. The Sharpe ratios of the both baskets beat those of the benchmark ranking baskets.

4.3.5 U.S. equity market: SPDR sector ETFs

The R-ratio momentum strategies in the SPDR U.S. sector ETF universe exhibit better performance than the traditional momentum strategy as seen in Table 4.9. Comparing with the benchmark momentum strategy providing the monthly return of 0.33% and the standard deviation of 4.34%, the R-ratio(50%,99%), R-ratio(50%,90%), and R-ratio(50%,95%) portfolios generate monthly 0.62%, 0.58%, and 0.58%, respectively. The standard deviations of the portfolio returns are decreased by about 25%. The R-ratio(90%,90%) and Sharpe ratio criteria not only outperform the cumulative return portfolio by 0.08% and 0.04% but also obtain lower volatility levels. The other stock selection rules follow the original momentum strategy in performance. The skewness of every reward-risk strategy is larger than the cumulative return

based strategy.

Table 4.9: Summary statistics of monthly 6/6 momentum portfolios in U.S. sector ETF

Criterion	Portfolio	Summary statistics				
		Mean	Std. Dev.	Skewness	Kurtosis	Final Wealth
Cumulative return	Winner (W)	0.5893	4.8317	-0.8700	1.9482	0.9547
	Loser (L)	0.2624	5.4676	-0.4482	0.7811	0.4251
	W – L	0.3269	4.3365	-0.2319	1.1894	0.5296
Sharpe ratio	Winner (W)	0.3945	4.6092	-0.7806	1.9449	0.6391
	Loser (L)	0.0234	5.5951	-0.7454	1.3787	0.0379
	W – L	0.3711	4.1907	0.0029	0.7015	0.6012
CVaR(99%)	Winner (W)	0.3114	3.8428	-0.6689	1.7318	0.5045
	Loser (L)	0.3166	5.7499	-0.3607	0.5737	0.5129
	W – L	-0.0052	3.9082	-0.1820	0.2317	-0.0084
CVaR(95%)	Winner (W)	0.2845	3.7622	-0.7628	1.9346	0.4608
	Loser (L)	0.2954	5.7979	-0.3878	0.6469	0.4786
	W – L	-0.0109	3.9062	-0.2081	0.7141	-0.0177
CVaR(90%)	Winner (W)	0.2743	3.8143	-0.8560	2.3086	0.4443
	Loser (L)	0.2854	5.8318	-0.4204	0.7283	0.4623
	W – L	-0.0111	4.0001	-0.1735	0.9543	-0.0180
STARR(99%)	Winner (W)	0.3455	3.8289	-0.6884	1.8070	0.5597
	Loser (L)	0.2731	5.7228	-0.3611	0.5414	0.4424
	W – L	0.0724	3.8656	-0.2519	0.3406	0.1173
STARR(95%)	Winner (W)	0.3444	3.7157	-0.7922	2.1487	0.5580
	Loser (L)	0.2810	5.7486	-0.4395	0.8571	0.4552
	W – L	0.0635	4.0613	0.0032	1.1248	0.1028
STARR(90%)	Winner (W)	0.3101	3.8911	-0.9767	2.8362	0.5024
	Loser (L)	0.3362	5.9748	-0.6140	1.1656	0.5447
	W – L	-0.0261	4.1620	0.1635	1.4122	-0.0423
R-ratio(99%,99%)	Winner (W)	0.3139	5.4340	-0.4896	1.3947	0.5085
	Loser (L)	0.4029	4.6333	-0.7555	1.0687	0.6527
	W – L	-0.0890	3.4372	0.2474	0.7772	-0.1442
R-ratio(95%,95%)	Winner (W)	0.4568	5.3861	-0.6746	2.2600	0.7400
	Loser (L)	0.3419	4.7851	-0.7264	0.9766	0.5538
	W – L	0.1149	3.3018	0.0994	1.0158	0.1862
R-ratio(90%,90%)	Winner (W)	0.5282	5.4281	-0.6998	2.1819	0.8557
	Loser (L)	0.1164	4.7575	-0.6552	0.9961	0.1886
	W – L	0.4117	3.4053	-0.0449	1.6380	0.6670
R-ratio(50%,99%)	Winner (W)	0.7366	4.8968	-0.5125	1.9995	1.1933
	Loser (L)	0.1178	4.7254	-0.6995	1.0059	0.1908
	W – L	0.6188	3.1334	0.0903	2.0793	1.0025
R-ratio(50%,95%)	Winner (W)	0.7152	4.9317	-0.5214	1.8685	1.1586
	Loser (L)	0.1396	4.5916	-0.7736	1.1658	0.2261
	W – L	0.5756	3.2177	0.1278	1.7826	0.9325
R-ratio(50%,90%)	Winner (W)	0.6417	4.7736	-0.4945	1.7924	1.0396
	Loser (L)	0.0568	4.7619	-0.6846	1.1489	0.0920
	W – L	0.5849	3.2278	-0.0048	1.5170	0.9475

The excellent performance of the R-ratio(50%,9X%) portfolios is achieved by the strong momentum in each basket. The winner groups of the portfolios

strongly outperform the winner group of the traditional momentum strategy. Meanwhile, the loser groups exhibit poorer performance than the loser of the benchmark strategy. The winner return of the R-ratio(90%,90%) portfolio is slightly worse but the loser return is much smaller than the momentum loser. The group behavior of the Sharpe ratio portfolio is similar to the R-ratio(90%,90%) case. Although the winner group underperforms the momentum winner by 0.20%, the weakest performance among all the ranking rules is obtained by the Sharpe ratio losers. For the R-ratio and Sharpe ratio strategies, the skewness of the long (short) baskets is larger (smaller) than that of the momentum strategy.

It is noteworthy that the performance of the R-ratio strategies, in particular, the performance of the R-ratio(50%,9X%) strategies is obtained by accepting less risks. Given in Table 4.10, all the R-ratio portfolios exhibit lower 95% VaRs and CVaRs than the benchmark momentum. The lower risks of the portfolios are also guaranteed by their larger λ_- values in the CTS model. Additionally, higher Sharpe ratios are achieved by the R-ratio(90%,90%) and R-ratio(50%,9X%) strategies. Moreover, smaller maximum drawdown than the traditional momentum strategy is the unique feature of the R-ratio(50%,9X%) strategies. Although all the CVaR and STARR portfolios are less riskier in the 95% VaR and CVaR levels, the performance of these strategies is poorer than the R-ratio portfolios.

The alternative portfolios are less riskier than the cumulative return strategy not only at the levels of entire portfolios but also in each ranking group of the portfolios. The winner and loser baskets of the R-ratio criteria, except for the R-ratio(95%, 95%) winner group, achieve lower 95% VaRs and CVaRs. In

Table 4.10: Summary risk statistics of monthly 6/6 momentum portfolios in U.S. sector ETF

Criterion	Portfolio	CTS parameters			Risk measures			
		α	λ_+	λ_-	Sharpe	$\text{VaR}_{95\%}$	$\text{CVaR}_{95\%}$	MDD
Cumulative return	Winner (W)	0.7510	2.3565	1.5212	0.0590	1.5412	1.8948	52.83
	Loser (L)	0.3234	2.1317	1.7751	-0.0029	1.9601	2.1292	62.58
	W – L	1.2096	1.4824	1.0474	0.0172	0.6720	0.9158	25.32
Sharpe ratio	Winner (W)	0.0500	3.0977	2.2654	0.0552	1.4819	1.8030	50.70
	Loser (L)	0.5778	2.3207	1.6956	0.0258	1.5013	1.8289	64.97
	W – L	1.3215	1.0726	0.7875	0.0001	0.6593	0.9272	35.56
CVaR(99%)	Winner (W)	0.2447	2.5717	1.9223	0.0449	1.1536	1.4848	42.45
	Loser (L)	0.0500	2.9443	2.3076	0.0416	1.6355	1.9388	60.41
	W – L	1.4094	1.1638	1.0081	-0.0100	0.7431	0.9087	36.32
CVaR(95%)	Winner (W)	0.0738	2.8638	2.1811	0.0457	1.1600	1.4861	39.80
	Loser (L)	0.0500	3.0203	2.3330	0.0435	1.6519	1.9624	61.22
	W – L	1.3516	1.1409	1.1704	-0.0114	0.7370	0.8886	35.79
CVaR(90%)	Winner (W)	0.6494	2.3053	1.5313	0.0460	1.1581	1.4960	39.80
	Loser (L)	0.4007	2.5791	1.8816	0.0429	1.6654	1.9852	60.65
	W – L	0.7996	1.8891	1.9635	-0.0120	0.7461	0.8990	37.93
STARR(99%)	Winner (W)	0.4908	2.3868	1.6844	0.0466	1.1495	1.4850	39.80
	Loser (L)	0.0500	2.9984	2.3374	0.0401	1.6376	1.9359	60.41
	W – L	1.3896	1.1154	1.0433	-0.0062	0.7236	0.8762	32.04
STARR(95%)	Winner (W)	0.7268	2.1082	1.4191	0.0485	1.1460	1.4937	39.80
	Loser (L)	0.1450	2.7832	2.1184	0.0432	1.6661	1.9790	61.22
	W – L	1.2936	1.2148	1.1946	-0.0031	0.7203	0.8599	36.49
STARR(90%)	Winner (W)	0.7726	2.0945	1.3625	0.0483	1.1549	1.5055	42.83
	Loser (L)	0.1435	2.8353	2.1773	0.0445	1.6583	1.9678	62.96
	W – L	1.4297	1.0748	1.0378	-0.0045	0.7255	0.8609	37.02
R-ratio(99%,99%)	Winner (W)	0.0500	2.6470	2.1651	0.0228	1.4620	1.7950	58.12
	Loser (L)	0.5290	2.2609	1.5640	0.0474	1.4211	1.7881	50.45
	W – L	0.7145	2.1055	2.5068	-0.0146	0.5459	0.6897	48.19
R-ratio(95%,95%)	Winner (W)	0.0501	2.6370	2.1358	0.0309	1.6082	1.9410	56.56
	Loser (L)	0.8360	1.9846	1.2608	0.0477	1.4153	1.7994	47.32
	W – L	0.0500	3.3436	3.8430	0.0003	0.6524	0.8080	44.55
R-ratio(90%,90%)	Winner (W)	0.0500	2.6752	2.1438	0.0353	1.4952	1.8316	52.73
	Loser (L)	0.3301	2.3987	1.8375	0.0398	1.3556	1.6775	53.38
	W – L	0.9987	1.5025	1.5760	0.0233	0.6390	0.8486	29.94
R-ratio(50%,99%)	Winner (W)	0.0500	2.8326	2.2048	0.0488	1.4879	1.7827	42.85
	Loser (L)	0.8534	1.8963	1.2870	0.0328	1.3333	1.6576	53.40
	W – L	0.9556	1.4507	1.3746	0.0233	0.6208	0.8352	17.11
R-ratio(50%,95%)	Winner (W)	0.0500	2.9408	2.2423	0.0535	1.5155	1.8095	42.85
	Loser (L)	0.8312	1.9537	1.3455	0.0418	1.3301	1.6550	53.40
	W – L	0.8906	1.6341	1.5288	0.0184	0.6306	0.8416	19.33
R-ratio(50%,90%)	Winner (W)	0.0500	2.9660	2.2672	0.0518	1.5180	1.8059	43.33
	Loser (L)	0.8150	1.9530	1.3654	0.0377	1.3322	1.6544	53.40
	W – L	0.7904	1.7991	1.6057	0.0211	0.6354	0.8506	22.56

particular, the short baskets in the R-ratio(50%,9X%) portfolios exhibit the lowest VaR and CVaR levels. Additionally, the long/short positions in the

R-ratio(50%,9X%) portfolio also feature smaller maximum drawdowns comparing with each long/short positions of the traditional momentum. With the CTS parameters, it is also cross-checked that these baskets in the R-ratio and Sharpe ratio portfolios are consistent with the directions of the price momentum. The λ_- parameters for the reward-risk winner groups are greater than that of the momentum strategy. Meanwhile, the λ_- values of the loser groups are smaller. This is much desirable for the momentum portfolio. Opposite to the R-ratio and Sharpe ratio strategies, the larger (smaller) λ_- for the short (long) baskets are the characteristics of the CTS parameters in the CVaR and STARR portfolios.

4.3.6 U.S. equity market: S&P 500

As shown in Table 4.11, the reward-risk momentum strategies in the S&P 500 universe outperform the traditional momentum and the best reward-risk portfolios are constructed by the R-ratio(50%,9X%) criteria. The R-ratio(50%,90%) strategy is the best portfolio of monthly 0.64%, almost three-times larger return than the cumulative return portfolio of 0.22%. Meanwhile, its standard deviation is monthly 2.73%, 50% smaller than the volatility of the original momentum strategy, 5.54%. Similar to the R-ratio(50%, 90%) case, the R-ratio(50%,95%) and R-ratio(50%,99%) portfolios obtain monthly 0.53% and 0.39% with the standard deviations of 2.83% and 2.64%, respectively. Comparing with the results in Rachev et al. [79], the returns of the R-ratio(50%,9X%) portfolios are increased and the volatility are reduced. However, the other strategies are not interesting because the performance of the

portfolios are based on taking larger volatility. Additionally, the performance of these selection rules including the cumulative return becomes poorer since the original study [79].

Table 4.11: Summary statistics of monthly 6/6 momentum portfolios in U.S. S&P 500

Criterion	Portfolio	Summary statistics				
		Mean	Std. Dev.	Skewness	Kurtosis	Final Wealth
Cumulative return	Winner (W)	0.5589	5.5887	-0.7507	1.0164	0.6371
	Loser (L)	0.3369	7.8426	-0.2007	2.3590	0.3841
	W – L	0.2220	5.5408	-0.8821	4.2380	0.2531
Sharpe ratio	Winner (W)	0.4825	5.4366	-1.2614	3.0440	0.5501
	Loser (L)	0.3417	6.4953	-0.7847	2.9677	0.3895
	W – L	0.1408	4.7980	-0.4827	2.5523	0.1605
CVaR(99%)	Winner (W)	0.4648	2.9705	-1.8157	6.4702	0.5299
	Loser (L)	0.4934	7.7577	-0.2225	1.5735	0.5625
	W – L	-0.0287	5.9358	-0.3818	2.4592	-0.0327
CVaR(95%)	Winner (W)	0.4653	2.8899	-1.7931	6.2756	0.5304
	Loser (L)	0.2432	8.3895	-0.4173	1.1078	0.2773
	W – L	0.2220	6.7451	-0.0358	1.4197	0.2531
CVaR(90%)	Winner (W)	0.4953	2.8628	-1.8302	6.4437	0.5646
	Loser (L)	0.3187	8.6751	-0.2324	1.2326	0.3633
	W – L	0.1766	7.0064	-0.2602	1.6025	0.2013
STARR(99%)	Winner (W)	0.5020	2.9350	-1.7080	5.7548	0.5722
	Loser (L)	0.4631	7.8568	-0.2536	1.6442	0.5280
	W – L	0.0388	6.0815	-0.3588	2.6549	0.0443
STARR(95%)	Winner (W)	0.5010	2.8426	-1.7691	6.1334	0.5712
	Loser (L)	0.2534	8.4243	-0.3394	0.9851	0.2888
	W – L	0.2477	6.7372	-0.1568	1.0950	0.2823
STARR(90%)	Winner (W)	0.5056	2.8500	-1.8692	6.5580	0.5764
	Loser (L)	0.3594	8.6919	-0.1974	1.1333	0.4098
	W – L	0.1462	7.0042	-0.3702	1.7272	0.1666
R-ratio(99%,99%)	Winner (W)	0.5720	5.1224	-1.1428	4.3427	0.6520
	Loser (L)	0.7517	5.2703	-0.8659	1.8257	0.8570
	W – L	-0.1798	2.0233	0.9705	5.9285	-0.2049
R-ratio(95%,95%)	Winner (W)	0.6804	4.8809	-1.3971	5.3933	0.7756
	Loser (L)	0.5968	5.2557	-1.0893	2.3207	0.6804
	W – L	0.0836	2.0793	0.6011	0.9863	0.0952
R-ratio(90%,90%)	Winner (W)	0.5715	4.7584	-1.3633	5.6386	0.6515
	Loser (L)	0.3841	5.3097	-1.0707	2.4322	0.4379
	W – L	0.1874	2.3672	-0.0205	0.1447	0.2137
R-ratio(50%,99%)	Winner (W)	0.7587	5.0256	-0.9462	5.0715	0.8649
	Loser (L)	0.3654	5.3213	-0.9708	2.1627	0.4166
	W – L	0.3933	2.6369	0.2485	1.1724	0.4484
R-ratio(50%,95%)	Winner (W)	0.7762	4.7852	-1.0896	5.3304	0.8849
	Loser (L)	0.2483	5.4449	-1.0573	2.2293	0.2830
	W – L	0.5279	2.8255	-0.0482	1.8141	0.6018
R-ratio(50%,90%)	Winner (W)	0.7654	4.7863	-1.0044	4.9962	0.8726
	Loser (L)	0.1296	5.3085	-1.0210	2.2957	0.1477
	W – L	0.6358	2.7326	-0.0795	1.3808	0.7249

The ranking group properties of the R-ratio(50%,9X%) portfolios are also attractive because each ranking group of the portfolios exhibit strong momentum. All the winner groups of these strategies outperform the traditional momentum long basket. Moreover, the loser groups of the R-ratio(50%,95%) and R-ratio(50%,90%) criteria underperform the momentum short basket and the performance of the R-ratio(50%,99%) loser group is slightly better by 0.03%. The ranking group characteristics of the STARR(90%) and Sharpe ratio portfolios are exactly opposite to those of the R-ratio(50%,99%) criterion, i.e. the winners underperform and the losers outperform the benchmark. In the cases of the STARR(95%), CVaR(90%) and CVaR(95%) measures, the weaker performance is observed for all the winner and loser groups. All winner and loser groups of every stock selection rules perform worse than those ranking groups of the reward-risk strategies in the previous study on the reward-risk momentum strategy [79].

The alternative ranking portfolios in the S&P 500 universe are less riskier according to Table 4.12. All the reward-risk momentum strategies feature lower 95% CVaRs. The 95% VaR levels depends on the criteria. In particular, the VaR and CVaR levels of the R-ratio strategies are substantially smaller than the risk measures of the cumulative return strategy. The Sharpe ratio portfolio also shows lower VaR and CVaR levels. Additionally, the λ_- parameters of the R-ratio and Sharpe ratio strategies, except for the R-ratio(95%,95%) and R-ratio(90%,90%) measures, are larger than that of the cumulative return. The larger λ_- of the reward-risk momentum strategies are good at controlling the downside tail risks. For maximum drawdown, the Sharpe ratio and the R-ratio portfolios exhibit better maximum drawdown values than the origi-

nal momentum strategy. The maximum drawdowns of the R-ratio portfolios are impressively decreased. For example, the maximum drawdowns of the R-ratio(50%,9X%) portfolios are around 15% and it imposes that 75% of the maximum drawdown by the cumulative return criterion is gone away by choosing the R-ratio(50%,9X%) measures. The additional advantage of adopting the R-ratio(50%, 9X%) and Sharpe ratio as the stock selection rules is that the Sharpe ratios of the portfolios are about 2–5 times higher than the cumulative return portfolio.

The risk characteristics of the winner and loser groups also show that the reward-risk selection rules are desirable to the risk management of the constituent baskets. The λ_{-} parameters of the winner groups are larger than that of the cumulative return winner. It is evident that the lower downside risks in the winner groups are obtained by the alternative portfolios. Opposite to the long baskets, the λ_{-} values for the loser baskets are smaller than the loser group in the cumulative return criterion and it is attractive for the short baskets to take the larger downside risks to earn the profits from short-selling the losers. Most of the reward-risk measures provide the less riskier winner and loser groups with smaller 95% VaRs and CVaRs. In addition to that, the maximum drawdown of each basket is also lower than that of each long/short basket by the cumulative return criterion. In the R-ratio and Sharpe ratio portfolios, the comparable sizes of maximum drawdowns are obtained by the winner and loser groups. Meanwhile, for the CVaR and STARR portfolios, the maximum drawdowns of the winner groups are much lower than those of the loser groups. This pattern is also observed in the cumulative return portfolio.

Table 4.12: Summary risk statistics of monthly 6/6 momentum portfolios in U.S. S&P 500

Criterion	Portfolio	CTS parameters			Risk measures			
		α	λ_+	λ_-	Sharpe	$\text{VaR}_{95\%}$	$\text{CVaR}_{95\%}$	MDD
Cumulative return	Winner (W)	0.8861	2.1267	1.1819	0.0003	1.8478	2.2138	59.55
	Loser (L)	0.0500	3.7818	2.7937	0.0358	1.9232	2.0562	78.90
	W – L	1.1751	1.5755	1.2925	0.0078	1.2477	1.6680	59.71
Sharpe ratio	Winner (W)	0.4746	2.5494	1.6115	0.0533	1.5337	1.9249	64.29
	Loser (L)	0.8142	3.4789	1.8520	0.0387	1.8531	1.9718	70.73
	W – L	0.5964	2.9640	2.5113	0.0182	1.0839	1.3332	49.50
CVaR(99%)	Winner (W)	0.0500	2.3656	1.8691	0.0686	1.0915	1.4658	43.31
	Loser (L)	0.7968	3.8780	1.9720	0.0357	1.8102	1.9908	72.92
	W – L	0.3462	3.1218	3.6005	-0.0071	1.1925	1.3448	60.29
CVaR(95%)	Winner (W)	0.0501	2.4449	1.9059	0.0708	1.0990	1.4700	41.14
	Loser (L)	0.7347	3.1873	1.8628	0.0353	1.8524	2.0175	78.53
	W – L	0.3278	3.1024	3.7552	-0.0114	1.3335	1.4625	60.63
CVaR(90%)	Winner (W)	0.0500	2.4971	1.9367	0.0721	1.1096	1.4723	39.82
	Loser (L)	0.2386	3.5081	2.4162	0.0366	1.9168	2.1219	78.57
	W – L	0.0614	3.3466	3.9793	-0.0151	1.3596	1.5191	61.41
STARR(99%)	Winner (W)	0.0500	2.3644	1.8484	0.0709	1.0980	1.4838	42.90
	Loser (L)	0.7670	3.7859	2.0132	0.0363	1.6748	1.8117	73.82
	W – L	0.2788	3.2625	3.7744	-0.0051	1.1199	1.2490	60.80
STARR(95%)	Winner (W)	0.0500	2.3256	1.8339	0.0708	1.0970	1.4780	40.41
	Loser (L)	0.7337	3.1198	1.8558	0.0341	1.8675	2.0504	78.24
	W – L	0.4629	2.8693	3.3958	-0.0078	1.3407	1.4872	60.85
STARR(90%)	Winner (W)	0.0501	2.4325	1.8814	0.0733	1.1099	1.4836	40.52
	Loser (L)	0.4306	3.4380	2.3083	0.0350	1.9809	2.1363	78.62
	W – L	0.0877	3.7570	4.2363	-0.0109	1.4510	1.5826	63.83
R-ratio(99%,99%)	Winner (W)	0.1787	3.1398	2.1485	0.0573	1.4580	1.7811	60.75
	Loser (L)	0.4969	2.7568	1.7266	0.0664	1.4836	1.7320	54.41
	W – L	0.7684	1.7629	2.0395	-0.0256	0.4299	0.5620	26.20
R-ratio(95%,95%)	Winner (W)	0.1662	2.8518	1.9817	0.0629	1.4310	1.7470	58.33
	Loser (L)	0.2141	2.9262	2.0650	0.0605	1.3994	1.6769	55.39
	W – L	1.5057	0.8361	0.8384	-0.0057	0.3827	0.5155	19.48
R-ratio(90%,90%)	Winner (W)	0.0500	2.8640	2.0565	0.0595	1.4001	1.7342	57.40
	Loser (L)	0.8505	2.6170	1.4780	0.0522	1.4632	1.7373	59.07
	W – L	1.5972	0.5932	0.5247	0.0063	0.4317	0.6008	15.72
R-ratio(50%,99%)	Winner (W)	0.4632	2.7405	1.6787	0.0650	1.4093	1.7276	54.79
	Loser (L)	0.5545	3.3607	2.0531	0.0489	1.4725	1.7052	59.64
	W – L	0.5909	2.4827	2.2535	0.0282	0.4856	0.6559	14.96
R-ratio(50%,95%)	Winner (W)	0.0500	2.8730	2.0207	0.0653	1.3924	1.7017	53.42
	Loser (L)	0.7764	2.8824	1.5795	0.0455	1.4935	1.7505	61.18
	W – L	1.0335	1.5251	1.3447	0.0303	0.4366	0.5966	15.78
R-ratio(50%,90%)	Winner (W)	0.2868	2.8634	1.8263	0.0665	1.4015	1.7125	54.69
	Loser (L)	0.8508	2.9716	1.5304	0.0417	1.5503	1.7739	62.20
	W – L	0.7900	1.7982	1.6932	0.0413	0.4813	0.6399	15.85

4.3.7 Overall results in various universes

In the various asset classes, the reward-risk measures are the better ranking rules that select the potential good and bad performers in next 6 months. In particular, the R-ratio(50%,9X%) measures generate the consistent outperformance with lower volatility. The outperformance of the R-ratio(50%,9X%) portfolios is also supported by the historical cumulative returns of the alternative portfolios given in Fig. 4.1. It is easy to find that the R-ratio(50%,9X%) not only outperform the traditional trend-following strategy but also tend to form consistent trends with less fluctuation. Additionally, the performance of the R-ratio(50%,9X%) strategies is still consistent even during the financial crisis in 2008. The R-ratio(9X%,9X%) and Sharpe ratio also provide good performance and the portfolios are less riskier than the benchmark momentum strategy in many asset classes. Each long/short basket is also superior to the momentum strategy in performance.

The outperformance of the reward-risk momentum strategies is achieved not by taking more risk but by accepting less risk. In particular, the R-ratio(50%,9X%) strategies are less riskier than the momentum portfolio in various risk measures such as Sharpe ratio, VaR, CVaR, and maximum drawdown. The dominance in risk profiles is also observed in the level of long/short baskets. Although the Sharpe ratio portfolio is not as good in performance as the R-ratio strategies, its risk profile imposes that the portfolio by the Sharpe ratio is also less riskier than the benchmark strategy.

In many asset classes, the patterns in performance and risk characteristics are categorized into two classes: The first class includes R-ratio and Sharpe

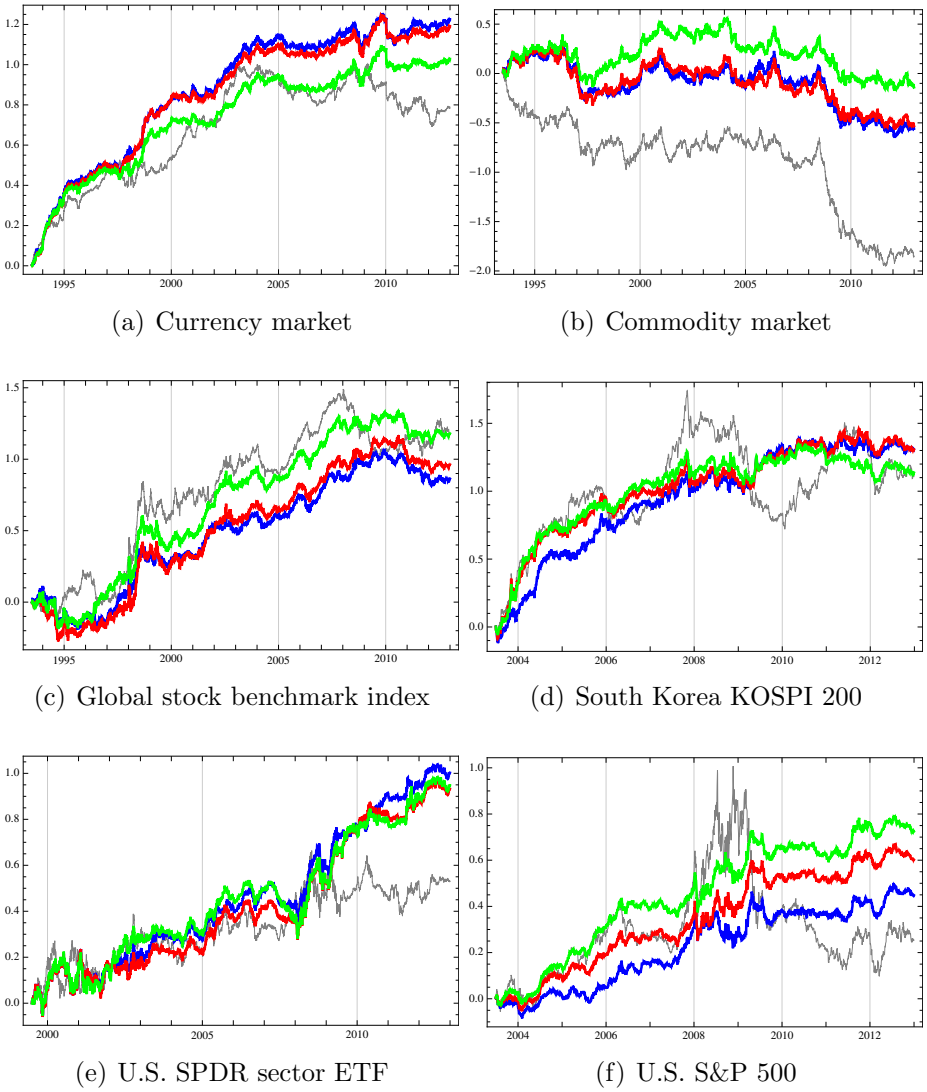

(a) Currency market (b) Commodity market

(c) Global stock benchmark index (d) South Korea KOSPI 200

(e) U.S. SPDR sector ETF (f) U.S. S&P 500

Figure 4.1: Cumulative returns for the traditional momentum (gray), R-ratio(50%,99%) (blue), R-ratio(50%,95%) (red), and R-ratio(50%,90%) (green).

ratio and the second group contains CVaR and STARR. It is noteworthy that the classification is also associated with the origin of the reward-risk measures. The reward-risk measures in the first category are all ratio-based measures. Meanwhile, the second category consist of the return/loss-based measures.

The possible explanation on the outperformance of the ratio-based reward-risk measures is that the R-ratio and Sharpe ratio consider not only downside risk but also upward latent profit in the normalized scale. Opposite to the ratio measures, the return/loss based strategies tend to select the low-risk instruments in non-normalized scale. It is likely not to consider the volatility along the upward direction which is not the actual risk but the source of potential gain.

4.4 Factor analysis

As found in the previous section, the reward-risk momentum strategies feature the better characteristics in performance and risk. For more robust tests, the alternative strategies need to be cross-checked with various market factors. In particular, the Fama-French three-factor model [40] is one of the well-known regression models in finance. We analyze the results in the S&P 500 universe with the Fama-French three-factor model.

As seen in Table 4.13, the intercepts of the factor analysis on the reward-risk momentum strategies in the S&P 500 universe are generally greater than that of the traditional momentum strategy. The ranges of the three-factor alpha are dependent with the types of the alternative stock selection rules. Additionally, the three-factor alphas are statistically significant in many portfolios. The different factor structures with respect to the criteria are also found.

The first category in the factor structure is generated by the Sharpe ratio

Table 4.13: Fama-French regression of monthly 6/6 momentum portfolios in U.S. S&P 500

Criterion	Portfolio	Factor loadings				
		$\alpha(\%)$	β_{MKT}	β_{SMB}	β_{HML}	R^2
Cumulative return	Winner (W)	-0.0643	1.0236**	0.3201*	0.0357	0.7699
	Loser (L)	-0.5487	1.4993**	0.2091	0.2665	0.8086
	W – L	0.4844	-0.4757**	0.1110	-0.2307	0.1616
Sharpe ratio	Winner (W)	-0.0887	1.0443**	0.0957	0.0302	0.7504
	Loser (L)	-0.3925	1.2375**	0.1571	0.2559*	0.8082
	W – L	0.3038	-0.1932	-0.0614	-0.2258	0.0643
CVaR(99%)	Winner (W)	0.1749	0.5892**	-0.1281	0.1025	0.7383
	Loser (L)	-0.4579	1.4739**	0.4497**	0.3284**	0.8873
	W – L	0.6328	-0.8847**	-0.5779**	-0.2259	0.6696
CVaR(95%)	Winner (W)	0.1887	0.5657**	-0.1222	0.0892	0.7139
	Loser (L)	-0.7810**	1.5448**	0.5892**	0.3184*	0.8625
	W – L	0.9696*	-0.9792**	-0.7114**	-0.2292	0.6568
CVaR(90%)	Winner (W)	0.2187	0.5621**	-0.1150	0.0886	0.7216
	Loser (L)	-0.7602**	1.5755**	0.6597**	0.4131**	0.8760
	W – L	0.9788**	-1.0134**	-0.7747**	-0.3245*	0.6873
STARR(99%)	Winner (W)	0.2116	0.5762**	-0.1088	0.1115	0.7384
	Loser (L)	-0.4920	1.4975**	0.4475**	0.2906*	0.8795
	W – L	0.7036*	-0.9213**	-0.5563**	-0.1790	0.6577
STARR(95%)	Winner (W)	0.2260	0.5592**	-0.1217	0.0969	0.7260
	Loser (L)	-0.7864**	1.5491**	0.6140**	0.3504**	0.8743
	W – L	1.0124**	-0.9899**	-0.7357**	-0.2535	0.6846
STARR(90%)	Winner (W)	0.2307	0.5631**	-0.1235	0.0889	0.7265
	Loser (L)	-0.7197*	1.5706**	0.6603**	0.4263**	0.8713
	W – L	0.9505*	-1.0075**	-0.7838**	-0.3374*	0.6886
R-ratio(99%,99%)	Winner (W)	-0.0609	1.0247**	0.2012**	0.2384**	0.9333
	Loser (L)	0.1324	1.0904**	0.1730*	0.0454	0.9057
	W – L	-0.1933	-0.0657	0.0282	0.1930*	0.0501
R-ratio(95%,95%)	Winner (W)	0.0875	0.9893**	0.1652**	0.1805**	0.9237
	Loser (L)	-0.0113	1.0796**	0.1245	0.0827	0.8846
	W – L	0.0988	-0.0903	0.0407	0.0979	0.0302
R-ratio(90%,90%)	Winner (W)	-0.0036	0.9603**	0.1500*	0.1877**	0.9157
	Loser (L)	-0.2248	1.1007**	0.1067	0.0573	0.8840
	W – L	0.2212	-0.1405*	0.0433	0.1304	0.0553
R-ratio(50%,99%)	Winner (W)	0.1429	0.9883**	0.2234**	0.2171**	0.9107
	Loser (L)	-0.2628	1.0583**	0.2204*	0.1057	0.8786
	W – L	0.4057	-0.0701	0.0030	0.1114	0.0157
R-ratio(50%,95%)	Winner (W)	0.1971	0.9518**	0.1862**	0.1795**	0.9051
	Loser (L)	-0.3787	1.0936**	0.1550	0.0983	0.8619
	W – L	0.5758*	-0.1418*	0.0312	0.0812	0.0389
R-ratio(50%,90%)	Winner (W)	0.1876	0.9459**	0.1847**	0.1904**	0.8980
	Loser (L)	-0.4812**	1.0830**	0.1425	0.0633	0.8737
	W – L	0.6688**	-0.1371*	0.0422	0.1270	0.0395

** 1% significance * 5% significance

and R-ratio. For the momentum portfolios by these reward-risk measures, the exposures on the market factor and size factor are smaller than any other strategies. Moreover, very small R^2 values impose that the Fama-French

three-factor model is not able to explain the return structures of the momentum portfolios constructed by the ratio-based reward-risk measures. The R-ratio(50%,90%) and R-ratio(50%, 95%) exhibit greater Fama-French three-factor alpha which is also statistically significant.

Another different factor structure is found in the CVaR and STARR portfolios. The statistically significant intercepts of the regression on these stock selection rules are much larger than the momentum strategies by the cumulative return and the ratio-based reward-risk measures. The sizes of the exposure on the market and size factors are substantially greater and statistically significant. The larger exposures to the Fama-French factors lead to the higher R^2. The large parts of the portfolio performance by these ranking rules are explained by the Fama-French three-factor model.

It is noteworthy that the classification for the different factor structures is also identical to the types of the stock selection rules. Not only performance and risk profiles but also the factor exposure highly depend the origin of the ranking criterion. These two groups of the momentum portfolio construction rules are considered the different categories of the reward-risk measures.

4.5 Concluding remarks

In this study, we test the alternative momentum portfolios based on the reward-risk measures in various asset classes and markets. The reward-risk measures include Sharpe ratio, CVaR, STARR, and R-ratio. The stock selection rules for the reward-risk momentum strategies are calculated from the

ARMA(1,1)-GARCH(1,1) model with CTS innovations in order to explain autocorrelation, volatility clustering, skewness, and kurtosis in asset returns.

The reward-risk momentum portfolios achieve the better performance and risk characteristics independent with asset class and market. In particular, the R-ratio(50%,9X%) strategies outperform the traditional momentum strategy in every asset classes. Additionally, the long/short positions of these strategies exhibit the stronger momentum than the benchmark strategy, i.e, the winners outperform the long basket of the traditional momentum portfolio and the losers underperform the loser in the cumulative return. The R-ratio(9X%,9X%) and Sharpe ratio strategies also perform well under the smaller deviation.

The alternative portfolios are less riskier than the traditional momentum portfolio in VaR, CVaR, and maximum drawdown. The larger λ_- parameters also guarantee the thinner downside tails of the portfolio returns. For each winner/loser group, the less riskier portfolios are also constructed by the alternative stock selection rules.

It is also observed that the performance and risk profile depend on the characteristics of the momentum group ranking criterion. The reward-risk measures such as R-ratio and Sharpe ratio construct the long/short portfolios with the better average returns and lower downside risks. This tendency is also found at the levels of long/short baskets.

The factor analysis in the S&P 500 universe supports the same conclusion that the factor structures are highly dependent with the types of the ranking criteria. Additionally, the Fama-French three-factor alpha is statistically significant and larger than that of the benchmark strategy and the momentum

strategies by the ratio-based stock ranking rules are inexplicable by the Fama-French three factor model which explains the performance of the CVaR and STARR portfolios.

In future study, various kinds of risk models will be tested for the construction of alternative momentum-style portfolios. In addition to that, the implementation of the reward-risk momentum strategies will be extended to weekly, daily, and high frequency scales.

Chapter 5

Physical approach to price momentum and its application to momentum strategy

In this chapter, we introduce various definitions for the physical momentum of equity price. Based on those definitions, the equity price momentum can be obtained from real historical data in the South Korean KOSPI 200 and S&500 universes. After computing the physical momentum, the implementation of the contrarian strategies based on the candidates for the price momentum increases the validity of our approach to measuring the physical momentum in equity price. Empirically, these new candidates for the selection criteria originated from the physical momentum idea provide the better returns and Sharpe ratios than the original criterion, i.e. the cumulative return. The structure of this paper is the following. In the next chapter, the definition of velocity in equity price space and possible candidates for financial mass are introduced and then the price momentum is defined with the financial velocity and mass. In section 5.2, we specify the datasets used for our analysis. In section 5.3, results for the physical momentum strategies are given. The Fama-French three-factor

analysis is given in section 5.4. In section 5.5, we conclude the chapter.

5.1 Theoretical background

When an one-dimensional space for price of a financial instrument is introduced, it is possible to consider that the price is in motion on the positive half-line. Although the negative price is conceptually proposed by Sornette [94], the negative price of the instrument is not allowed in practice.[1] The price dynamics of the financial instruments are now changed to an one-dimensional particle problem in physics. To extend the space to the entire line, the log price is mapped to the position $x(t)$ in the space by

$$x(t) = \log S(t)$$

where $S(t)$ is the price of the instrument. This transformation is not new to physicists because Baaquie [12, 13] already introduced the same transformation to derive path integral approach to option pricing theory. It was used in order to find the relation between the Black-Schole equation and Schrödinger equation. With this re-parametrization, an option pricing problem was transformed to an one-dimensional potential wall problem in quantum mechanics. However, it was not for introducing the physical momentum concept mentioned above. With the log return, $x(t)$ covers the whole line from the negative to positive infinity. In addition to the physical intuition, the log price has some

[1] Sornette not only pointed that the negative equity price is introduced only for symmetry breaking but also explained why the negative price is not observed under real situations using dividend payment as an external field in symmetry breaking.

advantages in finance. First of all, it is much simpler to calculate the log return from the log price because the difference of two log prices is the log return. Contrasting to the log return, the raw return is more complicated to compute than the log return. Secondly, one of the basic assumptions in mathematical finance is that the returns of financial instruments are log-normally distributed and we can handle normally-distributed log returns.

Having the advantages of the log price described above, it is natural to introduce a concept of velocity into the one-dimensional price space. In the case of the log price, the log return $R(t)$ per unit time scale is expressed in $x(t)$ by

$$\begin{aligned} R(t) &= \frac{\log S(t) - \log S(t-\Delta t)}{\Delta t} \\ &= \frac{x(t) - x(t-\Delta t)}{t - (t-\Delta t)} \\ &= \frac{\Delta x(t)}{\Delta t}. \end{aligned}$$

In the limit of infinitesimal time interval ($\Delta t \to 0$), the log return becomes

$$R(t) = \frac{dx(t)}{dt} = v(t)$$

where $v(t)$ is the velocity of the instrument in the log price space, $x(t)$. When the mapping between the log price and position in the one-dimensional space is introduced, it imposes the relation between the log return and velocity. Although this relation works only in the limit of $\Delta t \to 0$, it can be used as the approximation in the discrete time limit if the length of the whole time series is long enough to make the time interval relatively shorter.

The cumulative return $r(t)$ is expressed in $v(t)$ by

$$\begin{aligned} r(t) &= \frac{S(t) - S(t-\Delta t)}{S(t-\Delta t)} = \exp\left(R(t)\right) - 1 \\ &= v(t)\big(1 + \frac{1}{2}v(t) + \cdots + \frac{1}{n!}(v(t))^{n-1} + \cdots\big). \end{aligned}$$

Since the log return is usually small such as $|v(t)| \ll 1$ in real data, higher-order terms in $v(t)$ can be treated as higher-order corrections on $r(t)$ and it is possible to ignore the higher-order corrections if $|v(t)| \ll 1$. In this sense, the cumulative return can be approximated to $v(t)$. However this relation is broken in the cases of heavy tail risks caused by financial crisis or firm-specific events such as bankruptcy, merger and acquisition, and good/bad earning reports of the company. Since $|v(t)|$ in these events can be comparable to one or greater than one, the higher-order perturbations should be considered.

Based on the correspondence, the concept of the price momentum can be quantified by using the classical momentum in physics by

$$p = mv$$

where m has the same role to physical mass. In particular, when velocity is given in the log return, the contribution of the mass to the price momentum can be expressed in the following way,

$$\begin{aligned} p &= m \log\left(1 + r\right) \\ &= \log\left(1 + r\right)^m. \end{aligned}$$

The financial mass m plays a role of amplifying the price change as the mass becomes larger. This amplification is understood as filtering of market information on price. Consideration on the volume can catch more market information. For example, large transaction volumes at the peak or trough could impose the change in the trend from the viewpoint of technical analysis. Some instruments are heavily influenced by the investors' psychology and other market factors but other aren't. In this sense, the mass can act a role of the filter which is unique to each instrument and encodes the instrument-specific characters. This interpretation is also well-matched to the physical analogy that mass is a physical constant which is unique to each particle. The original ranking criterion in the traditional momentum strategy is a special case of this momentum definition. In the cumulative return momentum strategy, it is assumed that each of equities has the identical mass, $m = 1$. However, the identical mass assumption seems not to be reasonable because each equity has distinct properties and shows inherent price evolutions. In order to capture these heterogeneities between characteristics of each equity, the departure from the identical financial mass for all equities is more natural and the introduction of the financial mass concept to the momentum strategy look plausible. Although the physical momentum concept can be applied to other asset classes, we focus only on the equities in this paper.

As described in the previous paragraph, the financial mass can convey the instrument-specific information. However, it is obvious that all kinds of information cannot work as candidates of the mass because it should be well-matched to intrinsic properties of physical mass. In this sense, liquidity is a good candidate for the financial mass. Its importance in finance is already

revealed in many financial literatures in terms of bid-ask spread, volume, and fractional turnover rate [5, 6, 34, 49, 56, 60]. In particular, Datar et al.[34] reported that past turnover rate is negatively correlated to future return. With the same size of the momentum, the larger turnover rate brings the poorer future return i.e. illiquid stocks exhibit higher average returns. Even after controlling other factors such as firm-size, beta[2], and BM ratio, the past turnover rate has the significant negative correlation with the future return. It is possible to understand that the trading volume incorporates integrated opinions of investors and makes the price approach to the equilibrium asymptotically. In the viewpoint of information, trading can be understood as the exchange of information between investors with inhomogeneous information. More transactions occur, more information is widely disseminated over the whole market and the price change becomes more meaningful. Lee and Swaminathan [60] also provided the similar result that stocks with low past trading volumes tend to have high future returns. Additionally, the study found that the momentum strategy among high volume stocks is more profitable. The similar result is obtained in the South Korean market [56].

The possible mass candidates which are also well-matched to the analogy of physical mass are volume, total transaction value, and inverse of volatility. If the trading volume is larger, the price movement can be considered the more meaningful signal because the higher volume increases the market efficiency. The amount of the volume is proportional to mass m. As mentioned in the previous paragraph, the relation between the trading volume and asset return

[2]The beta in finance is the correlation between the stock return and benchmark return scaled by the market variance.

is already studied in finance [34, 49, 60]. Instead of the raw volume, we need to normalize the daily volumes with the total number of outstanding shares and this normalized value is also known as a turnover rate. The reason of this normalization is that some equities intrinsically have the larger trading volumes than others because the total number of shares enlisted in the markets are much larger than other equities or because they get more investors' attentions which cause more frequent trades between investors. The share turnover rate, trading volume over outstanding shares is expressed in v in the paper.

Similar to the volume, the daily transaction value in cash can be used as the financial mass. If an equity on a certain day has the larger transaction value, investors trade the equity frequently and the price change has more significant meanings. Additionally, the transaction value contains more information than the volume. For examples, even though two equities record the same daily volume and daily return on a given day, the higher priced equity has the larger trading value if two prices are different. The more important meaning is that even though market information such as close price, volume, return, and price band are identical, the trading value in cash can be different. As an instance, when one equity is traded more near the lowest price of the daily band but the other is traded mainly around the daily highest price region, the total transaction values of two equities are definitely different. It also needs to be normalized because each equity price is different. The normalization of dividing total transaction value by market capitalization is expressed in τ in the paper.

The return volatility σ is inversely proportional to the financial mass m. If the volatility of a certain equity in a given period is larger, the equity price is

easy to fluctuate much severely than other equities with the smaller volatilities. This correspond to the situation in physics that a lighter object can move more easily than a heavy object under the same force. So if it is heavy in the sense of the volatility, the asset price with larger mass is under the smaller volatility. This definition of the financial mass is also matched with the analogy used in Baaquie's works [12, 13]. In his works, the Black-Scholes equation was transformed into Hamiltonian of a particle under the potential which specifies the option. The mass of a particle in the Hamiltonian was exactly same to the inverse of the return volatility. Since the volatility is also interesting to economists and financiers, there are series of the literature covering the link between volatility and return [42, 45].

With the fractional volume and fractional transaction value as the proxies for the mass, it is possible to define two categories of the physical momentum,

$$p^{(1)}_{t,k}(m,v) = \sum_{i=0}^{k-1} m_{t-i} v_{t-i}$$

and

$$p^{(2)}_{t,k}(m,v) = \frac{\sum_{i=0}^{k-1} m_{t-i} v_{t-i}}{\sum_{i=0}^{k-1} m_{t-i}}$$

over the period of the size k. The latter one is the reminiscent of the center-of-mass momentum in physics and the similar concept is used as the embedded capital gain in Grinblatt and Han [46]. Since two different categories for the momentum calculation, two for return, and two for mass are available, there are eight different momentum definitions for an equity.

It is easily found that the cumulative return can be expressed in $p^{(1)}$ by

$$\begin{aligned} r_{t,k} &= \exp\left(\sum_{i=0}^{k-1} R_{t-i}\right) - 1 = \exp\left(p_{t,k}^{(1)}(1,R)\right) - 1 \\ &\approx p_{t,k}^{(1)}(1,R) + \mathcal{O}\Big(\left(p_{t,k}^{(1)}(1,R)\right)^2\Big) \end{aligned}$$

an this shows that the traditional momentum in finance is a special case of the physical momentum. In this sense, let's call $r_{t,k} = p_{t,k}^{(0)}$. In addition to that, since exponential function and log function are strictly increasing functions, the mapping between $p_{t,k}^{(0)}$ and $p_{t,k}^{(1)}(1,R)$ is one-to-one.

Since the return volatility over the period has more practical meanings than the sum of daily volatilities during the period, the third class of the physical momentum is defined by

$$p_{t,k}^{(3)}(m,v) = \bar{v}_{t,k}/\sigma_{t,k}$$

where $\bar{v}_{t,k}$ is the average velocity at time t during the past k periods. There are also two different definitions for $p_{t,k}^{(3)}$ computed from the normal return and log return. This is closely related to the Sharpe ratio, SR,

$$SR = \frac{\mu(r - r_f)}{\sigma(r - r_f)}$$

where r_f is the risk-free rate. If the risk-free rate is small and ignorable, $p_{t,k}^{(3)}$ approaches to the Sharpe ratio. The momentum strategy with this ranking criterion is reminiscent of the Sharpe ratio based momentum strategy by Rachev et al. [79]. Similar to the Sharpe ratio, $p_{t,k}^{(3)}$ can be related to the information

ratio that uses excessive returns over the benchmark instead of the risk-free rate in the definition. However, we don't consider the risk-free rate nor the benchmark return as a reference point of the portfolio returns in this paper.

With $p_{t,k}^{(1)}$, $p_{t,k}^{(2)}$, and $p_{t,k}^{(3)}$, total eleven different definitions of physical momentum including the traditional cumulative return are possible candidates for the physical equity momentum. Each of them is originated from the physical and financial foundations. Additionally, they are relatively easier to quantify than other risk measures used in Rachev's work [79]. Although it is possible to consider more complicated functions of other market data for the price momentum, it is beyond the scope of this paper.

5.2 Dataset

5.2.1 South Korea equity markets: KOSPI 200

The market data and component-change log of the KOSPI 200 universe are downloaded from Korea Exchange. The covered time horizon starts January 2003 and ends December 2012.

5.2.2 U.S. equity markets: S&P 500

The daily market information and roaster for S&P 500 components are collected from Bloomberg. The time window is identical to the KOSPI 200.

5.3 Results

5.3.1 South Korea equity market: KOSPI 200

In Table 5.1, all weekly contrarian strategies based on physical momentum except for the $p^{(3)}$ criteria outperform the traditional contrarian strategy. The $p^{(1)}(\upsilon, R)$ portfolio is the best contrarian strategy with the weekly return of 0.261% under the volatility of 2.444% while the benchmark contrarian strategy obtains weekly 0.069% with the standard deviation of 2.846%. The performance of other $p^{(1)}$ portfolios is as good as the $p^{(1)}(\upsilon, R)$ portfolio and is better than the $p^{(0)}$ criterion. Although the $p^{(2)}$ strategies are slightly worse than the $p^{(1)}$ cases, the performance is much better and less volatile than the mean-reversion strategy. Although all $p^{(3)}$ portfolios exhibit smaller standard deviations, the average returns are all negative. With a few exceptions, the skewness levels of the alternative weekly contrarian strategies are higher and the kurtosis is lower than the those of cumulative return strategy. The historical performance of the portfolios is given in Fig. 5.1.

The outperformance of the $p^{(1)}$ and $p^{(2)}$ portfolios is achieved by the stronger reversal in each ranking group. The average returns of the loser groups by those strategies are in the range of 0.278%–0.301% comparing with weekly 0.266% by the benchmark contrarian portfolio. Additionally, the volatility of the loser groups are lower than the loser in cumulative return. Meanwhile, the winner baskets in the alternative portfolios underperform its competitive winner basket. While the traditional mean-reversion winner group obtain weekly 0.198%, the performance of the winners in $p^{(1)}$ is in the range of 0.037%–0.048% and the $p^{(2)}$ winners gain weekly 0.121%–0.160% with the smaller standard devi-

Table 5.1: Summary statistics and risk measures of weekly 6/6 contrarian portfolios in South Korea KOSPI 200

Criterion	Portfolio	Summary statistics					Risk measures			
		Mean	Std. Dev.	Skewness	Kurtosis	Fin. Wealth	Sharpe	$\text{VaR}_{95\%}$	$\text{CVaR}_{95\%}$	MDD
$p^{(0)}$	Winner (W)	0.1977	3.8044	-1.2951	6.7842	1.0181	0.0689	1.7492	2.5255	67.27
	Loser (L)	0.2662	4.3629	-1.1757	7.6803	1.3708	0.0818	1.6779	2.5040	63.00
	L – W	0.0685	2.8461	0.1907	1.8784	0.3527	0.0149	1.6930	2.4344	33.40
$p^{(1)}(\upsilon, r)$	Winner (W)	0.0365	4.3618	-1.2676	6.7068	0.1880	0.0479	2.0039	2.9571	71.44
	Loser (L)	0.2781	4.2244	-1.2474	8.0932	1.4323	0.0888	1.6588	2.3910	64.92
	L – W	0.2416	2.3988	0.2320	1.0899	1.2443	0.0422	1.5481	2.1681	20.36
$p^{(1)}(\tau, r)$	Winner (W)	0.0433	4.3384	-1.2263	6.4733	0.2229	0.0487	2.0007	2.9610	71.20
	Loser (L)	0.2986	4.2776	-1.2293	8.1616	1.5376	0.0891	1.6558	2.3985	65.17
	L – W	0.2553	2.4203	0.2482	1.3236	1.3147	0.0431	1.5482	2.1747	21.30
$p^{(1)}(\upsilon, R)$	Winner (W)	0.0399	4.3078	-1.2111	6.2480	0.2053	0.0482	1.9968	2.9472	70.77
	Loser (L)	0.3006	4.3159	-1.2610	8.4086	1.5479	0.0892	1.6627	2.4087	65.53
	L – W	0.2607	2.4439	0.2286	1.4620	1.3427	0.0450	1.5289	2.1522	21.51
$p^{(1)}(\tau, R)$	Winner (W)	0.0481	4.2810	-1.1999	6.4031	0.2479	0.0490	1.9824	2.9382	70.31
	Loser (L)	0.3002	4.3536	-1.2939	8.5965	1.5462	0.0886	1.6676	2.4188	66.07
	L – W	0.2521	2.4656	0.1705	1.6283	1.2983	0.0422	1.5293	2.1521	23.29
$p^{(2)}(\upsilon, r)$	Winner (W)	0.1214	3.8635	-1.3671	7.6297	0.6251	0.0610	1.8278	2.6834	68.73
	Loser (L)	0.2842	3.9333	-1.6138	11.3616	1.4637	0.0951	1.4908	2.1750	65.07
	L – W	0.1628	2.1709	0.2235	1.4173	0.8386	0.0281	1.4383	2.0149	21.29
$p^{(2)}(\tau, r)$	Winner (W)	0.1407	3.8520	-1.3704	7.7786	0.7244	0.0624	1.8156	2.6577	68.59
	Loser (L)	0.2891	3.9623	-1.5753	11.1774	1.4889	0.0945	1.4799	2.1615	65.38
	L – W	0.1484	2.1738	0.2044	1.4014	0.7645	0.0280	1.4775	2.0766	20.54
$p^{(2)}(\upsilon, R)$	Winner (W)	0.1389	3.8274	-1.3849	7.7040	0.7151	0.0624	1.8149	2.6574	68.95
	Loser (L)	0.2875	3.9804	-1.5728	11.0874	1.4807	0.0940	1.5239	2.2234	65.53
	L – W	0.1487	2.1910	0.2024	1.6035	0.7657	0.0288	1.5139	2.1327	20.77
$p^{(2)}(\tau, R)$	Winner (W)	0.1597	3.8158	-1.4078	7.9932	0.8223	0.0654	1.8028	2.6433	69.02
	Loser (L)	0.2886	4.0066	-1.5608	10.9274	1.4865	0.0932	1.5209	2.2186	65.49
	L – W	0.1290	2.2188	0.1553	1.6056	0.6642	0.0258	1.5409	2.1789	21.88
$p^{(3)}(1/\sigma, r)$	Winner (W)	0.2722	3.4612	-1.4260	7.9900	1.4019	0.0794	1.5697	2.2775	62.39
	Loser (L)	0.2486	3.8970	-1.3369	8.6249	1.2801	0.0887	1.4988	2.1919	59.58
	L – W	-0.0237	2.5536	0.3605	2.1385	-0.1218	0.0055	1.5935	2.2586	49.46
$p^{(3)}(1/\sigma, R)$	Winner (W)	0.2871	3.4144	-1.3862	7.6921	1.4783	0.0813	1.5474	2.2447	61.26
	Loser (L)	0.2401	3.9418	-1.3097	8.6519	1.2364	0.0865	1.5137	2.2094	59.65
	L – W	-0.0470	2.6091	0.3298	2.3515	-0.2419	0.0036	1.6149	2.2948	55.65

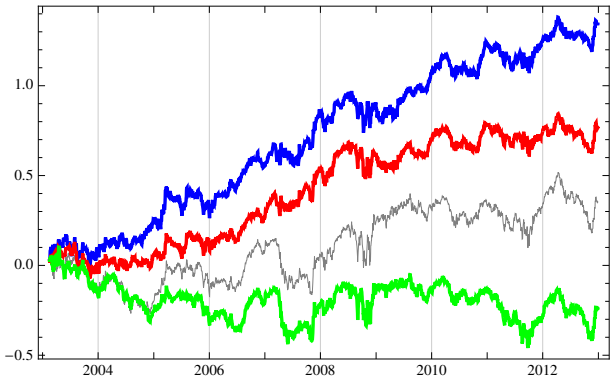

Figure 5.1: Cumulative returns for the traditional contrarian (gray), $p^{(1)}(\upsilon, R)$ (blue), $p^{(2)}(\upsilon, R)$ (red), and $p^{(3)}(1/\sigma, R)$ (green) in South Korea KOSPI 200.

ations than other strategies. In the cases of the $p^{(3)}$ criteria, the loser groups are as good as the other loser basket but the winner groups show the strongest momentum.

An interesting finding in Table 5.1 is that the outperformance of all the $p^{(1)}$ and $p^{(2)}$ portfolios is achieved by taking low risk. All the strategies in these classes are less riskier in every risk measures such as 95% VaR, CVaR, and maximum drawdown. The maximum drawdowns are almost 50% decreased with respect to the benchmark strategy. Additionally, the portfolios in both categories exhibit much higher Sharpe ratios. In particular, the risk measures of every selection rules in $p^{(1)}$ are at the lowest levels. The risk measures and Sharpe ratios of these alternative portfolios are in the narrow ranges. This fact indicates that the consistent risk management is valid for any choices of price momentum definition. The $p^{(2)}$ strategies also show the same pattern: higher Sharpe ratios and lower risk measures in the narrow ranges. Additionally, the risk measures are slightly lower than any other contrarian portfolios.

The risk profiles of each ranking basket is also consistent with the purpose of the ranking group. Every alternative losers are less riskier than the benchmark loser and the winner groups are much exposed to the risk. In particular, the 95% VaR and CVaR levels of the alternative loser groups are lower than those of the loser in cumulative return. Meanwhile, the winner groups are under the greater exposure of the risk than the winner basket in the traditional contrarian portfolio. The same pattern is observed for the Sharpe ratio. The Sharpe ratios of the loser (winner) baskets in $p^{(1)}$ and $p^{(2)}$ portfolios are greater (smaller) than that of cumulative return loser. The $p^{(2)}$ losers (winners) exhibits the slightly better (worse) reward-risk measures than $p^{(1)}$.

5.3.2 U.S. equity market: S&P 500

In Table 5.2, every alternative momentum strategies outperform the traditional contrarian strategy. The best portfolios are from the $p^{(3)}$ criteria with weekly 0.107% and 0.106%, respectively. These average returns are almost seven-times greater than the performance of the original mean-reversion portfolios. Additionally, the volatility levels of the portfolio performance are almost 50% decreased with respect to the benchmark strategy. The $p^{(3)}$ portfolios also exhibit the higher skewness and lower kurtosis. The strategies constructed by $p^{(1)}$ and $p^{(2)}$ also obtain the better performance under the smaller standard deviation. However, the skewness is decreased with respect to the cumulative return strategy. There is no significant improvement in kurtosis. The performance of the alternative portfolios can be found in Fig. 5.2.

In weekly scale, the contrarian strategies exhibit the strong reversal in

Table 5.2: Summary statistics and risk measures of weekly 6/6 contrarian portfolios in U.S. S&P 500

Criterion	Portfolio	Summary statistics					Risk measures			
		Mean	Std. Dev.	Skewness	Kurtosis	Fin. Wealth	Sharpe	$\text{VaR}_{95\%}$	$\text{CVaR}_{95\%}$	MDD
$p^{(0)}$	Winner (W)	0.1545	3.4269	-0.8186	6.8648	0.7970	0.0560	1.3386	1.7016	63.77
	Loser (L)	0.1685	4.6130	-0.1908	11.7318	0.8693	0.0494	1.3727	1.7022	81.06
	L – W	0.0140	2.7235	0.5559	18.0504	0.0722	-0.0018	0.5749	0.7774	68.14
$p^{(1)}(\upsilon, r)$	Winner (W)	0.1480	4.0676	-0.5063	7.2687	0.7636	0.0507	1.4203	1.8365	71.54
	Loser (L)	0.1807	4.3508	-0.0870	9.3735	0.9326	0.0541	1.4668	1.8387	77.10
	L – W	0.0327	1.9516	-0.5294	17.1004	0.1690	-0.0013	0.6181	0.8700	42.67
$p^{(1)}(\tau, r)$	Winner (W)	0.1488	3.9203	-0.5343	6.6807	0.7679	0.0507	1.4777	1.9006	70.37
	Loser (L)	0.1877	4.4446	-0.0486	9.7044	0.9684	0.0530	1.4598	1.8298	77.38
	L – W	0.0388	2.0502	0.1013	14.3828	0.2004	-0.0004	0.6148	0.8658	47.63
$p^{(1)}(\upsilon, R)$	Winner (W)	0.1500	3.8309	-0.5550	6.2724	0.7738	0.0517	1.4125	1.8306	69.49
	Loser (L)	0.1930	4.4955	-0.0530	9.7263	0.9960	0.0522	1.4650	1.8419	78.09
	L – W	0.0431	2.1074	0.3413	14.9428	0.2221	-0.0002	0.6133	0.8613	51.78
$p^{(1)}(\tau, R)$	Winner (W)	0.1537	3.6880	-0.5759	5.5509	0.7931	0.0518	1.4104	1.8286	67.46
	Loser (L)	0.1937	4.5815	-0.0799	10.3110	0.9997	0.0515	1.4634	1.8409	78.35
	L – W	0.0401	2.2530	0.4616	20.3251	0.2067	0.0003	0.6102	0.8587	56.16
$p^{(2)}(\upsilon, r)$	Winner (W)	0.1402	3.7924	-0.5654	8.0133	0.7236	0.0519	1.3162	1.6957	71.08
	Loser (L)	0.1786	4.0685	-0.1258	9.3141	0.9217	0.0564	1.4230	1.7917	76.01
	L – W	0.0384	1.8332	-0.3775	16.0465	0.1981	0.0011	0.5720	0.7977	42.57
$p^{(2)}(\tau, r)$	Winner (W)	0.1435	3.6434	-0.6414	7.2830	0.7404	0.0526	1.3151	1.6962	69.64
	Loser (L)	0.1805	4.1670	-0.1287	9.9820	0.9314	0.0559	1.4263	1.7964	76.92
	L – W	0.0370	1.9170	0.0761	13.1334	0.1910	0.0017	0.5696	0.7971	49.00
$p^{(2)}(\upsilon, R)$	Winner (W)	0.1416	3.5544	-0.6954	6.9265	0.7308	0.0530	1.3084	1.6894	68.87
	Loser (L)	0.1834	4.2449	-0.1108	10.3969	0.9462	0.0556	1.4250	1.7955	77.25
	L – W	0.0417	1.9983	0.3715	14.2958	0.2154	0.0047	0.5727	0.7993	51.69
$p^{(2)}(\tau, R)$	Winner (W)	0.1504	3.4075	-0.7225	6.0400	0.7759	0.0544	1.3142	1.7000	67.00
	Loser (L)	0.1877	4.3447	-0.1401	11.1255	0.9687	0.0555	1.4290	1.8006	77.82
	L – W	0.0374	2.1262	0.4476	19.4093	0.1927	0.0047	0.5662	0.7880	56.10
$p^{(3)}(1/\sigma, r)$	Winner (W)	0.0920	2.8331	-1.0490	8.6160	0.4746	0.0591	1.1677	1.4724	61.18
	Loser (L)	0.1992	3.4731	-0.4319	8.3765	1.0281	0.0635	1.2578	1.5768	70.11
	L – W	0.1073	1.7319	0.7020	5.0542	0.5535	0.0158	0.4963	0.6816	40.08
$p^{(3)}(1/\sigma, R)$	Winner (W)	0.0968	2.6887	-1.0728	7.7348	0.4995	0.0598	1.1644	1.4695	59.05
	Loser (L)	0.2024	3.5789	-0.3583	8.8179	1.0444	0.0620	1.2602	1.5817	71.17
	L – W	0.1056	1.8802	0.8292	7.1623	0.5449	0.0145	0.5023	0.6938	45.90

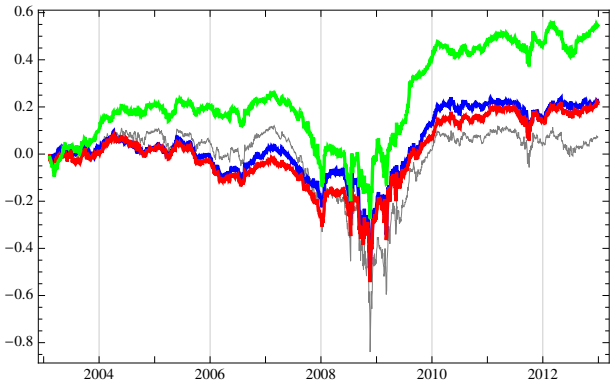

Figure 5.2: Cumulative returns for the traditional contrarian (gray), $p^{(1)}(\upsilon, R)$ (blue), $p^{(2)}(\upsilon, R)$ (red), and $p^{(3)}(1/\sigma, R)$ (green) in U.S. S&P 500.

each ranking group. First of all, all loser groups outperform the traditional contrarian loser group. In particular, the performance of the two $p^{(3)}$ loser baskets is much better than any other alternative and benchmark loser baskets. Additionally, the standard deviations of these $p^{(3)}$ loser groups are much lower than other losers constructed by the $p^{(0)}$, $p^{(1)}$, and $p^{(2)}$ physical momentum. Opposite to the loser groups, the winner groups underperform the winner basket in cumulative return. Although the performance of other winner groups is slightly worse than the short basket in cumulative return portfolio, the winner baskets in the $p^{(3)}$ criteria achieve the lowest average returns.

According to Table 5.2, the $p^{(3)}$ portfolios are less riskier in 95% VaR, CVaR, and maximum drawdown. The portfolio with inverse volatility and raw return for the physical momentum definition achieves the lowest risk measures. Additionally, its Sharpe ratio is the largest Sharpe ratio among all the alternative portfolios including the benchmark. Another $p^{(3)}$ strategy is ranked to the next in every measures to the $p^{(3)}(1/\sigma, r)$ portfolio. Meanwhile,

other alternative contrarian portfolios constructed by the physical momentum are riskier in 95% VaR and CVaR although the maximum drawdowns are improved. Moreover, the Sharpe ratios are better than the benchmark case but much lower than the $p^{(3)}$ portfolios.

The $p^{(3)}$ portfolios are less riskier at the level of each ranking basket. The winner and lower baskets in the $p^{(3)}$ portfolios achieve the lowest 95% VaR, CVaR, and maximum drawdown among every competitive baskets including the traditional contrarian portfolio. Additionally, the Sharpe ratios of the loser groups by $p^{(3)}$ are the largest Sharpe ratios. The winner groups of $p^{(3)}$ portfolios also obtains the highest reward-risk ratios. The ranking baskets in the $p^{(2)}$ portfolios are slightly less risker but the winner and loser groups in the $p^{(1)}$ definitions exhibit worse risk measures.

5.4 Factor analysis

The intercepts and factor exposures of the Fama-French three-factor analysis on the S&P 500 results are given in Table 5.3. All the intercepts by the physical momentum definitions are greater than the three-factor alpha of the traditional contrarian strategy. In particular, the $p^{(3)}$ portfolios achieve the largest and positive three-factor alphas.

The market and value factors are statistically significant. Meanwhile, the size factor doesn't show any significance in any portfolios. The factor loadings on the size factor in the $p^{(3)}$ portfolios are only positive. For any contrarian portfolios in the S&P 500 universe, the performance of the contrarian portfolios

Table 5.3: Fama-French regression of weekly 6/6 contrarian portfolios in U.S. S&P 500

Criterion	Portfolio	Factor loadings				
		$\alpha(\%)$	β_{MKT}	β_{SMB}	β_{HML}	R^2
$p^{(0)}$	Winner (W)	-0.0494	1.1237**	0.2532**	0.2906**	0.8744
	Loser (L)	-0.0965	1.4406**	0.1721*	0.6591**	0.8445
	L – W	-0.0471	0.3169**	-0.0810	0.3685**	0.1602
$p^{(1)}(\upsilon, r)$	Winner (W)	-0.1003	1.2949**	0.3612**	0.5236**	0.8936
	Loser (L)	-0.0762	1.4045**	0.2632**	0.4818**	0.8704
	L – W	0.0241	0.1096**	-0.0980	-0.0418	0.0172
$p^{(1)}(\tau, r)$	Winner (W)	-0.0901	1.2575**	0.3567**	0.4547**	0.8911
	Loser (L)	-0.0744	1.4219**	0.2594**	0.5389**	0.8680
	L – W	0.0157	0.1644**	-0.0973	0.0841	0.0518
$p^{(1)}(\upsilon, R)$	Winner (W)	-0.0837	1.2310**	0.3670**	0.4165**	0.8890
	Loser (L)	-0.0719	1.4297**	0.2567**	0.5782**	0.8673
	L – W	0.0118	0.1986**	-0.1102	0.1617*	0.0849
$p^{(1)}(\tau, R)$	Winner (W)	-0.0708	1.1925**	0.3693**	0.3448**	0.8842
	Loser (L)	-0.0762	1.4482**	0.2549**	0.6252**	0.8671
	L – W	-0.0053	0.2557**	-0.1144	0.2805**	0.1450
$p^{(2)}(\upsilon, r)$	Winner (W)	-0.0885	1.2362**	0.2405**	0.4664**	0.9034
	Loser (L)	-0.0603	1.3269**	0.1972**	0.4441**	0.8757
	L – W	0.0282	0.0907*	-0.0433	-0.0222	0.0139
$p^{(2)}(\tau, r)$	Winner (W)	-0.0764	1.2063**	0.2370**	0.3831**	0.9074
	Loser (L)	-0.0638	1.3386**	0.2013**	0.5146**	0.8699
	L – W	0.0127	0.1323**	-0.0357	0.1315	0.0513
$p^{(2)}(\upsilon, R)$	Winner (W)	-0.0731	1.1870**	0.2396**	0.3311**	0.9088
	Loser (L)	-0.0650	1.3536**	0.1942**	0.5621**	0.8681
	L – W	0.0080	0.1666**	-0.0454	0.2310**	0.0928
$p^{(2)}(\tau, R)$	Winner (W)	-0.0553	1.1538**	0.2384**	0.2512**	0.9110
	Loser (L)	-0.0660	1.3701**	0.1897**	0.6280**	0.8656
	L – W	-0.0107	0.2163**	-0.0487	0.3768**	0.1676
$p^{(3)}(1/\sigma, r)$	Winner (W)	-0.0721	1.0048**	0.0652	0.0936**	0.9099
	Loser (L)	-0.0012	1.1691**	0.0816	0.3046**	0.8830
	L – W	0.0709	0.1642**	0.0164	0.2111**	0.1188
$p^{(3)}(1/\sigma, R)$	Winner (W)	-0.0582	0.9689**	0.0661*	0.0187	0.9125
	Loser (L)	-0.0042	1.1906**	0.0865	0.3578**	0.8791
	L – W	0.0540	0.2217**	0.0204	0.3391**	0.2082

** 1% significance * 5% significance

are not explicable with the Fama-French three-factor model.

For each ranking basket, the intercepts of the regression are all negative. The stronger reversal in the ranking baskets is also found in the Fama-French three-factor analysis. The largest loser alphas are achieved by the winner groups by $p^{(3)}$. The alphas of the loser groups are exceptionally smaller than other loser baskets. The worst alphas are obtained by the $p^{(1)}$ portfolios. The

three-factor alphas of the $p^{(3)}$ losers are also worse than the cumulative return case.

The factor exposures of the contrarian portfolios are similar to other strategies except for $p^{(3)}$. Although all the factor loadings for the winner and loser baskets in $p^{(0)}, p^{(1)}$, and $p^{(2)}$ are positive and statistically significant, the $p^{(3)}$ strategies exhibit the weaker dependence on the size factor. The Fama-French three-factor model can explain the large parts of the portfolio performance with high R^2 values.

5.5 Concluding remarks

In this chapter, the various definitions of the physical momentum on equity price are introduced. Using the mapping between the price of an financial instrument and position of a particle in the one dimensional space, the log return corresponds to the velocity in equity price space. Up to the higher-order correction terms, the cumulative return is also considered as the velocity. The candidates for the financial mass to define the equity momentum quantitatively are the fractional volume, fractional transaction amount in cash, and the inverse of volatility. These definitions have the plausible origins not only from the viewpoint of physics but also based on financial viewpoint.

With the financial mass and velocity concepts, it is capable of defining the physical momentum in price that is called as the price momentum in finance. Measuring the physical momentum for each equity, the contrarian strategies using the physical momentum as a ranking criteria are implemented in the

KOSPI 200 and S&P 500 universes.

Its performance and reward-risk ratios surpass those of the traditional contrarian strategy in the weekly level. The outperformance of the physical momentum definition is based on the strong mean-reversion in each ranking basket. The winner in physical momentum definition underperform the winner group of the traditional contrarian portfolio.

The performance of the physical momentum portfolios is not explained by the Fama-French three-factor model. The intercepts are higher than the cumulative return strategy and the R^2 values are much lower.

In future work, the similar test will be conducted in different markets and asset classes. It will be interesting to implement the physical momentum portfolios in different trading strategies such as high frequency.

Chapter 6

Spontaneous symmetry breaking of arbitrage

In this chapter, the concept of spontaneous symmetry breaking is applied to arbitrage modeling. Unlike Sornette's work [94] which uses spontaneous symmetry breaking to explain speculation in the asset valuation theory, the phase transition is emergent directly from arbitrage dynamics. Wyarta and Bouchaud also consider symmetry breaking [105] but their concern is self-referential behavior explained by spontaneous symmetry breaking of correlation in macroeconomic markets such as indexes not of arbitrage return generated by the trading strategy. From the viewpoint of symmetry breaking, this paper pays attention to portfolio/risk management rather than explanations on macroeconomic regime change on which both of the previous works focus. Based on the dynamics which gives a spontaneous arbitrage phase and a no-arbitrage phase, the arbitrage strategy can be executed upon the phases of arbitrage. The phases are decided by a control parameter which has the same meaning to speed of adjustment in finance. The execution of the strategy aided by spontaneous symmetry breaking provides better performance than

the naive strategy and also diminishes risk of the strategy. In Section 6.1, a brief introduction to arbitrage modeling is given and then the spontaneous arbitrage modes are emergent from the return dynamics. The momentum strategy aided by spontaneous symmetry breaking is simulated on real data and the results in various markets are posted in Section 6.2. In Section 6.3, we conclude the chapter with some discussions and future directions.

6.1 Spontaneous symmetry breaking of arbitrage

6.1.1 Arbitrage modeling

Introducing the existence of arbitrage opportunity, the value of portfolio Π is governed by the following differential equation,

$$d\Pi\big(t, r(t)\big) = \big(r_f + r(t)\big)\Pi\big(t, r(t)\big)dt + \sigma(t)\Pi\big(t, r(t)\big)dW(t)$$

where r_f is risk free rate, $r(t)$ is excessive return of the portfolio Π, $\sigma(t)$ is volatility of portfolio return, and $W(t)$ is a stochastic noise term. If the no-arbitrage theorem is imposed, the excessive return becomes zero guaranteed by the Girsanov theorem that the risk-neutral measure $\widetilde{\mathbb{P}}(t)$ and the Brownian motion $\widetilde{W}(t)$ always exist under no-arbitrage situation [44]. If the existence of arbitrage is assumed, there is no risk-neutral measure $\widetilde{\mathbb{P}}(t)$ nor related Brownian motion $\widetilde{W}(t)$. In this case, it is more important to know how its return series has evolved. The reason why the dynamics is important has two facets.

First of all, for theorists, the dynamics encodes large amount of information on market macro- and microstructure. Secondly, it is helpful for practitioners to exploit the arbitrage opportunity by implementing trading strategies based on the dynamics.

The excessive return $r(t)$ is modeled by

$$\frac{dr(t)}{dt} = f\big(r(t)\big) + \nu(t) \tag{6.1}$$

where $\nu(t)$ is a white noise term. The structure of $f\big(r(t)\big)$ is decided by properties of arbitrage. One of the simplest forms for $f(r)$ is a polynomial function of r. Two properties of arbitrage dynamics help to guess the structure of the function [50]. When the excessive return of the strategy is large enough, the arbitrage opportunity usually disappears very quickly because many market participants are easily able to perceive the existence of the arbitrage and can use the opportunity profitably even with trading costs. This property imposes a constraint that coefficients of $f(r)$ have negative values. Additionally, Eq. (6.1) should be invariant under parity transformation $r \to -r$ because negative arbitrage return is also governed by the same dynamics. This property makes even order terms in the function vanish. Considering these properties of arbitrage, the form of $f(r)$ is given by

$$f(r) = -\lambda_1 r - \lambda_3 r^3 - \cdots \tag{6.2}$$

where $\lambda_i > 0$ for odd positive integer i. In traditional finance, these λs are also able to be considered as the proxies incorporating the information on changes

of discount rates which are covered in [28]. The dynamics describes reversal of return that the return becomes decreased when being large and it is increased when under the trend line. In other words, the reversal makes the return stay near the equilibrium around the trend line. By dimensional analysis, λ_1 is a speed of adjustment and is broadly studied in finance [7, 32, 99, 100]. Larger λ_i means the arbitrage opportunity dies out much faster. Meanwhile, smaller λ_i corresponds to the situation that chances for arbitrage can survive longer. As λ_i goes to infinity, the arbitrage return goes to zero extremely quickly and this limit corresponds to the no-arbitrage theorem. When only the linear term is considered for the simplest case, the dynamics is an Ornstein-Uhlenbeck process in mathematical finance,

$$dr_t = (\mu - \lambda_1 r_t)dt + \sigma dW_t$$

where the trend line μ is zero. This stochastic differential equation is invariant under parity transformation of r_t because W_t is an Ito process with standard normal distribution which has symmetric distribution around mean zero. Although there are higher order terms in Eq. (6.2), the dynamics is still considered as a generalized Ornstein-Uhlenbeck process because it is the mean-reverting process around the trend line.

6.1.2 Asymptotic solutions

We begin to introduce a cubic term to the Ornstein-Uhlenbeck process to extend it to more general cases. The introduction of higher order terms is already used in the market crash model [19]. Then the dynamics is changed

to

$$\frac{dr(t)}{dt} = -\lambda_1 r(t) - \lambda_3 r^3(t) + \nu(t)$$

where $\lambda_1 > 0$, $\lambda_3 > 0$, and $\nu(t)$ is a white noise term. After the cubic term is introduced, adjustment on arbitrate return occurs quicker because the coefficients are all negative. The negative coefficient condition needs to be modified in order to describe not only reversal but also trend-following arbitrage return which is explained by positive coefficients. In real situations, the trend-following arbitrage strategies are also possible to make profits by exploiting market anomalies because arbitrage opportunities fortified by transaction feedback do not disappear as quickly as expect and there could be more chances for investors. Speculation, as one of the examples, can create more opportunities for the trend-following arbitrage and increases expected return. Under speculation, the investors buy the instrument even though the price is high. This transaction induces to generate the trend line and is able to give feedback to the investors' trading patterns. During market crash or bubble collapse, they want to sell everything at very low prices although the intrinsic values of instruments are much higher than the price at which they want to sell. Not in extreme cases but under the normal market condition, people tend to buy financial instruments which have shown better performance than others because they expect that the instruments will provide higher returns in the future. The prices of the instruments become higher because the investors actually buy with the expectation [48, 101]. It seems to be very irrational but happens frequently in the markets. To integrate these kinds of situations,

we can introduce the cutoff value which can decide whether the arbitrage is originated from reversal or trend-following dynamics rather than the negative speed of adjustment. With the cutoff value, let us change λ_1 and λ_3 into the forms of

$$\begin{aligned} \lambda_1 &\rightarrow \lambda - \lambda_c \\ \lambda_3 &\rightarrow \lambda_c / r_c^2 \end{aligned}$$

where λ, λ_c, and r_c are positive. Although the number of parameters seems to be increased, this is not true because λ_c is an external parameter. Under these changes, the arbitrage dynamics is given by

$$\frac{dr(t)}{dt} = -(\lambda - \lambda_c) r(t) - \lambda_c \frac{r^3(t)}{r_c^2} + \nu(t). \tag{6.3}$$

After relaxation time τ, Eq. (6.3) becomes zero up to the noise term because other transient effects die out. In other words, the deterministic part of arbitrage dynamics arrives at the equilibrium state. By setting the deterministic part of the r.h.s. in Eq. (6.3) to zero, stationary solutions are found. The interesting point is that the number of stationary solutions is dependent with λ and λ_c. In the spontaneous symmetry breaking argument, λ is a control parameter and r is an order parameter. When $\lambda \geq \lambda_c$, there is only one asymptotic solution $r(t > \tau) = 0$ which shows the property of usual arbitrage opportunities. The meaning of this solution is that the arbitrage return finally becomes zero up to noise. It is obvious that the arbitrage opportunity vanishes after the relaxation time because it is taken by market participants who know

the existence and use the chance.

For $\lambda < \lambda_c$, there are three asymptotic solutions with $r(t > \tau) = 0$ and

$$r(t > \tau) = \pm\sqrt{1 - \frac{\lambda}{\lambda_c}} r_c = \pm r_v.$$

The solution $r = 0$ has the same meaning to the solution for $\lambda \geq \lambda_c$. It means that the arbitrage opportunity finally dies out. The latter solutions, $r = \pm r_v$, are more interesting because there exist long-living arbitrage modes in return. After the relaxation time, the arbitrage chance still exists and lifetime of the spontaneous market anomaly is longer than that of the usual short-living arbitrage. It is noteworthy that these solutions unlike $r = 0$ are symmetry breaking solutions although the dynamics is conserved under parity. The spontaneous mode also has the coherent meaning in the sense of speed of adjustment λ. If λ is smaller than the critical value λ_c, it is slower adjustment and the arbitrage opportunity can have longer lifetime. These solutions are also well-matched to the no-arbitrage theorem that the arbitrage chance does not exist because it disappears very quickly. The no-arbitrage theorem which corresponds to $\lambda \to \infty$ does not make the arbitrage possible after the relaxation time because λ is always greater than λ_c.

When a weak field term is introduced to Eq. (6.3), the observation becomes more interesting. Introducing the constant term ρ, the equation is given by

$$\frac{dr(t)}{dt} = \rho - (\lambda - \lambda_c) r(t) - \lambda_c \frac{r^3(t)}{r_c^2} + \nu(t)$$

where ρ can be considered the velocity of r. If $\lambda < \lambda_c$, the asymptotic solution

is also changed from r_v to $-r_v$ as positive ρ is changed to negative.

6.1.3 Exact solutions

The asymptotic behaviors described in the previous subsection can be cross-checked with exact solutions. In the long run, the noise term is ignored because its average is zero. Under this property, the exact solutions of Eq. (6.3) are given by

$$r(t) = \pm r_v \frac{r(t') \exp\left(-(\lambda - \lambda_c)(t - t')\right)}{\sqrt{r_v^2 - r^2(t')(1 - \exp\left(-2(\lambda - \lambda_c)(t - t')\right))}} \tag{6.4}$$

where t' is the initial time. When $\lambda \geq \lambda_c$, exponential functions in the nominator and the denominator go to zero in the large t region and it makes $r(t)$ zero. This corresponds to the symmetry preserving solution which is the usual arbitrage. If $\lambda < \lambda_c$, the exponential functions become dominant as t goes to infinity. At that time, $r(t)$ approaches $\pm r_v$ which are the symmetry breaking solutions. These solutions are already seen in the asymptotic solutions.

With the long-living arbitrage solutions in Eq. (6.4), properties of the solutions are checked graphically in Fig. 6.1 and 6.2.

In Fig. 6.1, the left graph shows time evolution of the solutions as $t \to \infty$. In the small t region, there exist non-zero arbitrage returns regardless of the value of λ/λ_c. However, as $t \to \infty$, the return approaches to non-zero if $\lambda/\lambda_c < 1$ and it vanishes if $\lambda/\lambda_c \geq 1$. In the asymptotic region, the difference becomes clear and phase transition happens where λ is at the critical value λ_c. It is easily seen in the graph on the right. The region $\lambda/\lambda_c < 1$ is called the long-living arbitrage phase, spontaneous return phase, or arbitrage phase.

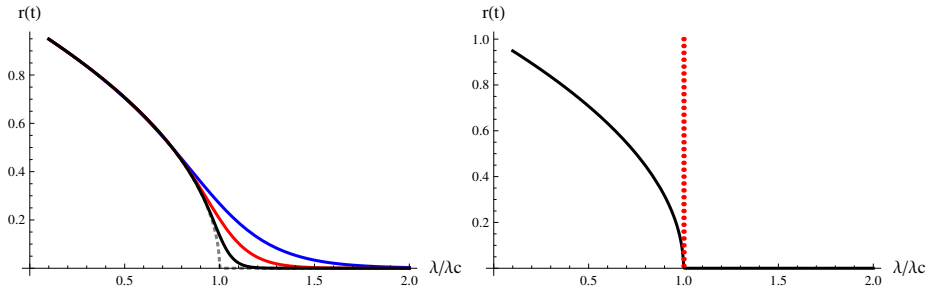

(a) (b)

Figure 6.1: Return vs. λ/λ_c. In the left graph, t=5 (blue), t=10 (red), t=25 (black), and t=∞ (gray dashed). In the right graph, t=∞ (black) and $\lambda/\lambda_c = 1$ (red dotted)

Another region where $\lambda/\lambda_c \geq 1$ is considered the short-living arbitrage phase or no-arbitrage phase. In the model, market anomalies survive if they are in the long-living modes.

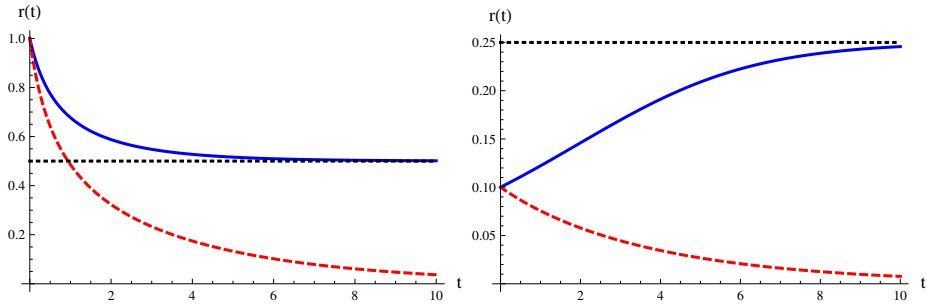

(a) r(0)> r_v (b) r(0)< r_v

Figure 6.2: Return vs. time. long-living arbitrage mode (blue), short-living arbitrage mode (red dashed), and asymptotic return (gray dashed)

In Fig. 6.2, the spontaneous arbitrage returns approach to r_v whatever initial return values are. However, the no-arbitrage phase finally goes to zero. This property does not depend on the size of the initial return values. Even if the initial value is smaller than the asymptotic value, it grows up to the

asymptotic value. For example, if investors realize the arbitrage opportunity and if they begin to invest into the chance, their trading behavior affects price dynamics and the trend-following investors pay attention to the instruments. The interest leads to trading which gives feedback to their trading patterns and can increase the profitability. In other words, money flows into the instrument, boosts its price, and gives feedback to investors' behaviors. If transaction cost is smaller than the asymptotic value, arbitrage opportunities created by spontaneous symmetry breaking can be utilized by the investors.

When the long-living arbitrage mode is possible, $r(t)$ can be re-parametrized by

$$r(t) = \pm r_v + \psi_\pm(t)$$

where $\psi(t)$ is a dynamic field for expansion around $\pm r_v$. Plugging this re-parametrization into (6.3), the differential equation for ψ is solved and its solutions are given by

$$\psi_\pm(t) = 0, \mp \frac{2r_v}{1 - \exp\left(-(\lambda_c - \lambda)t\right)}$$

Since the latter solution goes to $\mp 2r_v$ in the asymptotic region, we can check the transition between r_v and $-r_v$. If $\psi = 0$, the initial modes stay in themselves, i.e. $\pm r_v$ go to $\pm r_v$. However, if ψ is the latter solution, they evolve to $\mp r_v$ in large t limit even though we start at $\pm r_v$ initially.

6.2 Application to real trading strategy

6.2.1 Method and estimation of parameters

In order to test the validity of spontaneous symmetry breaking of arbitrage, we apply the following scheme depicted in Fig. 6.3 to trading strategies over real historical data. In backtest, the control parameter λ for the strategy should be forecasted based on historical data. At certain specific time t', it is assumed that data only from $t < t'$ are available and the control parameter for next period is forecasted from them. If the forecasted λ is smaller than the forecasted λ_c, the strategy which we want to test is expected to be in spontaneous arbitrage mode in the next period and the strategy will be executed. When the forecast tells that the strategy would not be in spontaneous arbitrage mode, it will not be exploited and the investor waits until the next execution signals. The weak field is also able to decide the method of portfolio construction. If the constant term is positive, the portfolio which the strategy suggests to build will be constructed. However, if the constant term becomes negative, weights of portfolio will become opposite to those of the portfolio originated from the positive constant term. Simply speaking, the portfolio is not constructed if the speed of adjustment is larger than the critical speed. When it is smaller than the critical value, the weight of the portfolio is $(w_1, w_2, \cdots, w_n)$ if the weak field is positive and the portfolio is $(-w_1, -w_2, \cdots, -w_n)$ if the weak field is negative. This kind of multi-state models is popular in the names of hidden Markov model [17] or threshold autoregressive model [102] in econometrics and finance. The scheme is repeated in every period over the whole data set.

To apply the model to real data, the model considered in the continuous

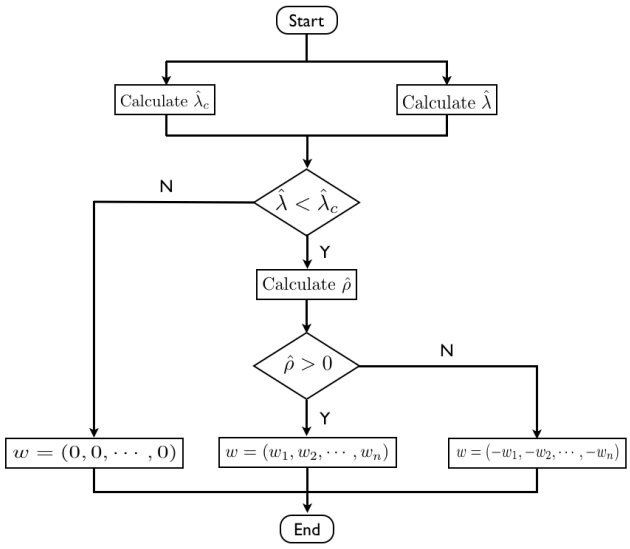

Figure 6.3: Flow chart of the scheme based on spontaneous symmetry breaking concept

time frame needs to be modified to discrete version because all financial data are in the forms of discrete time series. In the discrete form, Eq. (6.3) is changed into

$$r_{i+1} = \big(1 - (\lambda - \lambda_c)\big) r_i - \frac{\lambda_c}{r_c^2} r_i^3 + \epsilon_{i+1} \tag{6.5}$$

and an additional r_i related to the coefficient 1 in the first term on the r.h.s comes from the time derivative in Eq. (6.3).

The next step is estimation of parameters in Eq. (6.5) with real data. Regression theory gives help on estimation but it is not easy to estimate the parameters with real data because the model is nonlinear and many methods in the regression theory are for linear models. In statistics, these parameters can be estimated by nonlinear regression theory but it is not discussed in this

paper. Instead of using nonlinear regression theory directly, we can get some hints from linear regression theory. With consideration on financial meanings and physical dimensions of the parameters, linear regression theory enables us to estimate the model parameters.

There are some issues on the estimation of parameters. The first issue is related to stability of the parameters. When the parameters are fit to real data, if values of the parameters severely fluctuate over time, those abruptly-varying parameters hardly give a steady forecast. One of the best ways to avoid this is taking a moving average (MA) over a certain period. Moving average over the period can make the parameters smoothly-changing parameters. For longer MA windows, the parameter is stable but it would be rather out of date to tell more on the recent situation of the market. If it is short, they can encode more recent information but they tend to vary too abruptly to forecast the future values. To check MA window size dependency, a range of MAs needs to be tested and the results from different MAs should be compared.

Another issue is the method to estimate parameters in the model. Since two or three[1] internal parameters and one external parameter are given in the model, the same number of equations should be prepared. For the simpler case, the coefficient for each term can be considered as one parameter. In this case, two equations need to be set up. However, the values of two parameters found from two equations sometimes diverge when real data are plugged. Since λ and λ_c are the speeds of adjustment and have same physical and financial meanings, they need to be derived from the same origin. The only difference is that λ_c is external. In addition to that, the symmetry breaking needs comparison

[1]If the weak field is considered, we have three internal parameters.

between two different speeds, λ and λ_c.

One of the possible solutions is that λ is derived from the return series of the strategy and λ_c comes from the benchmark return as the definition of an external parameter. This interpretation can give two parameters the same physical dimensions and financial meanings. The specification on λs is also reasonable in the sense of the efficient market hypothesis. Since the hypothesis tells that it is impossible to systematically outperform the benchmark, it is obvious that we compare the performance of the strategy with that of the benchmark in order to test the hypothesis. In the case of r_c^2, the volatility of the strategy or benchmark return can be a good candidate because r_c^2 also has the same meaning and dimension to variance. For the constant term ρ, the average value of strategy return or benchmark return would be considered. Dividend payment rate is also a good candidate. However, since the most important parameters in the model are λ and λ_c, we focus on the estimation of these two parameters.

The intuitive way to get λ and λ_c is using a hint from the autoregressive model of order 1 called the AR(1) model. Ignoring the cubic term is also justified by the fact that the returns are much smaller than 1. Starting with the simpler model which does not have the cubic term, multiplying r_i to both sides and taking MA over k periods make the last term zero on the r.h.s. of Eq. (6.5) and give the form of λ. The one-step ahead forecasted λ is

$$\hat{\lambda}_{i+1,k} = 1 - \frac{\langle r_i r_{i-1} \rangle_k}{\langle r_{i-1}^2 \rangle_k}$$

where $\langle X_i \rangle_k = \frac{1}{k} \sum_{j=0}^{k-1} X_{i-j}$. In longer MA windows, we can change $\langle r_{i-1}^2 \rangle_k$

in the denominator to $\langle r_i^2 \rangle_k$ because $\langle r_{i-1}^2 \rangle_k$ is close to $\langle r_i^2 \rangle_k$. In shorter MA windows, the change is meaningful because it is capable of considering more recent informations[2]. Based on this argument, the final form of forecasted speed of adjustment is given by

$$\hat{\lambda}_{i+1,k} = 1 - \frac{\langle r_i r_{i-1} \rangle_k}{\langle r_i^2 \rangle_k}. \tag{6.6}$$

This λ has the same form to the parameter in AR(1) model which is found in

$$\begin{aligned} r_{i+1} &= \phi r_i + \epsilon_{i+1} \\ \phi &= \frac{E[x_i x_{i-1}]}{E[x_i x_i]} \end{aligned}$$

where $E[...]$ is the expectation value.

The estimator (6.6) is intuitively estimated but the hand-weaving argument is available. Since the benchmark return tends to be weakly autocorrelated and the return series by the arbitrage strategy is expected to be strongly positive-autocorrelated, the estimator for the arbitrage strategy is usually smaller than that for the benchmark. In this case, the strategy is in the long-living arbitrage mode. When the estimator for the strategy is larger than that for the benchmark, it is highly probable that return series for the strategy becomes much more weakly autocorrelated than the benchmark return. This tells that the strategy has recently suffered from large downslide and it can be used as the stop signal to strategy execution. Additionally, since the estimator is related to the correlation function which is in the range of -1 and 1, the value of the

[2]Actually, these two different definitions for λ will be tested in next subsections.

estimator fluctuates between 0 and 2 and it is well-matched to the positiveness condition on λ.

6.2.2 Data sets for the strategy

Two different market universes are used for analysis to avoid sample selection bias. The first universe is the S&P 500 index that is the value/float-weighted average of the top 500 companies in market capitalization in NYSE and NASDAQ. It is one of the main indexes such as the Dow Jones Index and Russell 3000 in the U.S. market. Standard & Poor's owns and maintains the index with regular rebalancing and component change. Another universe is KOSPI 200 in the South Korean market operated by Korea Exchange (KRX). It is the value-weighted average of 200 companies which represent the main industrial sectors. Unlike the S&P 500 index, KOSPI 200 contains small-sized companies in market capitalization and considers sector diversification. Its components and weights are maintained regularly and are also irregularly replaced and rebalanced in the case of bankruptcy or upon sector representation issues such as change of core business field or increase/descrease of relative weight in the sector. The significance of each index in the market is much higher than those of other main indexes such as Dow Jones 30 Index or Russell 3000 in the U.S. and the KOSPI index, the value-weighted average of all enlisted equities in the South Korean market, because futures and options on the indexes have enough liquidities to make strong interactions between equity and derivative markets. In the case of the Korean market, the KOSPI 200 index among main indexes is the only index which has the futures and options related to the main

indexes. Additionally, many mutual funds target the indexes as their benchmarks and various index-related exchange-traded funds are highly popular in both markets.

The whole time spans considered for two markets are slightly different but have large overlaps. S&P 500 is covered in the term of Jan. 1st, 1995 and Jun. 30th, 2010, 15.5 years which includes various macro-scale market events such as the Russian/Asian crisis (1997–1998), Dot-com bubble (1995–2000), its collapse (2000–2002), bull market phase (2003-2007), sub-prime mortgage crisis (2007–2009), and the recovery boosted by Quantitative Easing I (2009–2010). In the case of KOSPI 200, the market in the period of Jan. 1st. 2000 to Dec. 31st. 2010, had experienced not only economic coupling to the U.S. market but also local economic turmoils such as the credit bubble and crunch (2002–2003). Given the market and time span, the price history of each stock and whether it was bankrupt or not are stored on a database in order to remove survivor bias and all records for component change are also tracked to keep the number of index components the same. The S&P 500 data are downloaded from Bloomberg. The whole data of KOSPI 200 components and their change records are able to be downloaded from KRX. The total number of equities in the database during the covered period is 968 and 411 for S&P 500, KOSPI 200, respectively[3].

[3]Unfortunately, S&P 500 data is not completely free of survivor bias. Histories of 14 equities are not trackable and are left empty in the database. However, it might not give any serious impact on the result because the size of missing data is relatively small compared with the whole dataset.

6.2.3 Results

In both markets, 1/1 weekly strategies are considered and the contrarian portfolios are constructed. The reason for choosing 1/1 weekly strategies is that they show the best performance in each market among 144 strategies derived from maximum 12-week lookbacks and holdings. Excessive weekly returns of the portfolios are calculated from risk-free rates and proxies for the risk-free rate are from the U.S. Treasury bill with 91 days duration for S&P 500, CD with 91 days duration for KOSPI 200. Since the weekly momentum portfolio is constructed at the closing price of the first day in the week and is liquidated at the closing price of the last day, the benchmark return is also calculated from the closing prices of the first and the last days in the week. The results for these markets are given in Fig. 6.4

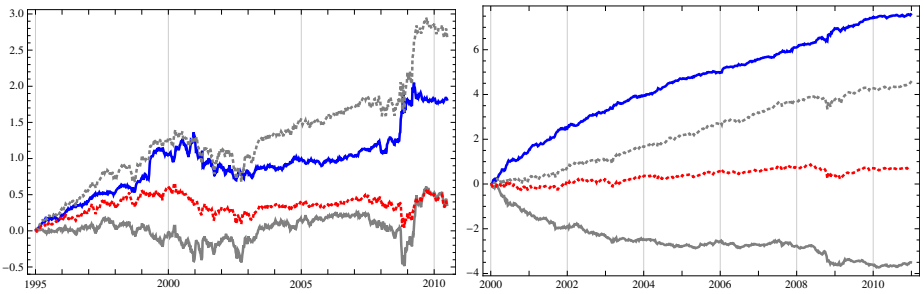

(a) S&P 500 (b) KOSPI 200

Figure 6.4: Cumulative excessive weekly returns in S&P 500 and KOSPI 200. Return time series by contrarian strategy (blue), by winner (gray), by loser (gray dashed), and by benchmark (red dashed)

There are similarities and differences in two markets. First of all, it is easily seen that 1/1 strategy shows a reversal that if the winner basket is bought, it is impossible to get a significant positive return but we can achieve posi-

tive return from the loser basket. In particular, the contrarian portfolio beats the benchmark over whole periods and this comes from the fact that the loser basket outperforms and the winner basket underperforms the benchmark. Additionally, the contrarian strategy looks more profitable in the Korean market and it can be explained that developed markets have weaker anomalies than emerging markets because the investors in the developed market have utilized the anomalies during longer periods. In the South Korea market, the winner and the loser have more clear directions and magnitudes of the returns are much greater than those of the U.S. market. It is easily seen in Table 6.1.

Table 6.1: Statistics for contrarian strategy and benchmark in S&P 500 and KOSPI 200.

		mean	std.	skewness	kurtosis	t-statistics	Sharpe ratio
S&P 500	Winner	0.045%	3.350%	0.419	11.181	0.379	0.013
	Loser	0.334%	3.973%	1.899	23.666	2.385	0.084
	Contrarian	0.225%	3.097%	1.011	21.447	2.065	0.073
	Benchmark	0.040%	2.368%	-0.150	8.097	0.482	0.017
KOSPI 200	Winner	-0.612%	4.189%	-1.051	7.444	-3.496	-0.146
	Loser	0.796%	4.747%	0.339	9.581	4.013	0.168
	Contrarian	1.325%	3.349%	1.293	9.839	9.491	0.396
	Benchmark	0.136%	3.662%	-0.125	7.052	0.889	0.037

In Table 6.1[4], the numbers from the KOSPI 200 confirm much stronger and clearer contrarian patterns as shown in Fig. 6.4. The contrarian return in the Korean market is weekly 1.325% which is much greater than 0.225% from S&P 500 contrarian strategy and the t-value of the KOSPI 200 contrarian strategy is 9.491 which is 0.1% statistically significant but the U.S. strategy has only 2.065, 5% statistically significant. The null hypothesis is that the expected excessive return is zero. Similar to the contrarian returns, the winner basket and the loser basket have larger absolute returns and t-statistics in KOSPI 200. Both of them are 0.1% statistically significant but the S&P 500

[4]The numbers are from excessive weekly return series.

loser return only has a 5% statistically significant t-value and a less significant t-value for another. In both markets, benchmarks have much smaller weekly expected returns than those by the contrarian strategies and t-values are not significant. Standard deviation gives another reason why the portfolio by the momentum/contrarian strategy needs to be constructed. After construction of the contrarian portfolio, the volatility of the portfolio is smaller than the volatility of the winner group and the loser group. In particular, in the South Korea market, the contrarian portfolio has a smaller volatility than the benchmark and has a greater Sharpe ratio than each of the winner and the loser basket has. A larger Sharpe ratio imposes that the strategy is good at minimizing the risk and maximizing the return. Winners, losers, and contrarian portfolios have large kurtosis by fat-tailed distribution.

The results by symmetry breaking with 99 different MA windows are given in Fig. 6.5 and 6.6. The strategies aided by spontaneous symmetry breaking show better performance than the naive momentum strategy in both markets and the results are not particularly dependent on the market where the strategy is used. In the case of return, the strategies with shorter MA windows have improved returns than longer MA windows or naive momentum strategy. As the length of the MA window becomes longer, the return plunges sharply and this plummet is observed in both markets. The Sharpe ratio is also increased with the SSB-aided strategy and it is obvious that the modified strategy is under better risk management. The winning percentage also increases and it is larger for shorter MA windows.

The application of spontaneous symmetry breaking also has the minor market dependencies. In S&P 500, average returns and Sharpe ratios increase

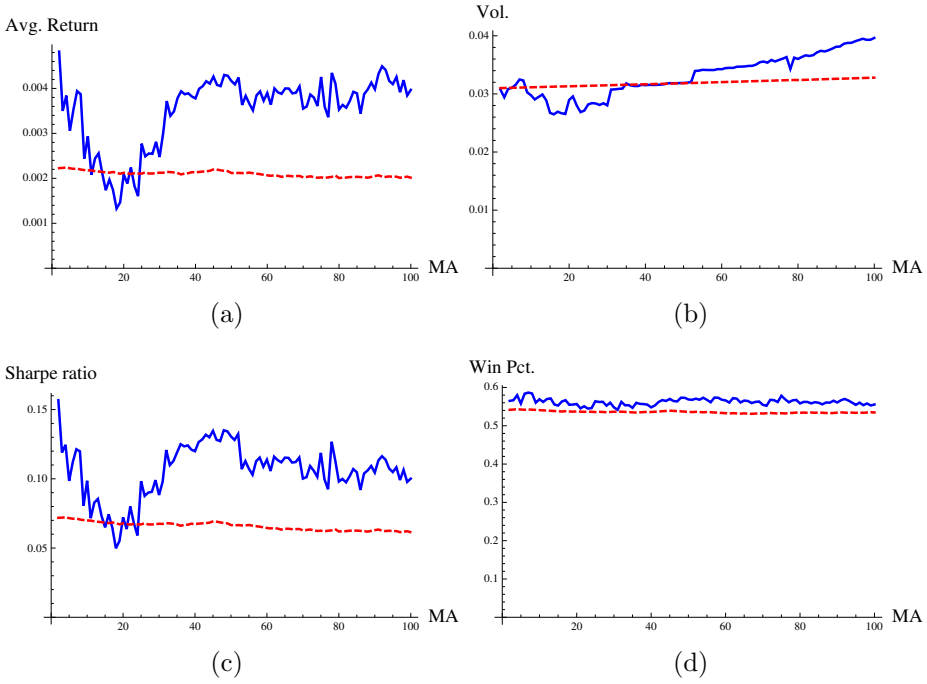

Figure 6.5: S&P 500. SSB-aided weekly contrarian strategy (blue) and naive weekly contrarian strategy (red dashed). MA window size ranges from 2 to 100.

after a drop around the 20-MA window but the KOSPI 200 momentum does not recover its average return level and remains stagnated around returns by the naive strategies. In the case of volatility, it is helpful to reduce volatility with SSB in KOSPI 200 but is not useful in S&P 500.

The constant term in spontaneous symmetry breaking is also considered. As described before, average return over the MA window or return in previous term of the raw strategy are used as the forecasted constant term. If the constant is positive, the contrarian portfolio is constructed and if the constant is negative, the momentum strategy is used. However, the strategy including the constant term does not provide better results than the strategy without the

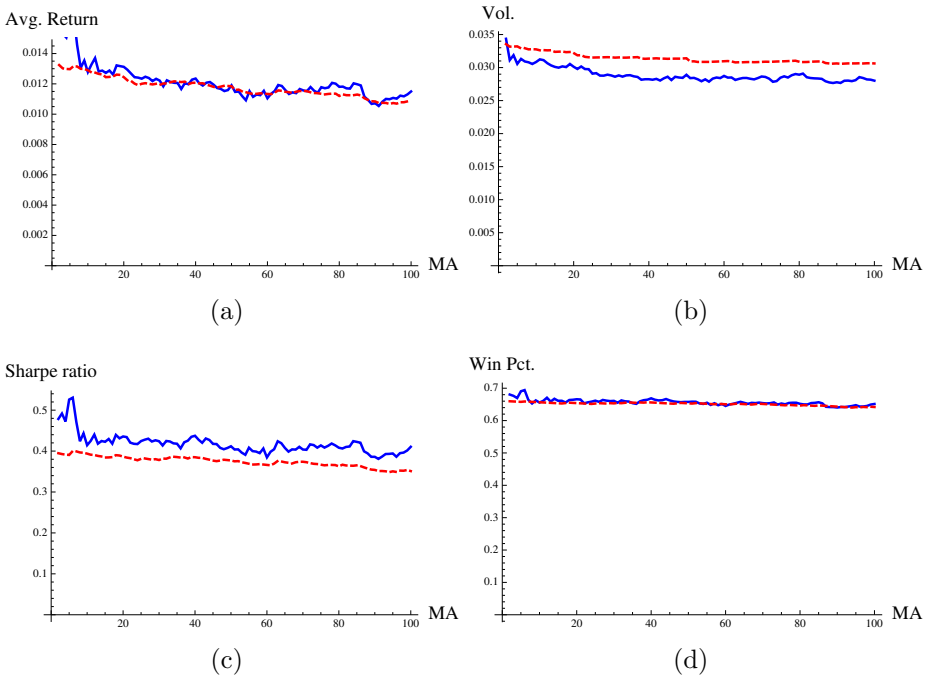

Figure 6.6: KOSPI 200. SSB-aided weekly contrarian strategy (blue) and naive weekly contrarian strategy (red dashed). MA window size ranges from 2 to 100.

constant. The same approach is applied to mean return or return in previous terms of the benchmark but it is not possible to find the better strategy. With these facts, it is guessed that the constant term is zero or the constant term is always positive if it exists and if these returns are the only possible candidates for the constant. The positiveness of the constant can be guaranteed by the fact that the arbitrage portfolio is constructed to get a positive expected return.

With other estimators for speed of adjustment, it is found that the SSB-guided strategies provide similar results although the results are not given in the paper. In both markets, the patterns of results are similar to the results depicted in Fig. 6.5 and 6.6. Specifically speaking, the estimator with $\langle r_{i-1}^2 \rangle_k$

in the denominator gives similar patterns in KOSPI 200 but the performance is slightly poorer than the result in Fig. 6.6. In the U.S. market, similar patterns in longer MA windows are found but the results with shorter MA windows are worse than the result given in the paper. This is well-matched to the assumption that $\langle r_{i-1}^2 \rangle_k$ is almost identical to $\langle r_i^2 \rangle_k$ in longer MA windows. When the estimator uses the covariance of r_i and r_{i-1}, similar results are found but the performance becomes much poorer, especially in shorter window length.

Although the whole time period is same for each of the MA windows, longer MA strategies have fewer data points when the performance is calculated in backtest. This difference in number of data points comes from the assumption that even though we work with historical data already known, we pretend to be unaware of the future after the moment at which the forecast is made in backtest. In the simulation with each MA, the first few data whose length is the same as the size of the MA window are used for forecast and are ignored in the calculation of performance. However, the difference does not make any serious difference in the patterns of performance. When the tests to calculate the performance are repeated over the same sample period for all MA windows, notable differences are not observed and the results are similar to Fig. 6.5 and 6.6.

6.3 Concluding remarks

The cubic order term and parity symmetry on return introduce the concept of spontaneous symmetry breaking to arbitrage dynamics. In the asymptotic time region, the dynamics has symmetry breaking modes triggered by the control parameter. It can provide the long-living arbitrage modes including the short-living mode in the dynamics. Spontaneous symmetry breaking generated by the control parameter λ imposes phase transition between the arbitrage phase and no-arbitrage phase. Contrasting to the short-living mode which is expected in the frame of the efficient market hypothesis, the long-living modes are totally new and exotic. The existence of a spontaneous arbitrage mode explains why the arbitrage return survives longer than expected and why the trading strategies based on market anomalies can make long term profits. With the existence of the weak field, it is possible to consider the transition between two long-living arbitrage modes, $\pm r_v$ in the asymptotic region.

Based on spontaneous symmetry breaking of arbitrage, the control parameter enables to decide execution of the trading strategy. If λ for the strategy is smaller than λ_c for the benchmark, the strategy will be executed in next period. If the speed of adjustment for the strategy is greater than that of the benchmark, nothing will be invested. Since it is difficult to estimate the parameter in the nonlinear model, the AR(1) model gives an insight for estimation. The estimated λ based on the AR(1) model has the theoretical ground that the speed of estimation is derived from the autocorrelation function. It is also reasonable in the sense of testing the efficient market hypothesis because it is capable of comparing the strategy with the benchmark. The simplest but

most meaningful estimator for the control parameter is applied to momentum strategy in the U.S and South Korean stock markets. The SSB-aided momentum strategy outperforms and has lower risk than the naive momentum strategy has. Since the strategy applied to two different markets shows similar patterns, the results are not achieved by data snooping. It is also not by estimator bias because three different estimators for speed of adjustment are tested and provide similar results with some minor differences.

The future study will be stretched into a few directions. First of all, parameter estimation needs to be more precise and statistically meaningful. In this paper, the estimator for the control parameter λ is from the AR(1) model and λ for benchmark serves as the critical value λ_c although the cubic term exists. Although it provides better performance and lower risk, estimation of the parameters is from the reasonable intuition not from regression theory. For the more precise model, they need to be estimated from nonlinear regression theory. In particular, a statistical test on estimation should be done. In the case of λ_c, it can be estimated with the help of other researches on market phase such as Wyarta and Bouchaud's work [105]. Other parameters, r_c or ρ, also help to find the better performance strategy if they are statistically well-estimated. The second direction is considering the stochastic term in arbitrage dynamics. In the paper, only the deterministic part is considered and the stochastic term is out of interest in finding the exact solutions. If the spontaneous symmetry breaking modes are found not as the asymptotic solutions but as the exact solutions of the stochastic differential equation, they would extend our understanding on arbitrage dynamics. In addition to that, specification of relaxation time can be found from the correlation function of the

stochastic solutions. Finally, it would be interesting if validity of the arbitrage modeling with spontaneous symmetry breaking is tested over other arbitrage strategies. Since only the momentum/contrarian strategy is the main concern in the paper, tests on other trading strategies including high frequency trading look very interesting. Additionally, a cross-check with momentum strategies for different markets and frequencies would be helpful to check the effectiveness and usefulness of spontaneous symmetry breaking concepts in arbitrage modeling.

Chapter 7

Kählerian information geometry for signal processing

In this chapter, we prove the correspondence between the Kähler manifold and the information geometry of signal processing models. Under certain conditions on the transfer functions of time series models and filters, the Kähler manifold is the information geometry of the models. On the Kähler manfiold, the calculation of geometric objects and search for Bayesian predictive priors are much simpler than the non-Kähler geometry. Additionally, the α-correction terms on the geometric objects are linear in α on the Kähler manifold. The structure of this paper is following. In next section, we shortly review information geometry for signal processing and derive some basic lemmas in terms of spectral density function and transfer function. In section 7.2, the conditions for the Kähler manifold are derived and main results are given. The implications of the Kähler geometry to time series models are provided in section 7.3. We conclude the chapter in section 7.4.

7.1 Information geometry for signal processing

7.1.1 Spectral density representation in frequency domain

A signal processing filter with given model parameters $\boldsymbol{\xi} = (\xi^1, \xi^2, \cdots, \xi^n)$ is described by a transfer function $h(w; \boldsymbol{\xi})$ with

$$y(w) = h(w; \boldsymbol{\xi}) x(w; \boldsymbol{\xi})$$

where $x(w; \boldsymbol{\xi})$ and $y(w)$ are input and output signals in frequency domain w, respectively. The properties of the filter are characterized by the transfer function $h(w; \boldsymbol{\xi})$ and model parameters $\boldsymbol{\xi}$. A number of the parameters, n, is not only a number of the independent variables in the model but also a dimension of a statistical manifold in information geometry.

In signal processing, one of the most important quantities is spectral density function. The spectral density function $S(w; \boldsymbol{\xi})$ is defined as the absolute square of the transfer function

$$S(w; \boldsymbol{\xi}) = |h(w; \boldsymbol{\xi})|^2. \tag{7.1}$$

The spectral density function describes the way how energy in frequency domain is distributed by the filter. In terms of signal amplitude, the spectral density function encodes change in amplitude over frequency by the filter. For example, the spectral density function of the all-pass filter is constant in

frequency domain because the filter passes all inputs to outputs up to phase difference regardless of frequency. The high-pass filter only allows the signal in the high frequency domain. Meanwhile, the low-pass filter only permits the low frequency inputs. The properties of other well-known filters are also described by their own spectral density functions.

The spectral density function is also important in information geometry because it is well-known that the Fisher information matrix, that is also the metric tensor of a statistical manifold, is derived from the spectral density function [3]. The metric tensor of a given time series model with spectral density function $S(w;\boldsymbol{\xi})$ is written in the form of

$$g_{ij}(\boldsymbol{\xi}) = \frac{1}{2\pi}\int_{-\pi}^{\pi} \partial_i \log S \partial_j \log S dw \tag{7.2}$$

where partial derivative is the derivative with respect to the coordinate system of the model parameters $\boldsymbol{\xi}$. Since the dimension of the manifold is n, the metric tensor is an $n \times n$ matrix.

Additionally, other information geometric objects are also represented with the spectral density function. For examples, the α-connection, that encodes the correction to a vector in order to transport the vector along the curve in a parallel manner, is found in

$$\Gamma^{(\alpha)}_{ij,k}(\boldsymbol{\xi}) = \frac{1}{2\pi}\int_{-\pi}^{\pi} (\partial_i\partial_j \log S - \alpha \partial_i \log S \partial_j \log S)\partial_k \log S dw \tag{7.3}$$

where α is a real number. Notice that the α-connection is not a tensor. The α-connection is related to the Levi-Civita connection, $\Gamma_{ij,k}(\boldsymbol{\xi})$, also known as

the metric connection. The relation is given by the following equation

$$\Gamma^{(\alpha)}_{ij,k}(\boldsymbol{\xi}) = \Gamma_{ij,k}(\boldsymbol{\xi}) - \frac{\alpha}{2} T_{ij,k}(\boldsymbol{\xi}) \tag{7.4}$$

$$T_{ij,k}(\boldsymbol{\xi}) = \frac{1}{\pi}\int_{-\pi}^{\pi} \partial_i \log S \partial_j \log S \partial_k \log S dw \tag{7.5}$$

where the tensor $T_{ij,k}(\boldsymbol{\xi})$ is symmetric under the exchange of the indices. It is easy to verify that the Levi-Civita connection corresponds to the $\alpha = 0$ case.

The metric tensor and α-connection are derived from the α-divergence, also known as Chernoff's α-divergence. The α-divergence is the only divergence that are both f-divergence and Bregman divergence [4]. The α-divergence between two spectral densities S_1 and S_2 is defined as

$$D^{(\alpha)}(S_1||S_2) = \begin{cases} \frac{1}{2\pi\alpha^2}\int_{-\pi}^{\pi}\left\{\left(\frac{S_2}{S_1}\right)^{\alpha} - 1 - \alpha\log\frac{S_2}{S_1}\right\}dw & (\alpha \neq 0) \\ \frac{1}{4\pi}\int_{-\pi}^{\pi}\left(\log S_2 - \log S_1\right)^2 dw & (\alpha = 0) \end{cases}$$

and conventionally measures the distance from S_1 to S_2. The α-divergence except for $\alpha = 0$ is a pseudo-distance measure in information theory because it is not symmetric under the commutation of S_1 and S_2. In spite of the asymmetry, the α-divergence is used for measuring how different two time series models or filters are. Different α provides different α-family. Some α-divergences are used much frequently than others because they correspond to the divergences already known in information theory and statistics. In particular, the (-1)-divergence is the Kullback-Leibler divergence. The 0-divergence is well-known as the square of the Hellinger distance. It is recently reported that the Hellinger distance is locally identical to the information

distance but globally tightly-bounded by the information distance [77].

These information geometric objects have interesting properties with the reciprocal spectral density function. The inverse system is related to the α-dual description. The following lemma is for the correspondence between the reciprocality of the spectral density function and the α-duality.

Lemma 1. *The inverse system of a signal processing model has the α-dual geometry to the information geometry of the original system.*

Proof. It is easy to prove that the metric tensor is invariant under the reciprocality of the spectral density function. By plugging S^{-1} to eq. (7.2), the reciprocal spectral density function provides the identical metric tensor. Given a filter with the spectral density function, there is no way to discern whether the metric tensor is derived from the filter with S or S^{-1}.

Meanwhile, the α-connection is not invariant under the reciprocality and exhibit the more interesting property. The α-connection from the reciprocal spectral density function is given in

$$\begin{aligned}\Gamma^{(\alpha)}_{ij,k}(S^{-1};\boldsymbol{\xi}) &= \frac{1}{2\pi}\int_{-\pi}^{\pi}(\partial_i\partial_j \log S + \alpha\partial_i \log S\partial_j \log S)\partial_k \log S dw \\ &= \Gamma^{(-\alpha)}_{ij,k}(S;\boldsymbol{\xi})\end{aligned}$$

and it is obvious that the α-connection with the reciprocal spectral density function is the $(-\alpha)$-connection of the original spectral density function. For example, if the 1-connection for model S is chosen, it corresponds to the (-1)-connection for model S^{-1} after the transformation. Additionally, if the model S is α-flat, S^{-1} provides the $(-\alpha)$-flat connection. Obviously, the 0-connection is self-dual to itself under the reciprocality.

Similar to the α-connection, the α-divergence is equipped with the same property under the inversion. The α-divergence between two inverted spectral density functions is easily found from the definition of the α-divergence and it is represented with

$$D^{(\alpha)}(S_1^{-1}||S_2^{-1}) = D^{(-\alpha)}(S_1||S_2).$$

With the inverse system, we can construct the α-dual description of the signal processing model. Finding the multiplicative inverse of the spectral density function corresponds to the α-dual transformation. □

With Lemma 1, it is obvious that the following multiplication rule is true

$$\begin{aligned} D^{(\alpha)}(S_1||S_2^{-1}) &= \frac{1}{2\pi\alpha^2}\int_{-\pi}^{\pi}\left\{(S_1S_2)^{-\alpha} - 1 + \alpha\log(S_1S_2)\right\}dw \\ &= D^{(-\alpha)}(S_0||S_1S_2) = D^{(\alpha)}(S_1S_2||S_0) \end{aligned}$$

where S_0 is a spectral density function for the all-pass filter of which the spectral density function is unity. Plugging $S_1 = S_0$ and $S_2 = S$, $D^{(0)}(S_0||S^{-1}) = D^{(0)}(S_0||S) = D^{(0)}(S||S_0)$.

7.1.2 Transfer function representation in z-domain

It is also possible to reproduce all the previous results in terms of the transfer function instead of the spectral density function. By using z-transformation, $z = e^{iw}$, the transfer function $h(z;\boldsymbol{\xi})$ is expressed by a Laurent polynomial

function in z in the form of

$$h(z;\boldsymbol{\xi}) = \sum_{r=-\infty}^{\infty} h_r(\boldsymbol{\xi}) z^{-r} \tag{7.6}$$

where $h_r(\boldsymbol{\xi})$ is an impulse response function. It is a bilateral (or two-sided) transfer function expression which has both of positive and negative degrees in z including the zero-th degree. If all $h_r(\boldsymbol{\xi})$ for negative r, i.e. positive degrees in z, are zero, the transfer function is reduced to a unilateral expression. In many real applications, the main concern is the causality of filters which is represented with unilateral transfer functions. In this paper, we start with the bilateral transfer function as generalization and then will focus on the causal filters.

In z-domain, all fomulae for the information geometric objects are identical to the expressions in frequency domain except for change of integral measure:

$$\frac{1}{2\pi}\int_{-\pi}^{\pi} g(w;\boldsymbol{\xi})dw \to \frac{1}{2\pi i}\oint_{|z|=1} g(z;\boldsymbol{\xi})\frac{dz}{z}.$$

Since the evaluation of the integration is obtained by line integral along the unit circle on the complex plane, it is easy to calculate with the aid of the residue theorem. By the residue theorem, the poles only inside the unit circle contribute to the evaluation of the integration. If $g(z;\boldsymbol{\xi})$ is analytic on the unit disk, the constant term in z of $g(z;\boldsymbol{\xi})$ is the answer, If the function has poles inside the unit circle, those poles contribute to the integration. For more details, see Cima et al. [27] and reference therein.

One advantage of using z-transform is that the transfer function can be

understood in the viewpoint of functional analysis. The transfer function in z-coordinate is expanded by the orthonormal basis z^{-r} with the coefficients of impulse response function. The inner product between two functions is expressed in terms of integration

$$\langle f, g \rangle = \frac{1}{2\pi i} \oint_{|z|=1} f(z)\overline{g(z)}\frac{dz}{z}.$$

By using this expression, the condition for the stable system, $\sum_{i=0}^{\infty} |h_i|^2 < \infty$ is considered as the square norm of transfer function. In complex analysis, the condition for stable system is represented as Hardy norm

$$\sum_{i=0}^{\infty} |h_i|^2 = ||h(z;\boldsymbol{\xi})||_{H^2}^2 < \infty$$

and the function that satisfies the above is called H^2 or L^2 function. The transfer function for stable system is a function on the L^2 space if it is in the bilateral form. For unilateral transfer function, it is a function on the H^2 space.

Additionally, it is natural to complexify the coordinate as being used in the complex differential geometry. For example, with holomorphic and anti-holomorphic coordinates, the metric tensor is represented with

$$g_{\mu\nu} = \frac{1}{2\pi i} \oint_{|z|=1} \partial_\mu \big(\log h(z;\boldsymbol{\xi}) + \log \bar{h}(\bar{z};\bar{\boldsymbol{\xi}}) \big) \partial_\nu \big(\log h(z;\boldsymbol{\xi}) + \log \bar{h}(\bar{z};\bar{\boldsymbol{\xi}}) \big) \frac{dz}{z}$$

where both μ and ν run over all the holomorphic and anti-holomorphic coordinates, i.e. $\mu, \nu = 1, 2, \cdots, n, \bar{1}, \bar{2}, \cdots, \bar{n}$. Since the metric tensor is defined as the inner product between the basis vectors on the manifold, the expression for

the metric tensor is also consistent with the viewpoint of functional analysis.

The metric tensor is categorized into three components: one for pure holomorphic coordinates, one for pure anti-holomorphic coordinates, and one for mixed coordinates. The metric tensors in these three categories are given in

$$g_{ij}(\boldsymbol{\xi}) = \frac{1}{2\pi i}\oint_{|z|=1} \partial_i \log h(z;\boldsymbol{\xi})\partial_j \log h(z;\boldsymbol{\xi})\frac{dz}{z} \tag{7.7}$$

$$g_{i\bar{j}}(\boldsymbol{\xi}) = \frac{1}{2\pi i}\oint_{|z|=1} \partial_i \log h(z;\boldsymbol{\xi})\partial_{\bar{j}} \log \bar{h}(\bar{z};\bar{\boldsymbol{\xi}})\frac{dz}{z} \tag{7.8}$$

where $g_{\bar{i}\bar{j}} = (g_{ij})^*$ and $g_{\bar{i}j} = (g_{i\bar{j}})^*$. The indices i and j run from 1 to n. It is also possible to express the α-connection and α-divergence in terms of the transfer function by using eq. (7.1), the relation between the transfer function and the spectral density function.

It is noteworthy that the information geometry of a filter is not changed by the multiplicative factor of z in the transfer function because the metric tensors are invariant under the factorization. It is also valid for spectral density function.

Lemma 2. *The information geometry is invariant under the multiplicative factor of z and it is possible to reduce the transfer function with the finite upper bound in degrees of z to the unilateral transfer function.*

Proof. Any transfer function can be factored out z^R in the form of

$$h(z;\boldsymbol{\xi}) = z^R \tilde{h}(z;\boldsymbol{\xi})$$

where R is any integer. When the spectral density function is considered, contribution of the factorization is $|z|^{2R}$ which is a unity in line-integral. Be-

cause of this cancelation, the metric tensor, α-connection, and α-divergence are independent with the factorization.

When the transfer function is considered, the same conclusion is obtained. Since partial derivatives in the expressions for metric tensor and α-connection remove any contribution from $\log z^R$, the formulae are invariant under the factorization. It is easy to show that α-divergence is also invariant under the factorization. Another explanation is that $\partial_i \log h$ in the metric tensor and α-connection is scale invariant under z^R factor.

In particular, this property is useful in the case that the transfer function has finite number of terms in any unilateral direction. For example, if the highest degree in z of the transfer function is finite, the transfer function is given in

$$\begin{aligned} h(z;\boldsymbol{\xi}) &= z^R(h_{-R} + h_{-(R-1)}z^{-1} + \cdots + h_0 r^{-R} + h_1 r^{-(R+1)} \cdots) \\ &= z^R \tilde{h}(z;\boldsymbol{\xi}) \end{aligned}$$

where R is an integer and $\tilde{h}$ is a unilateral transfer function. □

The bilateral transfer function can be expressed with the multiplication of two functions that one is a unilateral transfer function and another is an analytical function in the disk with non-negative degrees:

$$\begin{aligned} h(z;\boldsymbol{\xi}) &= f(z;\boldsymbol{\xi})a(z;\boldsymbol{\xi}) \\ &= (f_0 + f_1 z^{-1} + f_2 z^{-2} + \cdots)(a_0 + a_1 z^1 + a_2 z^2 + \cdots) \end{aligned}$$

where f_r and a_r are functions of $\boldsymbol{\xi}$. For a causal filter, all a_is are zero except for

a_0. This expression also includes the case of the Lemma 2 by changing $a_i = 0$ for $i < R$ and $a_R = 1$. However, it is natural to take f_0 and a_0 as non-zero functions because powers of z could be factored out for non-zero coefficient terms with the maximum degree in $f(z;\boldsymbol{\xi})$ and the minimum degree in $a(z;\boldsymbol{\xi})$, and the transfer function is reduced to

$$h(z;\boldsymbol{\xi}) = z^R \tilde{h}(z;\boldsymbol{\xi})$$

where $\tilde{h}(z;\boldsymbol{\xi})$ has non-zero $\tilde{f}_0$ and $\tilde{a}_0$ and R is an integer which is the sum of the degrees in z with first non-zero coefficient terms from $f(z;\boldsymbol{\xi})$ and $a(z;\boldsymbol{\xi})$, respectively. By Lemma 2, $h(z;\boldsymbol{\xi})$ has the same information geometry with the information geometry of $\tilde{h}(z;\boldsymbol{\xi})$.

Since $f(z;\boldsymbol{\xi}), a(z;\boldsymbol{\xi})$, and $h(z;\boldsymbol{\xi})$ construct the Toeplitz system, f_rs are decided by coefficients of $a(z;\boldsymbol{\xi})$ for a given $h(z;\boldsymbol{\xi})$. The following lemma is noteworthy for further discussion. It is the generalization of Lemma 2.

Lemma 3. *The information geometry is invariant under the choice of* $a(z;\boldsymbol{\xi})$.

Proof. It is obvious that the information geometry of the system is only decided by the transfer function $h(z;\boldsymbol{\xi})$. Whatever $a(z;\boldsymbol{\xi})$ is chosen, the transfer function is the same because $f(z;\boldsymbol{\xi})$ is conformable in Toeplitz system. □

For further generalization, the transfer function is extended with the Blaschke product $b(z)$, corresponding to the all-pass filter in signal processing, to the following form

$$h(z;\boldsymbol{\xi}) = f(z;\boldsymbol{\xi})a(z;\boldsymbol{\xi})b(z)$$

where the Blaschke product $b(z)$ is given by

$$b(z) = \prod_s b(z, z_s) = \prod_s \frac{|z_s|}{z_s} \frac{z_s - z}{1 - \bar{z}_s z}$$

and all z_s is on the unit disk. When $z_s = 0$, the Blaschke product is given by $b(z, z_s) = z$. Regardless of z_s, the Blaschke product is analytic on the unit disk. Since the Taylor expansion of the Blaschke product provides positive order terms in z, it is also possible to incorporate the Blaschke product to $a(z; \boldsymbol{\xi})$. However, the Blaschke product is considered separately in the note.

The log of transfer function is found in terms of f, a, and b:

$$\begin{aligned} \log h(z; \boldsymbol{\xi}) &= \log (f_0 a_0) + \log (1 + \sum_{r=1}^{\infty} \frac{f_r}{f_0} z^{-r}) + \log (1 + \sum_{r=1}^{\infty} \frac{a_r}{a_0} z^r) + \log b(z) \\ &= \log (f_0 a_0) + \sum_s \log |z_s| + \sum_{r=1}^{\infty} \phi_r(\boldsymbol{\xi}) z^{-r} + \sum_{r=1}^{\infty} \alpha_r(\boldsymbol{\xi}) z^r + \sum_{r=1}^{\infty} \beta_r z^r \end{aligned}$$

where ϕ_r, α_r are r-th coefficients of log expansions and those are functions of $\boldsymbol{\xi}$ unless all f_r/f_0 and a_r/a_0 are constant. Meanwhile, β_r is a constant given in $\beta_r = \frac{1}{r} \sum_s \frac{|z_s|^{2r} - 1}{z_s^r}$.

It is easy to show that the information geometry is independent with the Blaschke product.

Lemma 4. *The information geometry is independent with the Blaschke product.*

Proof. It is obvious that the Blaschke product is independent with the coordinate system $\boldsymbol{\xi}$. Plugging the above series to the expression for the metric in complex coordinates, eq. (7.7) and (7.8), the metric component is expressed

in terms of ϕ_r and α_r

$$
\begin{aligned}
g_{ij} &= \partial_i \log(f_0 a_0) \partial_j \log(f_0 a_0) + \sum_{r=1}^{\infty} \partial_i \phi_r \partial_j \alpha_r + \sum_{r=1}^{\infty} \partial_i \alpha_r \partial_j \phi_r \\
g_{i\bar{j}} &= \partial_i \log(f_0 a_0) \partial_{\bar{j}} \log(\bar{f}_0 \bar{a}_0) + \sum_{r=1}^{\infty} \partial_i \phi_r \partial_{\bar{j}} \bar{\phi}_r + \sum_{r=1}^{\infty} \partial_i \alpha_r \partial_{\bar{j}} \bar{\alpha}_r
\end{aligned}
$$

and it is obvious that there are no β_r terms related to the Blaschke product because it is not dependent on $\boldsymbol{\xi}$. It is straightforward to repeat the same calculation for the α-connection. □

According to Lemma 3, there exists the degree of freedom in choosing $a(z;\boldsymbol{\xi})$ while the geometry is not changed. Since the metric tensor is invariant under the choice of $a(z;\boldsymbol{\xi})$, it is possible to choose the degree of freedom as a_r/a_0 constant. In that degree of freedom, the metric tensors are expressed in

$$
\begin{aligned}
g_{ij} &= \partial_i \log(f_0 a_0) \partial_j \log(f_0 a_0) && (7.9) \\
g_{i\bar{j}} &= \partial_i \log(f_0 a_0) \partial_{\bar{j}} \log(\bar{f}_0 \bar{a}_0) + \sum_{r=1}^{\infty} \partial_i \phi_r \partial_{\bar{j}} \bar{\phi}_r && (7.10)
\end{aligned}
$$

and it is easy to verify that the metric tensors are only dependent on $f_0 a_0$ and ϕ_r. In other words, the metric tensor is dependent only on the unilateral part of the transfer function and a constant term of the analytic part.

By Lemma 2, it is also possible to reduce any transfer function with the finite upper bound of the degree in z to the unilateral transfer function with a constant term. For this kind of transfer function, the similar expression for the metric tensor can be obtained. First of all, the log transfer function is in

following notation:

$$\begin{aligned}\log h(z;\boldsymbol{\xi}) &= \log z^R + \log h_{-R} + \log\left(1 + \sum_{r=1}^{\infty} \frac{h_{-R+r}}{h_{-R}} z^{-r}\right) \\ &= \log z^R + \log h_{-R} + \sum_{r=1}^{\infty} \eta_r z^{-r}\end{aligned}$$

where R is the highest degree in z. Plugging this equation to metric tensor expression, eq. (7.7) and (7.8), it is obtained that

$$g_{ij} = \partial_i \log\left(h_{-R}\right) \partial_j \log\left(h_{-R}\right) \tag{7.11}$$

$$g_{i\bar{j}} = \partial_i \log\left(h_{-R}\right) \partial_{\bar{j}} \log\left(\bar{h}_{-R}\right) + \sum_{r=1}^{\infty} \partial_i \eta_r \partial_{\bar{j}} \bar{\eta}_r \tag{7.12}$$

and these expressions for metric tensors are similar to eq. (7.9) and (7.10). They could be exchangeable by $(f_0 a_0, \phi_r) \leftrightarrow (h_{-R}, \eta_r)$.

As an extension of Lemma 4, it is possible to generalize it for the inner-outer factorization for H^2 function.

Lemma 5. *Given a holomorphic transfer function in H^2 space, the transfer function is the multiplication of outer and inner functions. The information geometry is independent with the inner function.*

Proof. The transfer function $h(z;\boldsymbol{\xi}) \in H^2$ is decomposed by

$$h(z;\boldsymbol{\xi}) = \mathcal{O}(z;\boldsymbol{\xi})\mathcal{I}(z;\boldsymbol{\xi})$$

where $\mathcal{O}(z;\boldsymbol{\xi})$ is an outer function and $\mathcal{I}(z;\boldsymbol{\xi})$ is an inner function. The α-divergence is expressed with $|h(z;\boldsymbol{\xi})|^2 = |\mathcal{O}(z;\boldsymbol{\xi})\mathcal{I}(z;\boldsymbol{\xi})|^2 = |\mathcal{O}(z;\boldsymbol{\xi})|^2$ because the inner function has the unit modulus on the circle. Since the α-divergence

is represented only by the outer function, other geometrical objects such as metric tensor and α-connection are independent with the inner function. $\square$

7.2 Kähler manifold for signal processing

In z-domain, an advantage of using the transfer function representation is that it is easy to verify whether the information geometry of a given signal processing filter is the Kähler manifold or not. As mentioned before, choosing the coefficients in $a(z;\boldsymbol{\xi})$ is considered as choosing the degrees of freedom in calculation without changing any dynamics similar to gauge fixing in physics. By setting $a(z;\boldsymbol{\xi})/a_0$ a constant function in $\boldsymbol{\xi}$, the description for a statistical model becomes much simpler and the emergence of Kähler manifold can be verified easily. Since the causal filters are our main concerns in practice, we concentrate on the unilateral transfer function. Although we will work with a causal filter, the results in this section are also able to be extended to the cases of bilateral transform functions.

Theorem 1. *Given a holomorphic transfer function $h(z;\boldsymbol{\xi})$, information geometry of a signal processing model is Kähler manifold if and only if $f_0 a_0$ is a constant in $\boldsymbol{\xi}$.*

Proof. ($\Rightarrow$) If the geometry is Kähler, it should be Hermitian and

$$g_{ij} \;=\; \partial_i \log(f_0 a_0)\partial_j \log(f_0 a_0) = 0$$

for all i and j. This equation imposes that $f_0 a_0$ is a constant in $\boldsymbol{\xi}$.

($\Leftarrow$) If $f_0 a_0$ is a constant in $\boldsymbol{\xi}$, the metric tensor is given in

$$\begin{aligned} g_{ij} &= 0 \\ g_{i\bar{j}} &= \sum_{r=1}^{\infty} \partial_i \phi_r \partial_{\bar{j}} \bar{\phi}_r \end{aligned} \tag{7.13}$$

and these metric tensor conditions impose that the manifold is the Hermitian manifold. It is noteworthy that the non-vanishing metric tensor is expressed only in ϕ_r and $\bar{\phi}_r$ that are functions of the impulse response functions in $f(z;\boldsymbol{\xi})$, the unilateral part of the transfer function. For the manifold to be the Kähler manifold, the Kähler two form Ω given in

$$\Omega = -i g_{i\bar{j}} d\xi^i \otimes d\bar{\xi}^j$$

needs to be a closed two form. The condition for the Kähler two form Ω to be closed is for the metric tensor to satisfy that $\partial_k g_{i\bar{j}} = \partial_i g_{k\bar{j}}$ and $\partial_{\bar{k}} g_{i\bar{j}} = \partial_{\bar{j}} g_{i\bar{k}}$. It is easy to verify that the metric, eq. (7.13) satisfies the conditions. The Hermitian manifold with the closed Kähler two form is the Kähler manifold.

□

The Theorem 1 is not limited to the entire manifold and it is possible to apply to the submanifold. For example, given that $h(z;\boldsymbol{\xi})$ is holomorphic and $a(z;\boldsymbol{\xi})/a_0$ is a constant function in z, a submanifold of the signal processing models is Kähler manifold if and only if $f_0 a_0$ is constant on the submanifold, i.e. a function of the coordinates orthogonal to the submanifold.

Additionally, it is also possible to find the similar relationship in the case of the transfer function with the finite upper degrees in z given in eq. (7.11)

and (7.12).

Theorem 2. *Given a holomorphic transfer function $h(z;\boldsymbol{\xi})$, information geometry of a signal processing model is Kähler manifold if and only if the highest degree in z of the log-transfer function is a constant.*

Proof. The proof is straightforward because it is the same to the proof of the Theorem 1 by changing $(f_0 a_0, \phi_r) \leftrightarrow (h_{-R}, \eta_r)$. □

The previous two theorems seem to be two separate theorems but those theorems are actually equivalent to each other if the highest degree in z is finite.

Theorem 3. *If the highest degree in z of the transfer function is finite, the previous two theorems are equivalent.*

Proof. Let's assume that the highest degree term in z is R. By Lemma 2, it always enables to reduce the transfer function to the unilateral transfer function. It is possible to represent h_{-R} with $f_0 a_0$. The two theorems are equivalent. □

On the Kähler manifold, a function called Kähler potential is very important because the metric tensors are derived from the

$$g_{i\bar{j}} = \partial_i \partial_{\bar{j}} \mathcal{K} \tag{7.14}$$

where $\mathcal{K}$ is the Kähler potential. It is also possible to find the Kähler potential for signal processing.

Corollary 1. *Given the Kählerian information geometry, the Kähler potential of the geometry is the square of the Hardy norm of the log-transfer function.*

Proof. From the transfer function $h(z;\boldsymbol{\xi})$, the metric tensors for signal processing models are given by eq. (7.8). By using integration by part, the metric tensor is represented by

$$g_{i\bar{j}} = \frac{1}{2\pi i}\int_{|z|=1}\left\{\partial_i\Big(\log h(z;\boldsymbol{\xi})\partial_{\bar{j}}\log\bar{h}(\bar{\xi};\bar{\boldsymbol{\xi}})\Big) - \log h(z;\boldsymbol{\xi})\partial_i\partial_{\bar{j}}\log\bar{h}(\bar{\xi};\bar{\boldsymbol{\xi}})\right\}\frac{dz}{z}$$

where the latter term goes zero definitely. When we integrate by part for anti-holomorphic derivative, the metric tensor is expressed by

$$g_{i\bar{j}} = \frac{1}{2\pi i}\int_{|z|=1}\left\{\partial_i\partial_{\bar{j}}\Big(\log h(z;\boldsymbol{\xi})\log\bar{h}(\bar{\xi};\bar{\boldsymbol{\xi}})\Big) - \partial_i\Big(\partial_{\bar{j}}\log h(z;\boldsymbol{\xi})\log\bar{h}(\bar{\xi};\bar{\boldsymbol{\xi}})\Big)\right\}\frac{dz}{z}.$$

and the latter term is also zero because $h(z;\boldsymbol{\xi})$ is a holomorphic function.

Finally, the metric tensor is obtained as

$$g_{i\bar{j}} = \partial_i\partial_{\bar{j}}\left(\frac{1}{2\pi i}\int_{|z|=1}\big(\log h(z;\boldsymbol{\xi})\big)\big(\log h(z;\boldsymbol{\xi})\big)^*\frac{dz}{z}\right)$$

and by the definition of the Kähler potential, eq. (7.14), the Kähler potential is given in

$$\mathcal{K} = \frac{1}{2\pi i}\int_{|z|=1}\big(\log h(z;\boldsymbol{\xi})\big)\big(\log h(z;\boldsymbol{\xi})\big)^*\frac{dz}{z}$$

up to a holomorphic function F and its complex conjugate. The r.h.s. of the above equation is known as the square of the Hardy norm for the log-transfer

function where the Hardy norm is defined as

$$||g(z;\boldsymbol{\xi})||_{H^2} = \Big(\frac{1}{2\pi i}\int_{|z|=1} \big(g(z;\boldsymbol{\xi})\big)\big(g(z;\boldsymbol{\xi})\big)^* \frac{dz}{z}\Big)^{1/2}.$$

It is straightforward to derive the relation between the Kähler potential and square of the Hardy norm of the log-transfer function:

$$\mathcal{K} = \frac{1}{2\pi i}\int_{|z|=1} \big(\log h(z;\boldsymbol{\xi})\big)\big(\log h(z;\boldsymbol{\xi})\big)^* \frac{dz}{z} = ||\log h(z;\boldsymbol{\xi})||^2_{H^2}. \tag{7.15}$$

□

By eq. (7.13), the Kähler potential is given in

$$\mathcal{K} = \sum_{r=1}^{\infty} \phi_r \bar{\phi}_r$$

and it is noticeable that the Kähler potential only depends on ϕ_r, the unilateral parts of the transfer function. It is possible to obtain the similar expression for the finite highest degree case by changin $\phi_r \to \eta_r$.

Since the Kähler potential is expected to be finite, the transfer function $h(z;\boldsymbol{\xi})$ in H^2 space satisfies

$$\mathcal{K} = ||\log h(z;\boldsymbol{\xi})||^2_{H^2} < \infty$$

and it imposes that the transfer function lives not only in H^2 but also in $\exp(H^2)$. From now on, we assume $h \in \exp(H^2)$ or $\log h \in H^2$ equivalently.

From its definition, eq. (7.14), the Kähler potential generates the metric tensor and it is related to the α-divergence.

Corollary 2. *The Kähler potential is the same to a zero-th degree term in α up to holomorphic and anti-holomorphic functions in α-divergence between a signal processing filter and the all-pass filter of unit transfer function.*

Proof. The divergence is given in

$$\begin{aligned} D^{(0)}(h_0||h) &= \frac{1}{2\pi i}\oint_{|z|=1}\frac{1}{2}(\log h+\log\bar{h})^2\frac{dz}{z} \\ &= \mathcal{K}+\frac{1}{2\pi i}\oint_{|z|=1}\frac{1}{2}\big((\log h)^2+(\log\bar{h})^2\big)\frac{dz}{z} \\ &= \mathcal{K}+F(\boldsymbol{\xi})+\bar{F}(\bar{\boldsymbol{\xi}}) \end{aligned}$$

where $F(\boldsymbol{\xi})=\frac{1}{2}(\log(f_0a_0))^2$. For bilateral transfer function, $F(\boldsymbol{\xi})=\frac{1}{2}(\log(f_0a_0)+\sum\log|z_s|)+\sum_{r=1}\phi_r(\alpha_r+\beta_r)$.

For non-zero α, the α-divergence is

$$\begin{aligned} D^{(\alpha)}(h_0||h) &= \frac{1}{2\pi i\alpha^2}\int_{-\pi}^{\pi}\big\{h^\alpha-1-\alpha(\log h+\log\bar{h})\big\}\frac{dz}{z} \\ &= \frac{1}{2\pi i}\int\Big(\frac{1}{2}(\log h+\log\bar{h})^2+\sum_{n=1}^{\infty}\frac{1}{(n+2)!}\alpha^n(\log h+\log\bar{h})^{n+2}\Big)\frac{dz}{z} \\ &= D^{(0)}(h_0||h)+\mathcal{O}(\alpha) \\ &= \mathcal{K}+F(\boldsymbol{\xi})+\bar{F}(\bar{\boldsymbol{\xi}})+\mathcal{O}(\alpha). \end{aligned}$$

When f_0a_0 is a unity, a zero-th degree term in α of the α-divergence is the Kahler potential. This shows the relation between α-divergence and the Kähler potential. □

The α-connection on the Kähler manifold is also derived from the transfer function.

Corollary 3. *The α-connection of the Kählerian information geometry is*

$$\begin{aligned}
\Gamma^{(\alpha)}_{ij,\bar{k}} &= \frac{1}{2\pi i}\int_{|z|=1}\big(\partial_i\partial_j \log h(z;\boldsymbol{\xi}) - \alpha\partial_i \log h(z;\boldsymbol{\xi})\partial_j \log h(z;\boldsymbol{\xi})\big)\big(\partial_k \log h(z;\boldsymbol{\xi})\big)^*\frac{dz}{z}\\
\Gamma^{(\alpha)}_{i\bar{j},k} &= \frac{1}{2\pi i}\int_{|z|=1} -\alpha\big(\partial_i \log h(z;\boldsymbol{\xi})\big)\big(\partial_j \log h(z;\boldsymbol{\xi})\big)^*\big(\partial_k \log h(z;\boldsymbol{\xi})\big)\frac{dz}{z}\\
\Gamma^{(\alpha)}_{i\bar{j},\bar{k}} &= \frac{1}{2\pi i}\int_{|z|=1} -\alpha\big(\partial_i \log h(z;\boldsymbol{\xi})\big)\big(\partial_{\bar{j}} \log h(z;\boldsymbol{\xi})\big)^*\big(\partial_k \log h(z;\boldsymbol{\xi})\big)^*\frac{dz}{z}
\end{aligned}$$

and the symmetric tensor is given by

$$T_{ij,\bar{k}} = \frac{1}{\pi i}\int_{|z|=1}\big(\partial_i \log h(z;\boldsymbol{\xi})\partial_j \log h(z;\boldsymbol{\xi})\big)\big(\partial_k \log h(z;\boldsymbol{\xi})\big)^*\frac{dz}{z}. \tag{7.16}$$

In particular, the non-vanishing 0-connections are

$$\begin{aligned}
\Gamma^{(0)}_{ij,\bar{k}} &= \frac{1}{2\pi i}\int_{|z|=1}\big(\partial_i\partial_j \log h(z;\boldsymbol{\xi})\big)\big(\partial_k \log h(z;\boldsymbol{\xi})\big)^*\frac{dz}{z}\\
\Gamma^{(0)}_{i\bar{j},k} &= \frac{1}{2\pi i}\int_{|z|=1}\big(\partial_i\partial_j \log h(z;\boldsymbol{\xi})\big)^*\big(\partial_k \log h(z;\boldsymbol{\xi})\big)\frac{dz}{z}
\end{aligned}$$

and the 0-connection is directly derived from the Kähler potential

$$\Gamma^{(0)}_{ij,\bar{k}} = \partial_i\partial_j\partial_{\bar{k}}\mathcal{K}. \tag{7.17}$$

Proof. After plugging eq. (7.1) into eq. (7.3), the derivation of α-connection formulae is straightforward by considering holomorphic and anti-holomorphic derivatives in the expression. The same procedure is applied to the derivation of symmetric tensor $T_{ij,\bar{k}}$.

The 0-connection is expressed in terms of Kähler potential. The proof is

following:

$$\begin{aligned}
\Gamma^{(0)}_{ij,\bar{k}} &= \frac{1}{2\pi i}\int_{|z|=1}\big(\partial_i\partial_j \log h(z;\boldsymbol{\xi})\big)\big(\partial_k \log h(z;\boldsymbol{\xi})\big)^* \frac{dz}{z} \\
&= \partial_i\partial_j\partial_{\bar{k}}\Big(\frac{1}{2\pi i}\int_{|z|=1}\big(\log h(z;\boldsymbol{\xi})\big)\big(\log h(z;\boldsymbol{\xi})\big)^* \frac{dz}{z}\Big) \\
&= \partial_i\partial_j\partial_{\bar{k}}||\log h(z;\boldsymbol{\xi})||^2_{H^2} \\
&= \partial_i\partial_j\partial_{\bar{k}}\mathcal{K}
\end{aligned}$$

□

The α-connection and symmetric tensor are expressed in terms of ϕ_r

$$\begin{aligned}
\Gamma^{(0)}_{ij,\bar{k}} &= \sum_r \partial_i\partial_j\phi_r\partial_{\bar{k}}\bar{\phi}_r \\
T_{ij,\bar{k}} &= 2\sum_{r,s}\partial_i\phi_r\partial_j\phi_s\partial_{\bar{k}}\bar{\phi}_{r+s}
\end{aligned}$$

and it is obvious that the α-connection and $T_{ij,\bar{k}}$ are also independent with $a(z;\boldsymbol{\xi})$.

It is possible to compare these expressions with the well-known results on the Kähler manifold. First of all, we can cross-check the fact that the 0-connection is the Levi-Civita connection:

$${}^{(0)}\Gamma^k_{ij} = g^{k\bar{m}}\Gamma^{(0)}_{ij,\bar{m}} = g^{k\bar{m}}\partial_i\partial_j\partial_{\bar{m}}\mathcal{K} = g^{k\bar{m}}\partial_i g_{j\bar{m}} = \partial_i(\log g_{m\bar{n}})^k{}_j = \Gamma^k_{ij}$$

where the last equality comes from the expression for the Levi-Civita connection on the Kähler manifold. It is obvious that this is well-matched to the Levi-Civita connection on Kähler manifold.

In Riemannian geometry, the Riemann curvature tensor, corresponding to the 0-curvature tensor, is given by

$$R^{\rho}{}_{\sigma\mu\nu} = \partial_\mu \Gamma^{\rho}_{\nu\sigma} - \partial_\nu \Gamma^{\rho}_{\mu\sigma} + \Gamma^{\rho}_{\mu\lambda}\Gamma^{\lambda}_{\nu\sigma} - \Gamma^{\rho}_{\nu\lambda}\Gamma^{\lambda}_{\mu\sigma}$$

where the greek letters are all for any holomorphic and anti-holomorphic indices. On the Kähler manifold, the non-vanishing curvature tensors are $R^{\rho}_{\sigma\bar{\mu}j}$ and its complex conjugate. The only non-vanishing 0-curvature tensor with three holomorphic indices and one anti-holomorphic index (and its complex conjugate tensor) is represented with

$$\begin{aligned} {}^{(0)}R^{l}{}_{k\bar{i}j} &= \partial_{\bar{i}}\Gamma^{l}_{jk} - \partial_j \Gamma^{l}_{\bar{i}k} + \Gamma^{l}_{\bar{i}m}\Gamma^{m}_{jk} - \Gamma^{l}_{jm}\Gamma^{m}_{\bar{i}k} \\ &= \partial_{\bar{i}}\Gamma^{l}_{jk} \\ &= \partial_{\bar{i}}(g^{l\bar{m}}\partial_j\partial_l\partial_{\bar{m}}\mathcal{K}) \end{aligned}$$

by using the fact that the 0-connection with the mixed coordinates is vanishing.

Taking trace on holomorphic upper and lower indices in the Riemann curvature tensor, the 0-Ricci tensor is obtained as

$$\begin{aligned} R^{(0)}_{i\bar{j}} &= R^{k}{}_{ki\bar{j}} = -R^{k}{}_{k\bar{j}i} \\ &= -\partial_{\bar{j}}\partial_i (\log g_{ij})^{k}{}_{\bar{k}} = -\partial_{\bar{j}}\partial_i tr(\log g_{ij}) \\ &= -\partial_{\bar{j}}\partial_i \log\det g \end{aligned} \tag{7.18}$$

and this result is consistent with the definition of the Ricci tensor on the Kähler manifold. It is also straightforward to get the 0-scalar curvature by

contracting the indices of the 0-Ricci tensor.

The α-generalization of curvature tensor, Ricci tensor, and scalar curvature is done by using the expression for α-connection, eq. (7.4). The α-curvature tensor is given in

$$\begin{aligned} {}^{(\alpha)}R^{l}{}_{k\bar{i}j} &= \partial_{\bar{i}}{}^{(\alpha)}\Gamma^{l}_{jk} = \partial_{\bar{i}}\Big({}^{(0)}\Gamma^{l}_{jk} - \frac{\alpha}{2}g^{l\bar{m}}T_{jk,\bar{m}}\Big) \\ &= R^{(0)l}{}_{k\bar{i}j} - \frac{\alpha}{2}\partial_{\bar{i}}\Big(g^{l\bar{m}}T_{jk,\bar{m}}\Big). \end{aligned}$$

The α-Ricci tensor and α-scalar curvature are obtained as

$$\begin{aligned} R^{(\alpha)}_{i\bar{j}} &= {}^{(\alpha)}R^{k}{}_{ki\bar{j}} = -{}^{(\alpha)}R^{k}{}_{k\bar{j}i} \\ &= -\partial_{\bar{j}}\Big({}^{(0)}\Gamma^{k}_{ik} - \frac{\alpha}{2}g^{k\bar{l}}T_{ik,\bar{l}}\Big) \\ &= R^{(0)}_{i\bar{j}} + \frac{\alpha}{2}\partial_{\bar{j}}T^{k}_{ik} \\ R^{(\alpha)} &= R^{(0)} + \frac{\alpha}{2}g^{i\bar{j}}\partial_{\bar{j}}T^{\rho}_{i\rho}. \end{aligned}$$

It is noteworthy that the α-curvature tensor, α-Ricci tensor, and α-scalar curvature on the Kähler manifold have only the linear order correction of α comparing the second order correction of α in non-Kähler manifold.

When the submanifold of dimension $m < n$ exists, the transfer function is splitted into two parts

$$h(z;\boldsymbol{\xi}) = h_{\parallel}(z;\xi^{1},\cdots,\xi^{m})h_{\perp}(z;\xi^{m+1},\cdots,\xi^{n})$$

where $h_{\parallel}$ is the transfer function on the submanifold and $h_{\perp}$ is the transfer function for the orthogonal coordinates to the submanifold. When it is

plugged into eq. (7.15), the Kähler potential is decomposed into three terms as following

$$\begin{aligned}
\mathcal{K} &= \frac{1}{2\pi i}\int_{|z|=1}(\log h_{\|}+\log h_{\perp})(\log h_{\|}+\log h_{\perp})^{*}dz \\
&= \frac{1}{2\pi i}\int_{|z|=1}\log h_{\|}\log \bar{h}_{\|}dz+\frac{1}{2\pi i}\int_{|z|=1}\log h_{\perp}\log \bar{h}_{\perp}dz \\
&\quad +\frac{1}{2\pi i}\int_{|z|=1}\log h_{\|}\log \bar{h}_{\perp}dz+(c.c.) \\
&= \mathcal{K}_{\|}+\mathcal{K}_{\perp}+\mathcal{K}_{\times}
\end{aligned}$$

where $\mathcal{K}_{\|}$ contains only submanifold index, $\mathcal{K}_{\times}$ for cross-terms, and $\mathcal{K}_{\perp}$ for orthogonal to the submanifold.

It is obvious that each part of the Kähler potential decomposition provides the metric tensors given by

$$\begin{aligned}
g_{M\bar{N}} &= \partial_{M}\partial_{\bar{N}}\mathcal{K}_{\|} \\
g_{M\bar{n}} &= \partial_{M}\partial_{\bar{n}}\mathcal{K}_{\times} \\
g_{m\bar{n}} &= \partial_{m}\partial_{\bar{n}}\mathcal{K}_{\perp}
\end{aligned}$$

where a uppercase index is for the submanifold and a lowercase index for the orthogonal coordinates to the submanifold. As we already know, the Kähler potential of the submanifold is $\mathcal{K}_{\|}$ which gives the induced metric for submanifold. Based on this decomposition, it is possible to use $\mathcal{K}$ for the submanifold because it endows the same metric. However, Riemann curvature tensors and Ricci tensors have the correction terms derived from embedding in the manifold because the inverse metric tensor contains the orthogonal coordinates by

Schur complement. In statistical inference, those tensors and scalar curvature play important roles.

The benefits of introducing the Kähler manifold are followings. First of all, on the Käher manifold, the calculation of geometric objects such as the metric tensor, α-connection, and Ricci tensor becomes simpler by using the Kähler potential. For example, the 0-connection on non-Kähler manifold is given by

$$\Gamma^{(0)}_{ij,k} = \frac{1}{2}(\partial_i g_{kj} + \partial_j g_{ik} - \partial_k g_{ij})$$

and it needs three-times more calculation than the Kähler case. Additionally, Ricci tensor is directly derived from the metric tensor on the Kähler manifold. In case of the non-Kähler manifold, the connection should be calculated from the metric tensor and taking the derivative on the connection provides Ricci tensor.

Secondly, the α corrections of the Riemann curvature tensor, Ricci tensor, and scalar curvature on the Kähler manifold are linear comparing the second order corrections in non-Kähler cases. The linear correction makes much easier to understand the effect of α-family.

Lastly, finding the superharmonic priors [59] is much easier in the Kähler setup because the Laplace-Beltrami operator on the Kähler manifold is much more straightforward than the non-Kähler cases. The Laplace-Beltrami operator on the Kähler manifold is

$$\Delta\psi = 2g^{i\bar{j}}\frac{\partial^2\psi}{\partial\xi^i\partial\bar{\xi}^j}$$

comparing the Laplace-Beltrami operator on non-Kähler manifold

$$\Delta\psi = \frac{1}{\sqrt{|g|}}\partial_i\big(\sqrt{|g|}g^{ij}\partial_j\psi\big).$$

It is obvious that on the Kähler manifold, partial derivative only on the superharmonic prior gives contribution to the Laplace-Beltrami operator. Meanwhile, the contribution from the metric tensor parts also should be considered in the non-Kähler cases.

7.3 Example: AR, MA, and ARMA models

The signal processing description enables to interpret time series models as a filter that transforms an input $x(z;\boldsymbol{\xi})$ to an output $y(z)$ in the viewpoint of signal processing. In particular, we cover AR, MA, and ARMA models as examples.

First of all, the transfer functions of these time series models need to be identified. The transfer functions of AR, MA, and ARMA models are represented with $\boldsymbol{\xi} = (\sigma, \xi^1, \cdots, \xi^n)$ by

$$h(z;\boldsymbol{\xi}) = \frac{\sigma^2}{2\pi}\prod_i (1-\xi^i z^{-1})^{c_i}$$

where $c_i = -1$ if ξ^i is the AR pole and $c_i = 1$ if ξ^i the MA root.

7.3.1 AR(p) and MA(q) models

The AR and MA models are related to each other by using the reciprocality of the transfer function. By Lemma 1, the AR model is α-dual to the MA model and vice versa. The correspondence is expressed as following:

$$\begin{aligned}
\mathrm{AR}(n) &\leftrightarrow \mathrm{MA}(n) \\
\text{poles} &\leftrightarrow \text{zeroes} \\
\sigma/\sqrt{2\pi} &\leftrightarrow \sqrt{2\pi}/\sigma \\
\alpha &\leftrightarrow -\alpha \\
\Gamma^{(\alpha)} &\leftrightarrow \Gamma^{(-\alpha)} \\
D^{(\alpha)}(h_0||h) &\leftrightarrow D^{(-\alpha)}(h_0||h^{-1})
\end{aligned}$$

where h_0 is the transfer function of the all-pass filter of unity. Since these two models have the same information geometry, we will only cover the AR(p) model.

Kählerian information geometry of AR(p) model

The AR(p) model is the (p+1)-dimensional model with $\boldsymbol{\xi} = (\sigma, \xi^1, \cdots, \xi^p)$ and is represented with its transfer function

$$h(z;\boldsymbol{\xi}) = \frac{\sigma^2}{2\pi} \frac{1}{(1-\xi^1 z^{-1})(1-\xi^2 z^{-1}) \cdots (1-\xi^p z^{-1})}$$

where σ is the standard deviation and ξ^i is a pole. The log-transfer function of the AR(p) model is

$$\log h(z;\boldsymbol{\xi}) = \log \frac{\sigma^2}{2\pi} - \sum_{i=1}^{p} \log\left(1 - \xi^i z^{-1}\right)$$

and it is easy to show that $f_0 a_0 = \sigma^2/2\pi$. By Theorem 1, information geometry of the AR(p) model is not the Kähler manifold because $f_0 a_0$ is not a constant in $\boldsymbol{\xi}$. However, the submanifold of the AR model on which σ is a constant is the Kähler manifold. Since it is possible to gauge σ by re-normalize the amplitude of the input signal, σ-coordinate or 0-th coordinate can be considered as the denormalization coordinate [3]. Even in non-Kähler AR model, the metric tensor g_{0i} is vanishing for all non-zero i by direct calculation from eq. (7.2). So there is no problem in working only with non-σ coordinates and the information geometry of the $AR(p)$ model is the Kähler manifold of dimension p.

As mentioned, the Käher potential is crucial on the manifold and defined with the square of the Hardy norm of the log-transfer function. For the AR(p) model, the Kähler potential is given by

$$\mathcal{K} = \sum_{n=1}^{\infty} \frac{1}{n^2} \Big| \sum_{i=1}^{p} (\xi^i)^n \Big|^2$$

and the metric tensor is simply derived from the Kähler potential by taking the partial derivatives, eq. (7.14),

$$g_{i\bar{j}} = \frac{1}{1 - \xi^i \bar{\xi}^j}$$

where other pure-holomorphic- and pure-anti-holomorphic-indexed metric tensors are zero. Its inverse metric tensor is given by

$$g^{i\bar{j}} = \frac{(1-\xi^i\bar{\xi}^j)\prod_{k\neq i}(1-\xi^k\bar{\xi}^j)\prod_{k\neq j}(1-\xi^i\bar{\xi}^k)}{\prod_{k\neq i}(\xi^k-\xi^i)\prod_{k\neq j}(\bar{\xi}^k-\bar{\xi}^j)}$$

and the determinant of the metric tensor is calculated as

$$g = \det g_{i\bar{j}} = \frac{\prod_{1\leq j<k\leq n}|\xi^k-\xi^j|^2}{\prod_{j,k}(1-\xi^j\bar{\xi}^k)}.$$

The 0-connection and $T_{ij,\bar{k}}$ can be obtained in the Kähler-AR model. The 0-connection is obtained by eq. (7.17)

$$\Gamma^{(0)}_{ij,\bar{k}} = \frac{\delta_{ij}\bar{\xi}^k}{(1-\xi^j\bar{\xi}^k)^2}$$

and $T_{ij,\bar{k}}$ is given by eq. (7.16)

$$T_{ij,\bar{k}} = \frac{2\bar{\xi}^k}{(1-\xi^i\bar{\xi}^k)(1-\xi^j\bar{\xi}^k)}.$$

Based on the above expressions, the α-connection is easily obtained by eq. (7.4).

The 0-Ricci tensor, eq. (7.18) is found

$$R^{(0)}_{i\bar{j}} = -\frac{1}{(1-\xi^i\bar{\xi}^j)^2}$$

and the 0-scalar curvature is calculated from the 0-Ricci tensor

$$R^{(0)} = -\sum_{i,j} \frac{\prod_{k\neq i}(1-\xi^k\bar{\xi}^j)\prod_{k\neq j}(1-\xi^i\bar{\xi}^k)}{(1-\xi^i\bar{\xi}^j)\prod_{k\neq i}(\xi^k-\xi^i)\prod_{k\neq j}(\bar{\xi}^k-\bar{\xi}^j)}.$$

It is straightforward to obtain the α-generalization of Riemann curvature tensor, Ricci tensor, and scalar curvature.

Superharmonic priors for Kähler-AR(p) model

As mentioned before, the Laplace-Beltrami operator on the Kähler manifold has much simpler form than those on non-Kähler manifold. The simpler Laplace-Beltrami operator imposes that it is easier to find the superharmonic priors on the Kähler manifold. Although it is valid in any arbitrary dimensions, let's confine ourselves to the AR(2) model for simplification. For $p = 2$, the metric tensor is given by

$$g_{i\bar{j}} = \begin{pmatrix} \frac{1}{1-|\xi^1|^2} & \frac{1}{1-\xi^1\bar{\xi}^2} \\ \frac{1}{1-\xi^2\bar{\xi}^1} & \frac{1}{1-|\xi^2|^2} \end{pmatrix}.$$

By the Laplace-Beltrami on Kahler manifold, it is obvious that $(1-|\xi^k|^2)$ for $k = 1, \cdots, p$ is a superharmonic function in arbitrary dimension by

$$\begin{aligned} \Delta(1-|\xi^k|^2) &= 2g^{i\bar{j}}\frac{\partial^2}{\partial\xi^i\partial\bar{\xi}^j}(1-|\xi^k|^2) \\ &= -2g^{i\bar{j}}\delta_{i,k}\delta_{j,k} = -2g^{k\bar{k}} \end{aligned}$$

because the diagonal components of the inverse metric tensor are all positive. By additivity, the sum of these priors $\sum_{k=1}^{n}(1-|\xi^k|^2)$ are also superharmonic.

It is obvious that $\psi_1 = (1 - |\xi^1|^2) + (1 - |\xi^2|^2)$ is a superharmonic prior in the two-dimensional case.

Another superharmonic prior for the AR(2) model is $\psi_2 = (1 - |\xi^1|^2)(1 - |\xi^2|^2)$. The Laplace-Beltrami operator on ψ_2 is represented with

$$\left(\frac{\Delta\psi_2}{\psi_2}\right) = -\frac{2(2 - \xi^1\bar{\xi}^2 - \xi^2\bar{\xi}^1)}{|\xi^1 - \xi^2|^2}$$

and it is easily verified that $\left(\frac{\Delta\psi_2}{\psi_2}\right) < 0$ because $2 - \xi^1\bar{\xi}^2 - \xi^2\bar{\xi}^1 > 0$. From this, it is obvious that $\psi_2 = (1 - |\xi^1|^2)(1 - |\xi^2|^2)$ because $\psi_2 > 0$ on the unit disk.

The prior $\psi_3 = (1 - \xi^1\bar{\xi}^2)(1 - \xi^2\bar{\xi}^1)(1 - |\xi^1|^2)(1 - |\xi^2|^2)$ is also a superharmonic prior. The Laplace-Beltrami operator act on this prior is obtained as

$$\begin{aligned}(\frac{\Delta\psi_3}{\psi_3}) &= -\frac{6}{g}\frac{|\xi^1 - \xi^z|^2}{(1 - \xi^1\bar{\xi}^2)(1 - \xi^2\bar{\xi}^1)(1 - |\xi^1|^2)(1 - |\xi^2|^2)} \\ &= -6\end{aligned}$$

and it is to verify that ψ_3 is superharmonic because ψ_3 is positive. This prior is similar to the prior found in Komaki's paper [59]. If Komaki's prior is represented in the complex coordinate, Komaki's prior is $(1 - |\xi^1|^2)$ because z_1 and z_2 in his paper are complex conjugate to each other.

7.3.2 ARMA(p, q) model

Since the determinant of the metric tensor in the ARMA model is the same to that in the AR or MA model, the Ricci tensor of the ARMA model is

identical to the Ricci tensor of the AR or MA model. The correspondence can be applied for ARMA(p,q) model. For example, ARMA(p,q) model with α-connection is α-dual to ARMA(q,p) model with $(-\alpha)$-connection under the inversion. The correspondence is given as following:

$$\begin{aligned}
\text{ARMA}(p,q) &\leftrightarrow \text{ARMA}(q,p) \\
\text{poles} &\leftrightarrow \text{zeroes} \\
\text{zeroes} &\leftrightarrow \text{poles} \\
\sigma &\leftrightarrow 2\pi/\sigma \\
\alpha &\leftrightarrow -\alpha \\
\Gamma^{(\alpha)} &\leftrightarrow \Gamma^{(-\alpha)} \\
D^{(\alpha)}(h_0||h) &\leftrightarrow D^{(-\alpha)}(h_0||h^{-1})
\end{aligned}$$

where h_0 is the transfer function of the unit all-pass filter. In the case of ARMA(p,q), the metric can be still same if we consider the coordinate exchange between the AR and MA parts.

Kählerian information geometry of ARMA(p,q) model

The transfer function of ARMA(p,q) model is represented by

$$h(z;\boldsymbol{\xi}) = \frac{\sigma^2}{2\pi}\frac{(1-\xi^{p+1}z^{-1})(1-\xi^{p+2}z^{-1})\cdots(1-\xi^{p+q}z^{-1})}{(1-\xi^{1}z^{-1})(1-\xi^{2}z^{-1})\cdots(1-\xi^{p}z^{-1})}$$

and log-transfer function is in the form of

$$\log h(z;\boldsymbol{\xi}) = \log \frac{\sigma^2}{2\pi} + \sum_{i=1}^{p+q} a_i \log\left(1-\xi^i z^{-1}\right)$$

where $a_i = 1$ if the ξ^i is a root, i.e. the MA part and $a_i = -1$ if the ξ^i is come from the AR part. Similar to the AR and MA models, information geometry of the full ARMA model is not the Kähler manifold because of σ-coordinate. The first term provides a constant term in z but it is not a constant in $\boldsymbol{\xi}$. However, the information geometry of the ARMA model on constant σ-plane is the Kähler manifold as the AR and MA models do.

The Kähler potential of the ARMA model can be derived from the square of the Hardy norm of the log-transfer function. The Kähler potential is given by

$$\mathcal{K} = \sum_{n=1}^{\infty} \frac{1}{n^2} \Big| \sum_{i=1}^{p+q} c_i (\xi^i)^n \Big|^2$$

and it is similar to that of the AR and MA models except for c_i factors. These c_i factors make the difference in the metric tensor because the metric tensor is derived from the Kähler potential. The metric tensor of the ARMA(p,q) is given by

$$g_{i\bar{j}} = \frac{c_i c_j}{1-\xi^i \bar{\xi^j}}$$

and it is easily verified that AR(p) and MA(q) submanifolds have the same metric tensors to the AR(p) and MA(q) models because a_i and a_j have the same signature if those are both from AR or MA models. In the case of the

mixed coordinate, there is only sign change in the metric tensor.

Considering Schur complement, the inverse metric tensor is represented with

$$g^{i\bar{j}} = c_i c_j \frac{(1-\xi^i\bar{\xi}^j)\prod_{k\neq i}(1-\xi^k\bar{\xi}^j)\prod_{k\neq j}(1-\xi^i\bar{\xi}^k)}{\prod_{k\neq i}(\xi^k-\xi^i)\prod_{k\neq j}(\bar{\xi}^k-\bar{\xi}^j)}$$

and the only difference is the sign change in AR-MA mixed components. With the sign change of the metric tensor in the mixed coordinate, the determinant of the metric tensor is found as

$$g = \det g_{i\bar{j}} = \frac{\prod_{1\leq j<k\leq n}|\xi^k-\xi^j|^2}{\prod_{j,k}(1-\xi^j\bar{\xi}^k)}$$

and is the same to that of the AR or MA model.

The 0-connection and $T_{ij,\bar{k}}$ are similar to those of the AR or MA models except for the sign change originated from the mixing between AR coordinates and MA coordinates. The 0-connection is found in

$$\Gamma^{(0)}_{ij,\bar{k}} = \frac{c_j c_k \delta_{ij}\bar{\xi}^k}{(1-\xi^j\bar{\xi}^k)^2}$$

and $T_{ij,\bar{k}}$ is given by

$$T_{ij,\bar{k}} = \frac{2c_i c_j c_k \bar{\xi}^k}{(1-\xi^i\bar{\xi}^k)(1-\xi^j\bar{\xi}^k)}.$$

Both of them are dependent with c_i which generates the sign difference by choosing the coordinates.

The Ricci tensor of the ARMA model is identical to that of the AR or MA

models because the determinant of the metric tensor is not changed. However, the scalar curvature is different because of the sign change in the inverse metric tensor. The scalar curvature is given in

$$R = -\sum_{i,j} \frac{c_i c_j \prod_{k\neq i}(1-\xi^k\bar{\xi}^j)\prod_{k\neq j}(1-\xi^i\bar{\xi}^k)}{(1-\xi^i\bar{\xi}^j)\prod_{k\neq i}(\xi^k-\xi^i)\prod_{k\neq j}(\bar{\xi}^k-\bar{\xi}^j)}.$$

Superharmonic priors for Kähler-ARMA(p,q) model

For ARMA$(1,1)$, the metric tensor is given by

$$g_{i\bar{j}} = \begin{pmatrix} \frac{1}{1-|\xi^1|^2} & -\frac{1}{1-\xi^1\bar{\xi}^2} \\ -\frac{1}{1-\xi^2\bar{\xi}^1} & \frac{1}{1-|\xi^2|^2} \end{pmatrix}.$$

It is trivial to show that $\psi_1 = (1-|\xi^1|^2)+(1-|\xi^2|^2)$ and $\psi_2 = (1-|\xi^1|^2)(1-|\xi^2|^2)$ are superharmonic priors similar to the AR(2) model. Oppose to the AR(2) model, $\psi_3 = (1-\xi^1\bar{\xi}^2)(1-\xi^2\bar{\xi}^1)(1-|\xi^1|^2)(1-|\xi^2|^2)$ is not a superharmonic prior.

7.4 Conclusion

In this chapter, we prove that the information geometry of a signal filter is the Kähler manifold under the conditions on the transfer function of the filter. The first condition for the transfer function to be Kähler manifold is whether multiplication of zero-th degree terms in z of the unilateral and analytic parts of the transfer function decomposition is a constant or not. The second is whether the coefficient of the highest degree in z is a constant or not. These

two conditions are equivalent to each other.

It is also found that the square of Hardy norm of log-transfer function is the Kähler potential for the Kählerian information geometry. With the Kähler potential, it is easy to derive the metric tensors and Ricci tensors. Additionally, the Kähler potential is a constant term in α of the α-divergence.

The Kählerian information geometry for signal processing is not only mathematically interesting but also computationally beneficial. It is relatively easier to calculate the metric tensors and Ricci tensors comparing with the non-Kähler manifold on which tedious and lengthy calculation is needed in order to get the tensors. On the Kähler manifold, taking derivatives on the Kähler potential provides these tensors. Moreover, α-corrections on the curvature tensor, Ricci tensor, and scalar curvature are linear in α contrary to the non-linear correction in the non-Kähler case. Additionally, since the Laplace-Beltrami operator is in much simpler form, it is easier to find superharmonic priors.

The AR, MA, and ARMA models, the most well-known time series models, include the Kähler manifold as their information geometry. The metric tensor, connection, and divergence are derived from the the Kähler potential with simpler calculation than the non-Kähler manifold. In addition to that, the superharmonic priors for those models are found within much shorter computational steps.

Chapter 8

Conclusion

In this dissertation, the concepts in physics and mathematics are applied to problems in finance. The price momentum, one of the most well-known market anomalies, is empirically tested and the theoretical framework from spontaneous symmetry breaking is proposed. Additionally, the differential geometric correspondence between Kähler manifold and information geometry of signal processing models is proven.

Introducing various ranking rules to momentum-style portfolio construction is a worthwhile approach to understanding the price momentum. Using the stock selection rules originated from risk management and physics, the alternative strategies in monthly and weekly scales outperform the portfolios constructed by cumulative return regardless of market universe. The alternative portfolios are less riskier in many reward-risk measures such as Sharpe ratio, VaR, CVaR, and maximum drawdown. Larger factor-neutral returns achieved by the reward-risk momentum strategies are statistically significant and the large portions of the performance are not explained by the Fama-French three-factor model.

Using spontaneous symmetry breaking, the trading strategies are consid-

ered being in the symmetry breaking phase. The model can explain why the statistical arbitrage is available even under the efficient market hypothesis. The application of the model to the contrarian strategies in various markets exhibits that the performance and risk profile are improved.

The information geometry of signal filters is the Kähler manifold under some conditions on transfer function. The Kähler manifold is emergent if and only if the impulse response function in the highest degree in z-transform is constant. The Kählerian information geometry takes the advantage of simpler calculation steps for metric tensors and Ricci tensors. Moreover, α-corrections on geometric tensors are linear. It is also easy to find Bayesian predictive priors such as superharmonic priors because Laplace-Beltrami operator on the Kähler manifold is more straightforward. Applications to time series models including AR, MA, and ARMA models are also given.

The dissertation shows that the physical and geometrical ideas would be useful in the various fields of finance including the implementation of trading strategy. The possibility of the approaches based on physical and geometrical ideas deserves to extend to various directions not only for finding the better understanding on the market phenomena but also for making the more profitable strategies.

Bibliography

[1] Ahn, Y. G., and Lee, J. D., Investment strategy based on past stock returns and trading volume, Asia-Pacific Journal of Financial Studies 33 (2004) 105-137

[2] Amari, S., Differential-Geometrical methods in statistics, Springer (1990)

[3] Amari, S. and Nagaoka, H., Methods of information geometry, Oxford University Press (2000)

[4] Amari, S., α-divergence is unique, belonging to both f-divergence and Bregman divergence classes, IEEE Transactions on Information Theory 55 (2009) 4925-4931

[5] Amihud, Y., Illiquidity and stock returns: cross-section and time-series effect, Journal of Finanicial Markets 5 (2002) 31-56

[6] Amihud, Y. and Mendelson, H., Asset pricing and the bid-ask spread, Journal of Financial Economics 17 (1986) 223-249

[7] Amihud, Y. and Mendelson, H., Trading mechanisms and stock returns: An empirical investigation, Journal of Finance 42 (1987) 533-553

[8] Artzner, P., Delbaen, F., Eber, J., and Heath, D., Coherent measures of risk, Mathematical Finance 9 (1999) 203-228

[9] Arwini, K. and Dodson, C. T. J., Information geometry: Near randomness and near independence, Springer (2008)

[10] Asness, C. S., Momentum in Japan: The exception that proves the rule, The Journal of Portfolio Management 37 (2011) 67-75

[11] Asness, C. S., Moskowitz, T., and Pedersen, L. H., Value and momentum everywhere, Journal of Finance 68 (2013) 929-985

[12] Baaquie, B. E., A path integral approach to option pricing with stochastic volatility: Some exact results, J. Phys. I France 7 (1997) 1733-1753

[13] Baaquie, B. E., Quantum finance: Path integrals and Hamiltonians for options and interest rates, Cambridge University Press (2004)

[14] Bachelier, L., Théorie de la spéculation, Annales Scientifiques de l'École Normale Supérieure 3 (1900) 21-86

[15] Barbaresco, F., Information intrinsic geometric flows, AIP Conf. Proc. 872 (2006) 211-218

[16] Barberis, N., Shleifer, A., and Vishny, R., A model of investor sentiment. Journal of Financial Economics 49 (1998) 307-343

[17] Baum, L. E. and Petrie, T., Statistical inference for probabilistic functions of finite state Markov chains. The Annals of Mathematical Statistics 37 (1966) 1554-1563

[18] Black, F. and Scholes M. The pricing of options and corporate liabilities, Journal of Political Economy 8 (1973) 637-654

[19] Bouchaud, J. P. and Cont R., A Langevin approach to stock market fluctuations and crashes, European Physical Journal B 6 (1998) 543-550

[20] Bradley, B. O. and Taqqu, M. S., Financial risk and heavy tails, Handbook of Heavy Tailed Distributions in Finance, Elsevier/North-Holland, 1-69 (2003)

[21] Brody, D. C. and Hughston, L. P., Interest rates and information geometry, Proc. R. Soc. Lond. A 457 (2001) 1343-1363

[22] Carhart, M. M., On persistence in mutual fund performance, Journal of Finance 52 (1997) 57-82

[23] Chae, J., and Eom, Y., Negative momentum profit in Korea and its source, Asia-Pacific Journal of Financial Studies 38 (2009) 211-236

[24] Choi, J., Spontaneous symmetry breaking of arbitrage, Physica A 391 (2012)

[25] Choi, J., Physical approach to price momentum and its application to momentum strategy, arXiv:1208.2775, SSRN 2128946

[26] Choi, J., Kim, Y. S., and Mitov, I., Reward-risk momentum strategies using classical tempered stable distribution, arXiv:1403.6093, SSRN 2414105

[27] Cima, J. A., Matheson, A. L., and Ross, W. T., The Cauchy transform, American Mathematical Society (2006)

[28] Cochrane, J. H., Presidential address: Discount rates, Journal of Finance 66 (2011) 1047-1108

[29] Conlisk, J., Bounded rationality and market fluctuation, Journal of Economic Behavior and Organization 29 (1996) 233-25

[30] Cootner, P., The random character of stock market prices, MIT Press, 1964

[31] Cox, J. C., Ingersoll, J. E. and Ross, S. A., A theory of the term structure of interest rates, Econometrica 53 (1985) 385-407

[32] Damodaran, A., A simple measure of price adjustment coefficients, Journal of Finance 48 (1993) 387-400

[33] Daniel, K., Hirshleifer, D., and Subrahmanyam, A., Investor psychology and security market under- and over-reactions. Journal of Finance 53 (1998) 1839-1886

[34] Datar, V., Naik, N., and Radcliffe, R., Liquidity and asset returns: An alternative test, Journal of Financial Markets 1 (1998) 203-220

[35] De Bondt, W. F. M. and Thaler, R., Does the stock market overreact?, Journal of Finance 40 (1985) 793-805

[36] Efron, B., Defining the curvature of a statistical problem (with applications to second order efficiency), Ann. Statist. 3 (1975) 1189-1217

[37] Erb, C. B., and Harvey, C. R., The strategic and tactical value of commodity futures, Financial Analysts Journal 62 (2006) 69-97

[38] Fama, E. F., The behavior of stock market prices, Journal of Business 38 (1965) 34-105

[39] Fama, E. F. and French, K. R., Common risk factors in the returns on stocks and bonds, Journal of Financial Economics 33 (1993) 3-56

[40] Fama, E. F. and French, K. R., Multifactor explanations of asset pricing anomalies, Journal of Finance 51 (1996) 55-84

[41] Farmer, J. D. and Lo, A. W., Frontiers of finance: Evolution and efficient markets, Proc. Natl. Acad. Sci. 96 (1999) 9991-9992

[42] French, K. R., Schwert, G. W., Stambaugh, R. F., Expected stock returns and volatility, Journal of Financial Economics 19 (1987) 3-29

[43] George, T. J., and Hwang, C., The 52-week high and momentum investing, Journal of Finance 59 (2004) 2145-2175

[44] Girsanov, I. V., On transforming a certain class of stochastic processes by absolutely continuous substitution of measures, Theory Prob. Appl. 5 (1960) 285-301

[45] Glosten, L. R., Jagannathan, R., and Runkle, D. E., On the relation between the expected value and the volatility of the nominal excess return on stocks, Journal of Finance 48 (1993) 1779-1801

[46] Griblatt, M., and Han, B., The disposition effect and momentum, Working paper, UCLA (2002)

[47] Heckman, J. J., Statistical inference and string theory, arXiv:1305.3621

[48] Hong, H. and Stein, J. C., A unified theory of underreaction, momentum trading and overreaction in asset markets, Journal of Finance 54 (1999) 2143-2184

[49] Hu, S., Trading turnover and expected stock returns: the trading frequency hypothesis and evidence from the Tokyo Stock Exchange, Working paper, University of Chicago (1997)

[50] Ilinski, K., Physics of finance: Gauge modelling in non-equilibrium pricing, Wiley, 2001

[51] Janke, W., Johnston, D.A., and Kenna, R., Information geometry and phase transitions, Physica A336 (2004) 181-186

[52] Jeffreys, H., An invariant form for the prior probability in estimation problems, Proc. Roy. Soc. London, Ser. A 196 (1946) 453-461

[53] Jegadeesh, N. and Titman, S., Returns to buying winners and selling losers: Implications for stock market efficiency, Journal of Finance 48 (1993) 65-91

[54] Kahneman, D., Slovic, P., and Tversky, A., Judgment under uncertainty: Heuristics and biases, Cambridge University Press, 1982

[55] Kahneman, D. and Tversky, A., Choices, values and frames, Cambridge University Press, 2000

[56] Kim, S., Kim, D., and Shin, H., Evaluating asset pricing models in the Korean stock market, Pacific-Basin Finance Journal 20 (2012) 198-227

[57] Kim, Y. S., Rachev, S. T., Bianchi, M. L., and Fabozzi, F. J., Tempered stable and tempered infinitely divisible GARCH models, Journal of Banking and Finance 34 (2010) 2096-2109

[58] Koh, B. C., Risk premium and profitability of relative strength strategies, Korean Journal of Financial Management 14 (1997) 1-21

[59] Komaki, F., Shrinkage priors for Bayesian prediction, Ann. Statistics 34 (2006) 2, 808-819

[60] Lee, C. and Swaminathan, B., Price momentum and trading volume, Journal of Finance 55 (2000) 2017-2070

[61] Lesmond, D. A., Schill, M. J., and Zhou, C., The illusory nature of momentum profits, Journal of Financial Economics 71 (2004) 349-380

[62] Lewellen, J., Momentum and autocorrelation in stock return, Review of Financial Studies 15 (2002) 533-563

[63] Liu, M., Liu, Q., and Ma, T., The 52-week high momentum strategy in international stock markets, Journal of International Money and Finance 30 (2011) 180-204

[64] Lo, A. W., The adaptive markets hypothesis: Market efficiency from an evolutionary perspective, Journal of Portfolio Management, Forthcoming

[65] Lo, A. W., Reconciling efficient markets with behavioral finance: The adaptive markets hypothesis, Journal of Investment Consulting 7 (2005) 21-44

[66] Lo, A. W. and MacKinlay, A., When are contrarian profits due to stock market overreaction?, Review of Financial Studies 3 (1990) 175-205

[67] Lo, A. W. and MacKinlay, A., A non-random walk down wall street, Princeton University Press, 2001

[68] Malevergne, Y. and Sornette, D., Multi-dimensional rational bubbles and fat tails, Quantitative Finance 1 (2001) 533-541

[69] Mantegna, R. N. and Stanley, H. E., Introduction to econophysics: Correlations and complexity in finance, Cambridge University Press, 2007

[70] Markowitz, H. M., Portfolio selection, Journal of Finance 7 (1952) 77-91

[71] Martin, R. D., Rachev, S., and Siboulet, F., Phi-alpha optimal portfolios and extreme risk management, Willmot Magazine of Finance (2003)

[72] Matsuyama, Y., The α-EM algorithm: Surrogate likelihood maximization using α-Logarithmic information measures, IEEE Transactions on Information Theory 49 (2003) 692-706

[73] Matsuyama, Y., Hidden Markov model estimation based on alpha-EM algorithm: Discrete and continuous alpha-HMMs, Proceedings of International Conference on Neural Networks, San Jose, California, USA (2011)

[74] Merton, R. C., Theory of rational option pricing, Bell Journal of Economics and Management Science (The RAND Corporation) 4 (1973) 141-183

[75] Moskowitz, T. J. and Grinblatt M., Do industries explain momentum?, Journal of Finance 54 (1999) 1249-1290

[76] Moskowitz, T. J., Ooi, Y. H., and Pedersen, L. H., Time series momentum, Journal of Financial Economics 104 (2012) 228-250

[77] Mullhaupt, A. P., Hellinger distance and information distance, unpublished

[78] Okunev, J. and Derek W., Do momentum-based strategies still work in foreign currency markets?, Journal of Financial and Quantitative Analysis 38 (2003) 425-447

[79] Rachev, S., Jasic, T., Stoyanov, S., and Fabozzi, F., Momentum strategies based on reward-risk stock selection criteria, Journal of Banking and Finance 31 (2007) 2325-2346 3206-3218

[80] Rao, C. R., Information and accuracy attainable in the estimation of statistical parameters, Bull Calcutta Math. Soc. 37 (1945) 81-89

[81] Ravishanker, N., Melnick, E. L., and Tsai, C., Differential geometry of ARMA models, Journal of Time Series Analysis 11 (1990) 259-274

[82] Ravishanker, N., Differential geometry of ARFIMA processes, Communications in Statistics - Theory and Methods 30 (2001) 1889-1902

[83] Rockafellar, R. T. and Uryasev, S., Optimization of conditional Value-at-Risk, Journal of Risk 2 (2000) 21-41

[84] Rockafellar, R. T. and Uryasev, S., Conditional Value-at-Risk for general loss distributions, Journal of Banking and Finance 26 (2002) 1443-1471

[85] Roehner, B. M., Patterns of Speculation: A study in observational econophysics, Cambridge University Press, 2005

[86] Rosinski, J., Tempering stable processes, Stochastic Processes and Their Applications 117 (2007) 677-707

[87] Rouwenhorst, K. G., International momentum strategies, Journal of Finance 53 (1998) 267-284

[88] Rouwenhorst, K. G., Local return factors and turnover in emerging stock markets, Journal of Finance 54 (1999) 1439-1464

[89] Samuelson, P., Proof that properly anticipated prices fluctuate randomly, Industrial Management Review 6 (1965) 41-49

[90] Sharpe, W. F., The Sharpe ratio, Journal of Portfolio Management 21 (1994) 45-58

[91] Shleifer, A., Inefficient markets : An introduction to behavioral finance, Oxford University Press, 2000

[92] Shleifer, A. and Vishny, R. W., The limits of arbitrage, Journal of Finance 52 (1997) 35-55

[93] Singal, V., Beyond the random walk: A guide to stock market anomalies and low risk investing, Oxford University Press, 2003

[94] Sornette, D., Stock market speculation : Spontaneous symmetry breaking of economic valuation, Physica A 284 (2000) 355-375

[95] Sornette, D., Why Stock Markets Crash: Critical events in complex financial systems, Princeton University Press, 2004

[96] Sornette, D. and Malevergne, Y., From rational bubbles to crashes, Physica A 299 (2001) 40-59

[97] Tanaka, F. and Komaki, F., A superharmonic prior for the autoregressive process of the second order, Mathematical Engineering Technical Reports, University of Tokyo (2006)

[98] Tanaka, F., Superharmonic priors for autoregressive models of the second order, Mathematical Engineering Technical Reports, University of Tokyo (2009)

[99] Theobald, M., and Yallup, P., Measuring cash-futures temporal effects in the UK using partial adjustment factors, Journal of Banking and Finance 22 (1998) 221-243

[100] Theobald, M., and Yallup, P., Determining security speed of adjustment coefficient, Journal of Financial Markets 7 (2004) 75-96

[101] Terence, H., Hong, H., Lim, T., and Stein, J., Bad news travels slowly: Size, analyst coverage, and the profitability of momentum strategies, Journal of Finance 55 (2000) 265-295

[102] Tong, H., Threshold Models in Nonlinear Time Series Analysis, Springer-Verlag, New York, 1983

[103] Vasicek, O., An equilibrium characterization of the term structure, Journal of Financial Economics 5 (1977) 177-188

[104] Hull, J. and White, A., Pricing interest-rate derivative securities, The Review of Financial Studies 3 (1990) 573-592

[105] Wyarta, M. and Bouchaud, J. P., Self-referential behaviour, overreaction and conventions in financial markets, Journal of Economic Behavior and Organization 63 (2007) 1-24

[106] Zanardi, P., Giorda, P., and Cozzini, M., Information-theoretic differential geometry of quantum phase transitions, Phys. Rev. Lett. 99, 100603 (2007)